# FINITE ELEMENT MODELING AND EARTHQUAKE SIMULATION OF A HIGHWAY BRIDGE USING MEASURED EARTHQUAKE DATA

A THESIS SUBMITTED TO
THE GRADUATE SCHOOL OF NATURAL AND APPLIED SCIENCES
OF
THE MIDDLE EAST TECHNICAL UNIVERSITY

BY



ÖNDER TÜRKER



IN PARTIAL FULFILLMENT OF THE REQUIREMENTS FOR THE DEGREE OF

MASTER OF SCIENCE

IN

THE DEPARTMENT OF CIVIL ENGINEERING



APRIL 2003

Approval of the Graduate School of Natural and Applied Sciences

Prof. Dr. Tayfur ÖZTÜRK
Director

I certify that this thesis satisfies all the requirements as a thesis for the degree of Master of Science.

Prof. Dr. Mustafa TOKYAY
Head of Department

This is to certify that we have read this thesis and that in our opinion it is fully adequate, in scope and quality, as a thesis for the degree of Master of Science.

Prof. Dr. Çetin YILMAZ
Co-Supervisor

Assist. Prof. Dr. Ahmet TÜRER
Supervisor

Examining Committee Members

Prof. Dr. Tanvir WASTI

Assist. Prof. Dr. Ahmet TÜRER

Prof. Dr. Çetin YILMAZ

Prof. Dr. Mehmet UTKU

Prof. Dr. Turgut TOKDEMİR

# ABSTRACT

## FINITE ELEMENT MODELING AND EARTHQUAKE SIMULATION OF A HIGHWAY BRIDGE USING MEASURED EARTHQUAKE DATA

TÜRKER, Önder

M.Sc., Department of Civil Engineering

Supervisor: Assist. Prof. Dr. Ahmet TÜRER

Co-Supervisor: Prof. Dr. Çetin YILMAZ

April 2003, 120 pages

This thesis analyzes the earthquake behavior of Bolu Viaduct, Bridge No:1 of the Anatolian Motorway Gümüşova-Gerede Section, which is one of the most important engineering structures and underwent extensive damage during the 12 November 1999 Düzce Earthquake. The thesis has two parts: computer modeling and earthquake simulation. In the first part, four different 3-dimensional and two different 2-dimensional computer models are generated at different levels of detail and complexity for the analyses to be performed with SAP2000

Structural Analysis Program. The geometry of the models is generated mainly by using a combination of Fortran 77 and Excel – Visual Basic routines. In the second part, Düzce Earthquake is simulated using Düzce station record and analysis results of different models are compared against each other, discussed, and conclusions are drawn.

Keywords: Bridge, Viaduct, Bolu Viaduct, Highway, Modeling, Computer Modeling, Finite Element, Earthquake Simulation, Düzce Earthquake, Time History Analysis, Dynamic Analysis

# ÖZ

ÖLÇÜLMÜŞ DEPREM VERİLERİ KULLANARAK BİR OTOYOL KÖPRÜSÜNÜN SONLU ELEMANLARLA MODELLENMESİ VE DEPREM SİMÜLASYONU

TÜRKER, Önder

Yüksek Lisans, İnşaat Mühendisliği Bölümü

Tez Yöneticisi: Yrd. Doç. Dr. Ahmet TÜRER

Ortak Tez Yöneticisi: Prof. Dr. Çetin YILMAZ

Nisan 2003, 120 sayfa

Bu çalışma, önemli mühendislik yapılarından biri olan ve 12 Kasım 1999 Düzce Depremi sırasında büyük ölçüde hasar görmüş bulunan, Anadolu Otoyolu Gümüşova-Gerede Kısmına ait Bolu Viyadüğü olarak da adlandırılan 1 nolu köprünün depremdeki davranışını incelemiştir. Tez, iki bölümden oluşmaktadır: bilgisayar modellemesi ve deprem simülasyonu. İlk bölümde, SAP2000 Yapısal Analiz Programı ile yapılacak olan analizler için, değişik detay ve komplekslik derecelerinde dört farklı üç boyutlu ve iki farklı iki boyutlu bilgisayar modeli

geliştirilmiştir. Modellerin geometrisi genel olarak Fortran 77 ve Excel – Visual Basic programlarıyla yazılan bilgisayar kodları kullanılarak oluşturulmuştur. İkinci bölümde, Düzce istasyonu kayıtları kullanılarak Düzce Depremi'nin simülasyonu gösterilmiş, değişik modellerin analiz sonuçları birbirleriyle karşılaştırılmış ve sonuçlar ortaya konmuştur.

Anahtar Kelimeler: Köprü, Viyadük, Bolu Viyadüğü, Otoyol, Modelleme, Bilgisayar Modellemesi, Sonlu Elemanlar, Deprem Simülasyonu, Düzce Depremi, Zaman Tanım Alanında Hesap, Dinamik Analiz

## ACKNOWLEDGEMENTS

I am very grateful to my M.Sc. thesis supervisor Assist. Prof. Dr. Ahmet Türer, who has shown me untiring patience and invaluable support in the completion of this thesis. Throughout my M.Sc. studying period, he was always helpful to me for the development of my thesis in a friendly manner even in his intensive working days.

I wish also thank and express my deep appreciation to my M.Sc. thesis co-supervisor Prof. Dr. Çetin Yılmaz for his support, encouragement, and the valuable knowledge I obtained from him.

Lastly, I am forever indebted to my parents, Mrs. Emel Türker and Mr. Şener Türker, who gave birth to me, raised me, supported me, taught me, and loved me. Moreover, they are the most important persons in my life, who encouraged me to start this Master of Science program. To them I dedicate this thesis.

## TABLE OF CONTENTS

## LIST OF TABLES

## LIST OF FIGURES

# CHAPTER 1

# INTRODUCTION

Bridges, which are called viaducts when they are long and high, sometimes need special considerations prior to modeling and simulation. In today's technology, it is easier to model structures by means of high technology computers and software compared to 5-10 years ago. However, special structures, such as in the case of this study, may require extra attention and even programming to a certain extent.

In this master's thesis study, both finite element modeling and earthquake simulation of a special type of viaduct are presented. Other than the finite element models, more simplistic frame type of models are also formed in order to understand and present the sensitivity and effect of using different modeling techniques.

In this thesis, four different 3-dimensional (3D) and two 2-dimensional (2D) computer models with different levels of complexity are presented and the seismic loading analysis results of different types of models are compared. For the analysis work, a general purpose commercially available structural analysis program SAP2000 [3] was used. In addition, some useful codes with Fortran 77 programming language [5] and Excel – Visual Basic macros were written in order to form the viaduct 3D geometrical coordinates and member connection information.

There are 5 additional chapters apart from this chapter throughout the thesis. In Chapter 2, the description of the problem including the reason why this study was carried out, and scope and objectives of the study are explained. In Chapter 3, general description of the bridge under focus is given. In Chapter 4, generated bridge computer models are explained in detail, and earthquake simulation and dynamic analysis considerations are presented. Chapter 5 includes the comparison of results (in the form of tables, graphs) and comments on the analysis results. Finally, the last chapter includes the summary and conclusions.

# CHAPTER 2

# DESCRIPTION OF THE PROBLEM, SCOPE AND OBJECTIVES

## 2.1 Description of the Problem

In 1999, two major earthquakes that occurred on the Northern Anatolian Fault (NAF) in Turkey had major impact on an important part, called as Bolu Mountain Pass, of Gümüşova-Gerede Highway Project. The first earthquake was Kocaeli-Gölcük Earthquake, which occurred on August 17, 1999 and lasted 45 seconds with a Richter Magnitude of 7.4. The second major earthquake was Bolu-Düzce Earthquake, which occurred on November 12, 1999 with a Richter Magnitude of 7.2.

Gümüşova-Gerede Highway Project is a part of Anatolian Motorway, which connects İstanbul and Ankara, two largest cities of Turkey (Figure 2.1). Bolu Mountain Pass is an important part of Gümüşova-Gerede Highway Project, which aims at meeting the demand of national and international transportation in Edirne-İstanbul-Ankara route, the main artery of Turkish highway network. This pass is the only part of the project which is under construction. When completed, the wholeness of the high quality highway and the continuity of safe traffic flow in the highway are going to be achieved. Bolu Mountain Pass, also known as

Stretch 2 of Gümüşova-Gerede Highway Project, is 25.6 km long and starts at 30th km of Gümüşova-Gerede Highway. It goes forward along Asarsuyu River towards east direction, passes over Bolu Mountain with a tunnel and ends at Yumrukaya location. The total cost of this part, Bolu Mountain Pass, of the project is US$ 570.5 million and the contractor for the project is a joint venture between an Italian company, Astaldi S.p.A and a Turkish company, Bayındır Construction.

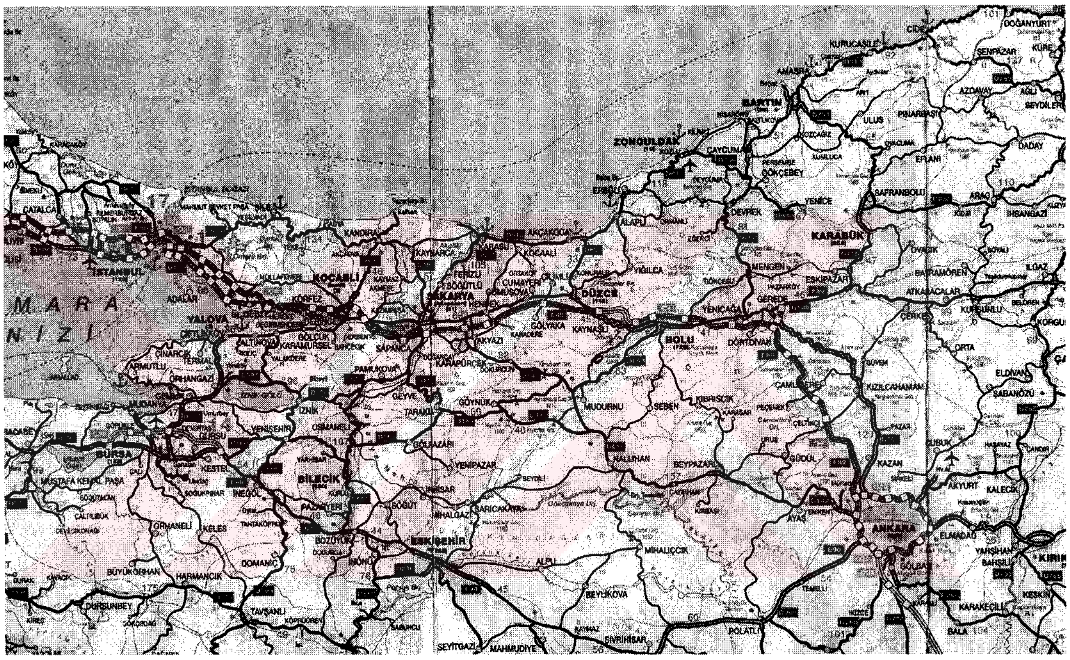


**Figure 2.1 North-Central Part of Turkey (Anatolian Motorway)**

Bolu Mountain Pass is composed of two viaducts and two long tunnels; and one of the two viaducts was almost completed in November 1999 when second major earthquake hit caused the viaduct to undergo extensive damage. This viaduct is called as "Bolu Viaduct" and is the main subject of this thesis study.

The viaduct was previously analyzed by Astaldi S.p.A, using 2-dimensional (2D) planar models in two perpendicular directions. This analysis work is explained in detail in Section 4.1.1.

Since the bridge underwent extensive damage during the major earthquakes, 3D computer modeling and 3D time history analysis of the bridge are considered to be necessary. The results of Astaldi's 2D models are also useful to be compared against different modeling techniques that are used in this thesis. Furthermore, the special characteristics of the bridge mentioned in Chapter 3 constitute an academically interesting subject and a real life application. Therefore, modeling the viaduct using different levels of complexity, earthquake simulation, and comparison of results are selected to be the main work load of this thesis study.

## 2.2 Scope and Objectives

The following are the main scope of this thesis study:

a) Construct six different analytical computer models to simulate the behavior of the bridge,
b) Write Fortran 77 routines and Excel – Visual Basic macros in order to generate the complicated 3D coordinates and member connection information to be used in the modeling efforts,
c) Calculate the sectional properties of discrete members that are used in each different model,

d) Simulate Düzce Earthquake, analyze generated models and find demands (internal member forces, pier top displacements)

e) Compare the results obtained from each different model and investigate the effect of model complexity on the results.

The following are the main objectives of this thesis study:

a) To find out internal forces at pier bases and to find out the displacements (drifts) at pier caps,

b) To compare the results from different models constructed for the same bridge and the results from existing Astaldi's 2D Model,

c) To investigate (indirectly) whether Astaldi's 2D model successfully simulates the bridge behavior and response,

d) To investigate the sensitivity of the calculated internal forces to using different modeling types, levels of complexity, and total number of members and degrees of freedom.

# CHAPTER 3

# BRIDGE DESCRIPTION

## 3.1 Location and Seismological Features of the Region

Bolu Mountain is located in Bolu, which is a city in the north-central part of Turkey. The main subject of the thesis, Bolu Viaduct, is located next to the Asarsuyu River around Bolu Mountain. The general view of the viaduct is given in Figure 3.1.

The route of Anatolian Motorway at Gümüşova-Gerede Section where Bolu Viaduct is being constructed was determined in the years 1988-89. North Anatolian Fault Line, which extends along approximately 1500 km in east-west direction, is passing through this region. Although the route was tried to be as far away from the fault lines as possible, some parts had to pass over fault lines due to economical reasons (Figure 3.2).

In Kocaeli-Gölcük Earthquake, Düzce station is 107 km away from the epicenter; however, it was within 11 km from the fault rupture. Although there are some minor effects of Kocaeli-Gölcük Earthquake, it is Bolu-Düzce Earthquake which caused Bolu Viaduct to undergo extensive damage. The epicenter of Bolu-

Düzce Earthquake was located about 6 km south of Düzce and the fault crossed Bolu Viaduct at an angle of 20-30 degrees with the viaduct axis. A right lateral offset of approximately 2.0-2.5 meters occurred (Figure 3.3). The earthquake caused substantial shifts between the supports and the pier. Some of the piers near the fault line rotated by 10-15 degrees.

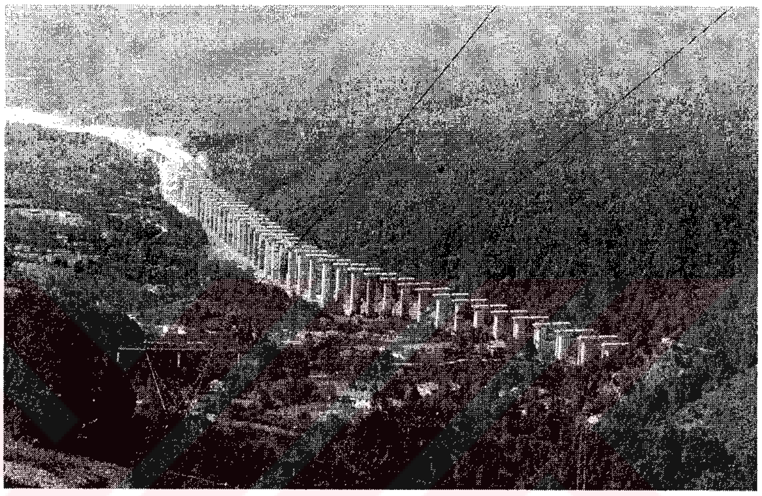

**(a)**

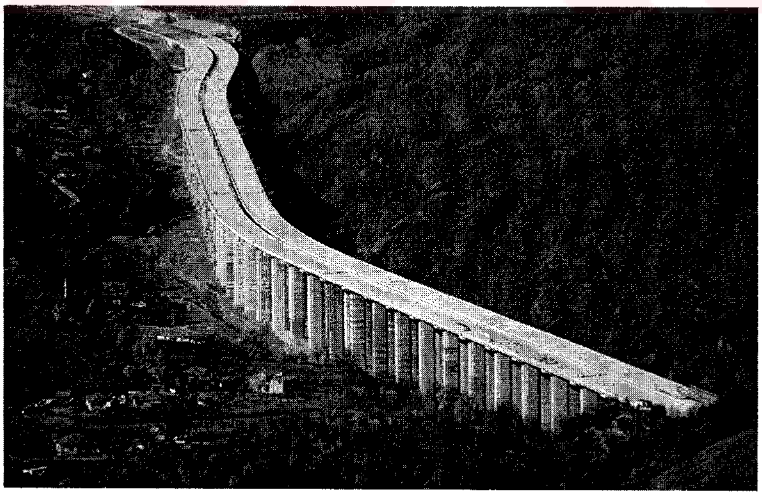

**(b)**

**Figure 3.1 General View of Bolu Viaduct**

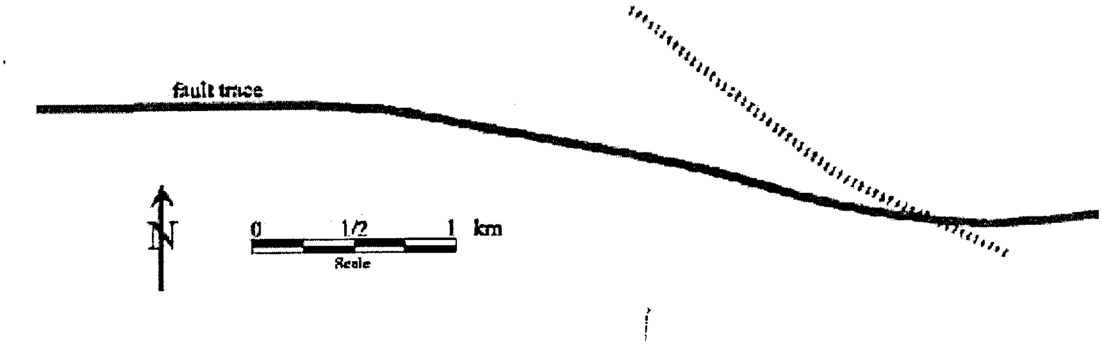


**Figure 3.2 Bolu Viaduct and Fault Trace of 12 November 1999 Düzce Earthquake**

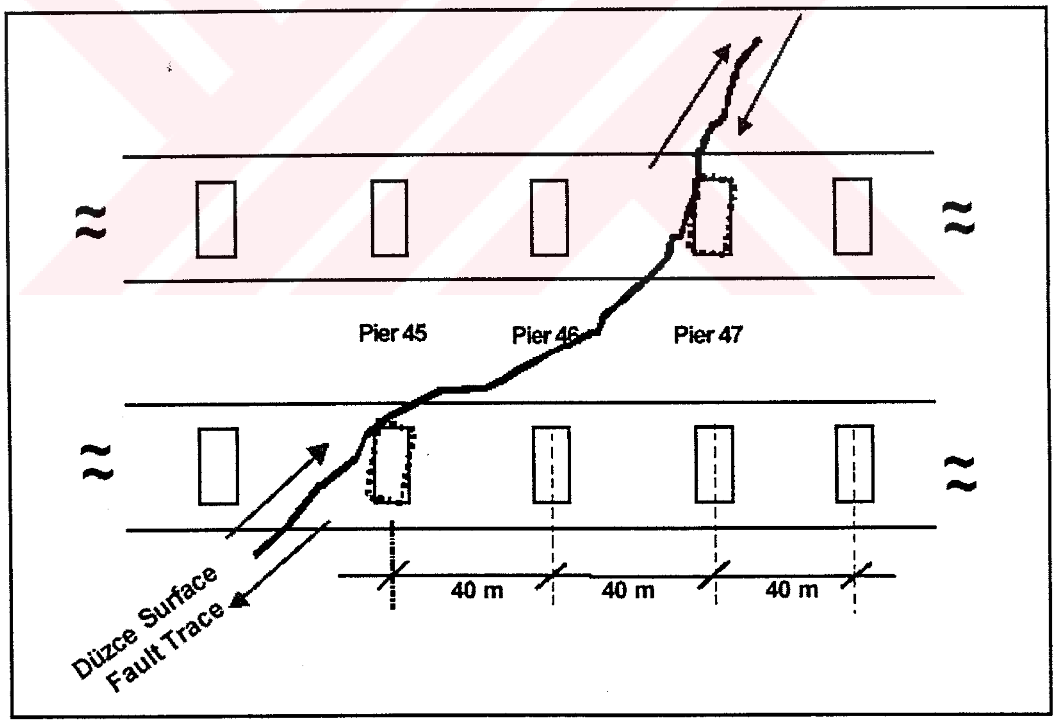


**Figure 3.3 Fault Trace and Fault Rupture in Bolu Viaduct**

### 3.2 Geometrical and Structural Features

The highway is curved in plan, has a vertical slope of approximately 4% towards İstanbul direction and consists of two parallel bridges, each having a separate traffic direction. The number of spans is 59 and 58 in left and right bridges, respectively. The total length of the bridge is 2313.03 meters and 2273.75 meters for the left and right carriage ways, respectively.

There are tall reinforced concrete piers with large and nearly rectangular hollow cross sections (Figure 3.4 and 3.5). Total number of piers is 58 for the left bridge and 57 for the right bridge. Piers are numbered starting from Düzce end towards Bolu direction from 1 to 58 and 1 to 57 for the left and right bridges, respectively. Piers lengths vary from 10 m to 49 m.

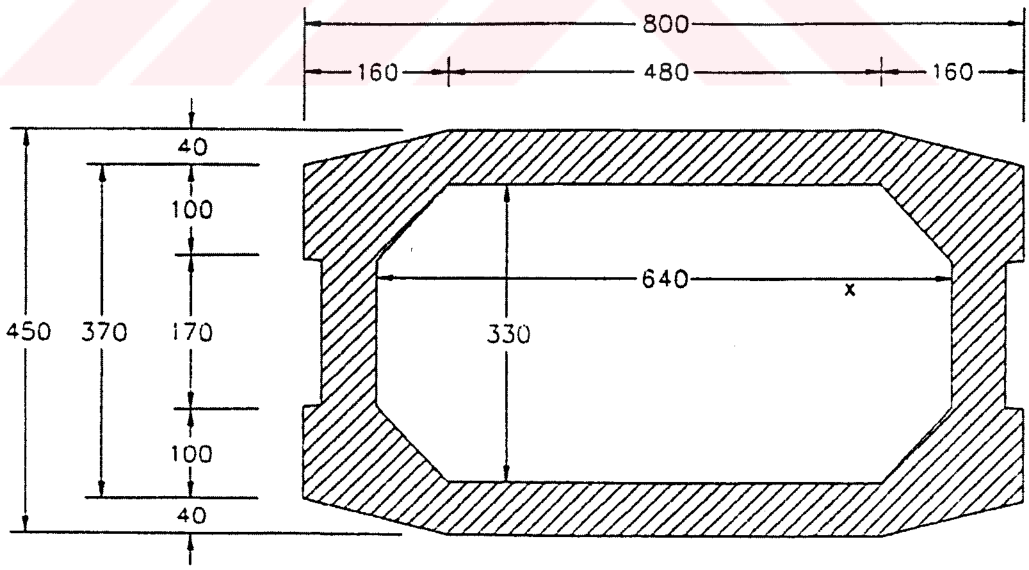


**Figure 3.4 Cross Section of a Typical Pier (dimensions in cm)**

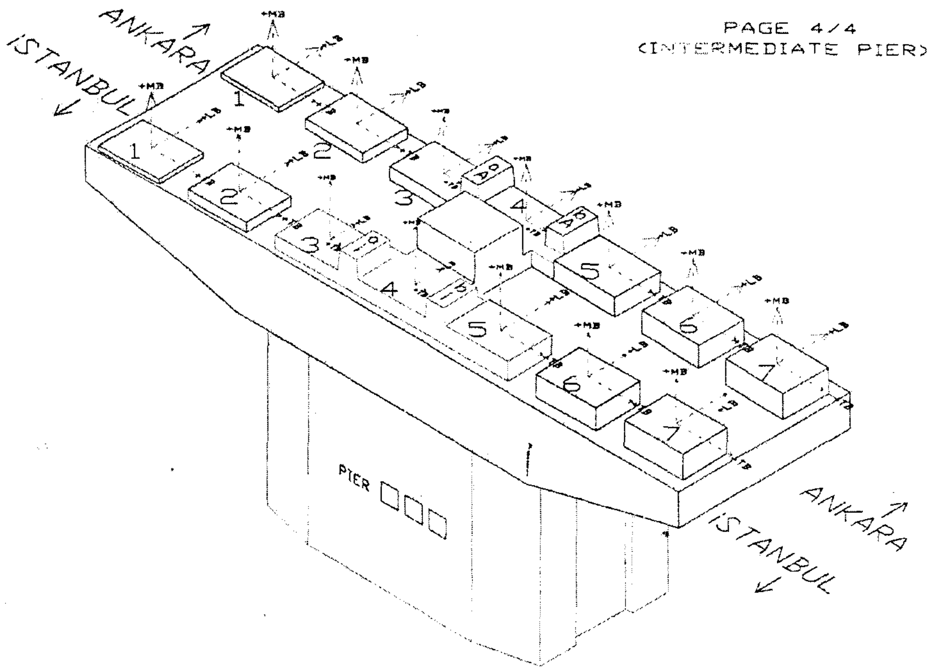


**Figure 3.5 Isometric View from a Typical Pier**

All piers rest on massive and monolithic column footings supported on 12 cast in drilled hole friction piles with a diameter of 1.8 m (Figure 3.6). The depth of the piles ranges from 20 m to 30 m. The typical size of the footing is 3 m deep, 18.7 m long in the bridge longitudinal direction and 16 m wide in the bridge transverse direction (Figure 3.7).

Pier spacing is 39.2 meters from center to center and the superstructure is made continuous over 10 spans of the section by means of 1.5 m long and 24 cm thick span connecting slabs. At the end piers of these 392 m long segments, suitable expansion joints are provided to the deck, which terminate with longitudinal cantilevers. The longitudinal section from Pier 10 to Pier 20 is given in Figure 3.8.

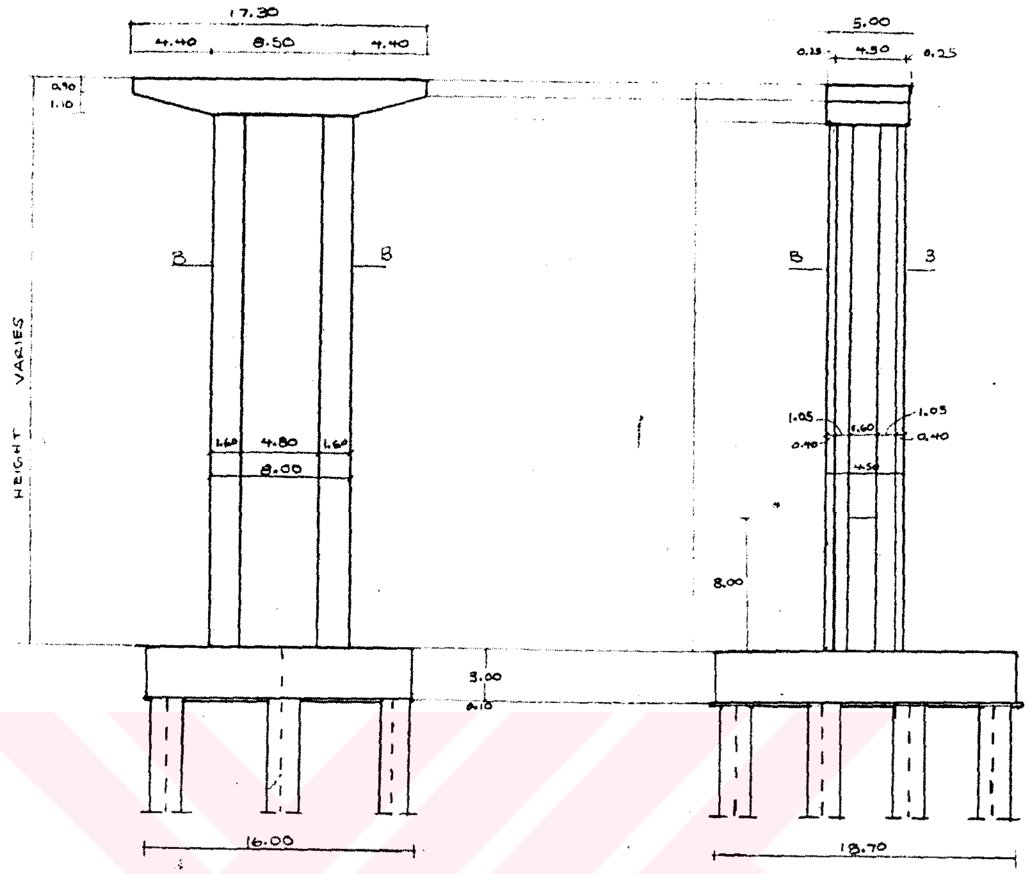


**Figure 3.6 Typical Pier Elevation (dimensions in meter)**

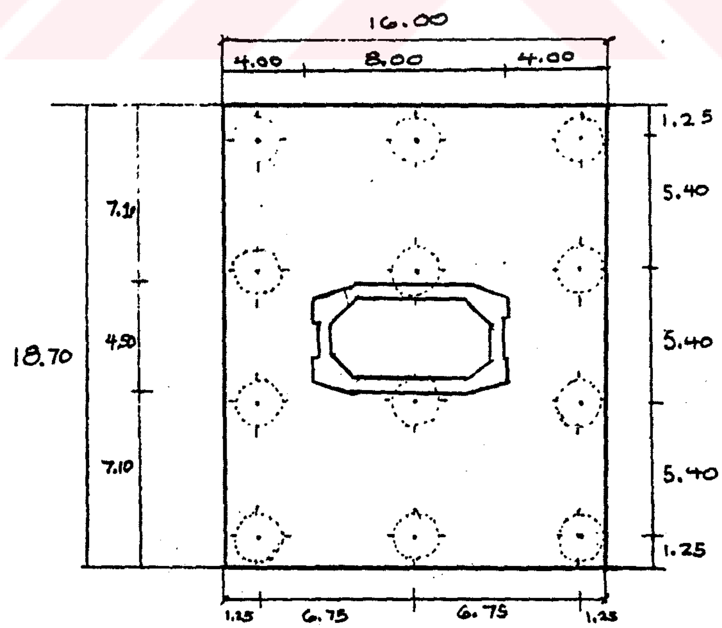


**Figure 3.7 Top View of Typical Pile Section (dimensions in meter)**

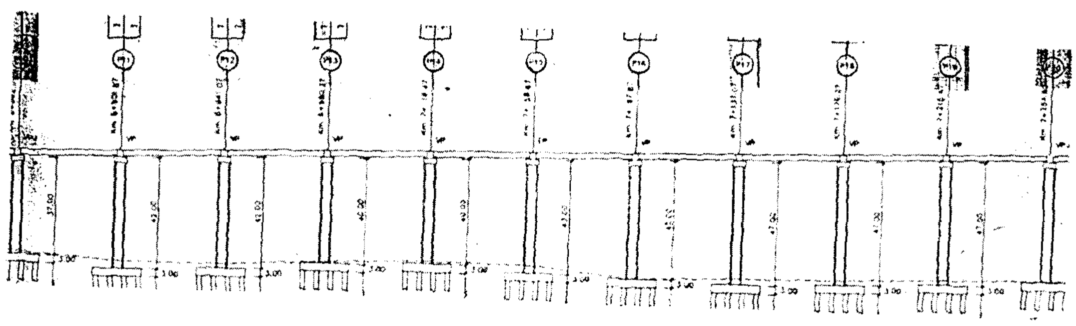

**Figure 3.8 Longitudinal Section between Pier 10 and Pier 20**

The superstructure is composed of seven prefabricated prestressed girders connected by a continuous cast-in-place slab of 24 cm thickness over the girders and of 54 cm thickness between the girders, as shown in Figure 3.9. The girders are 36.8 m long and simply supported at their ends. Typical cross section of the girders is shown in Figure 3.10.

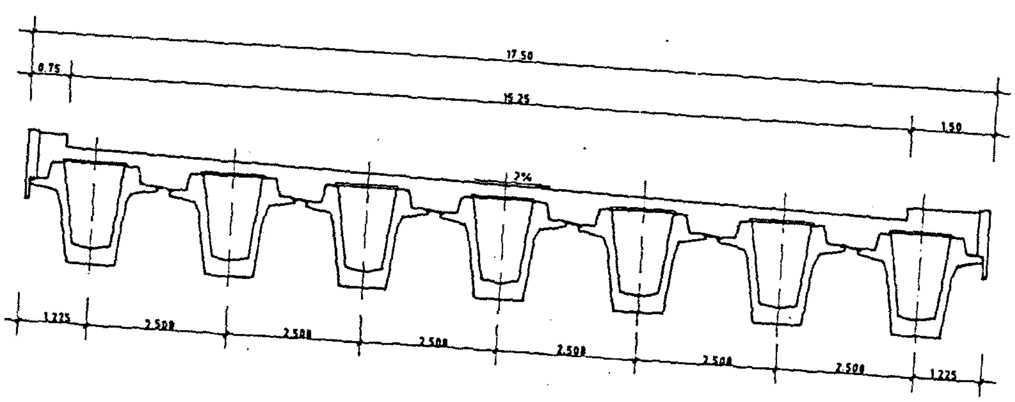


**Figure 3.9 Typical Cross Section of the Deck (dimensions in meter)**

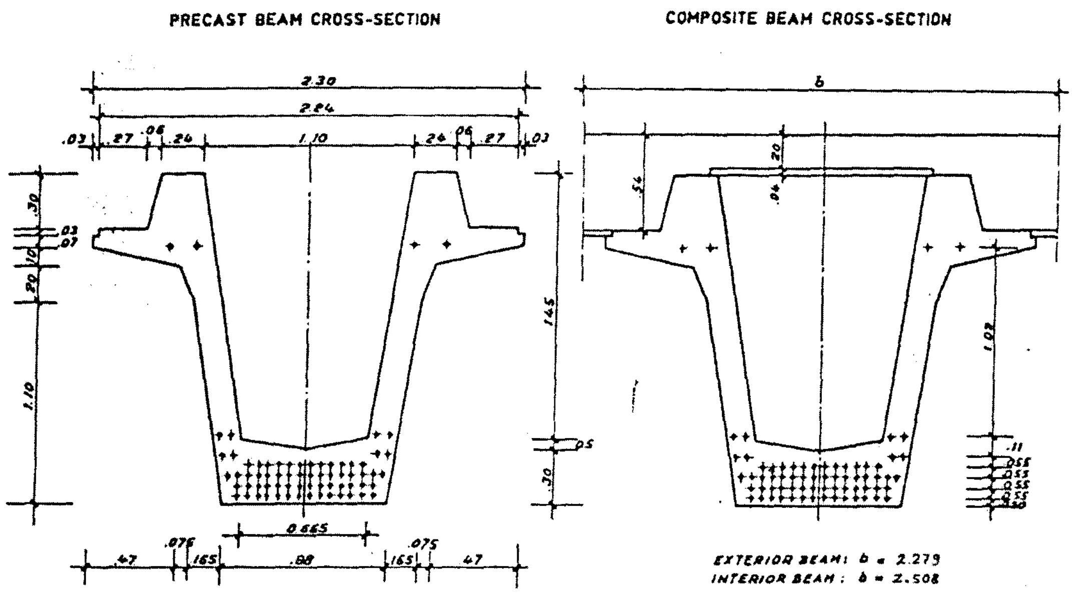


**Figure 3.10 Typical Cross Section of the Girders (dimensions in meter)**

### 3.3 Energy Dissipating Units

The deck is continuous over 10 spans and all the beams are simply supported on all piers by multi-directional free sliding bearings (Figure 3.11). Horizontal movements due to earthquake loads are transferred to the piers by means of Energy Dissipating Units (EDU) (Figure 3.12) which are placed between the piers and the deck.

The central supports of the continuous 10-span segments, considered as fixed point of the 10-span segment for thermal expansion, are provided with energy dissipating device of EP Type, which is a multidirectional crescent moon-type steel energy dissipating unit (Figure 3.13). Other supports of the 10-span segments are provided with Viscous Connecting Devices (VCD), allowing longitudinal displacements of the deck with respect to the pier; the whole device is called as VP (Figure 3.14). At the expansion joints, VPJ Type of EDU is placed. This device is designed in order to transfer the transversal earthquake force equally to the adjoining slabs and the longitudinal earthquake force to only the span it is connected. In Figure 3.15, the locations of these devices are shown roughly.

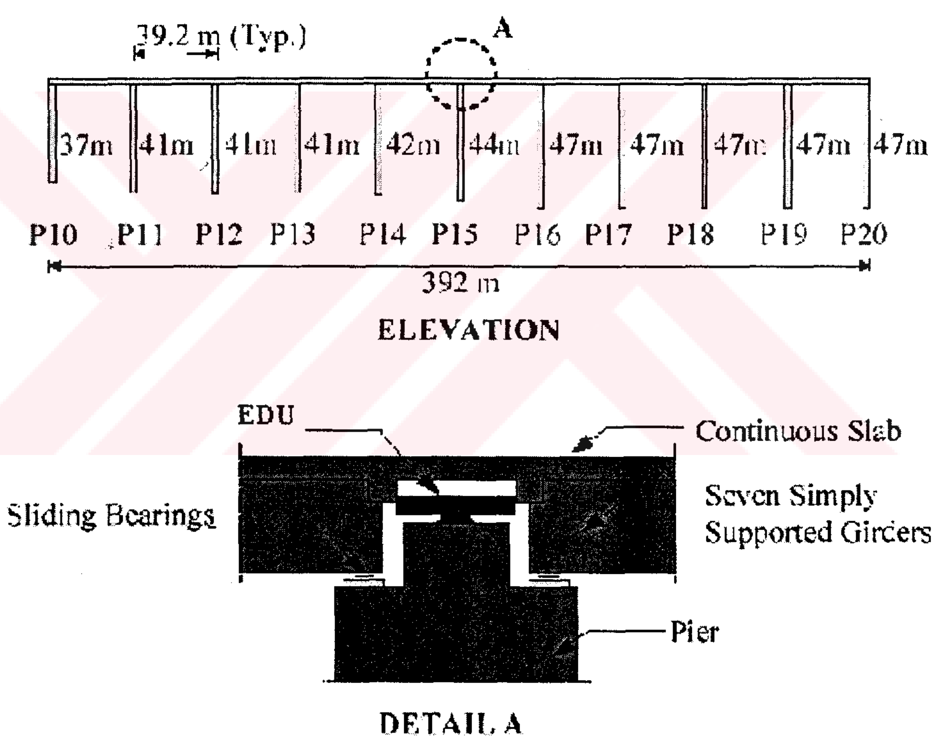


**Figure 3.11 Elevation of Viaduct at Piers**

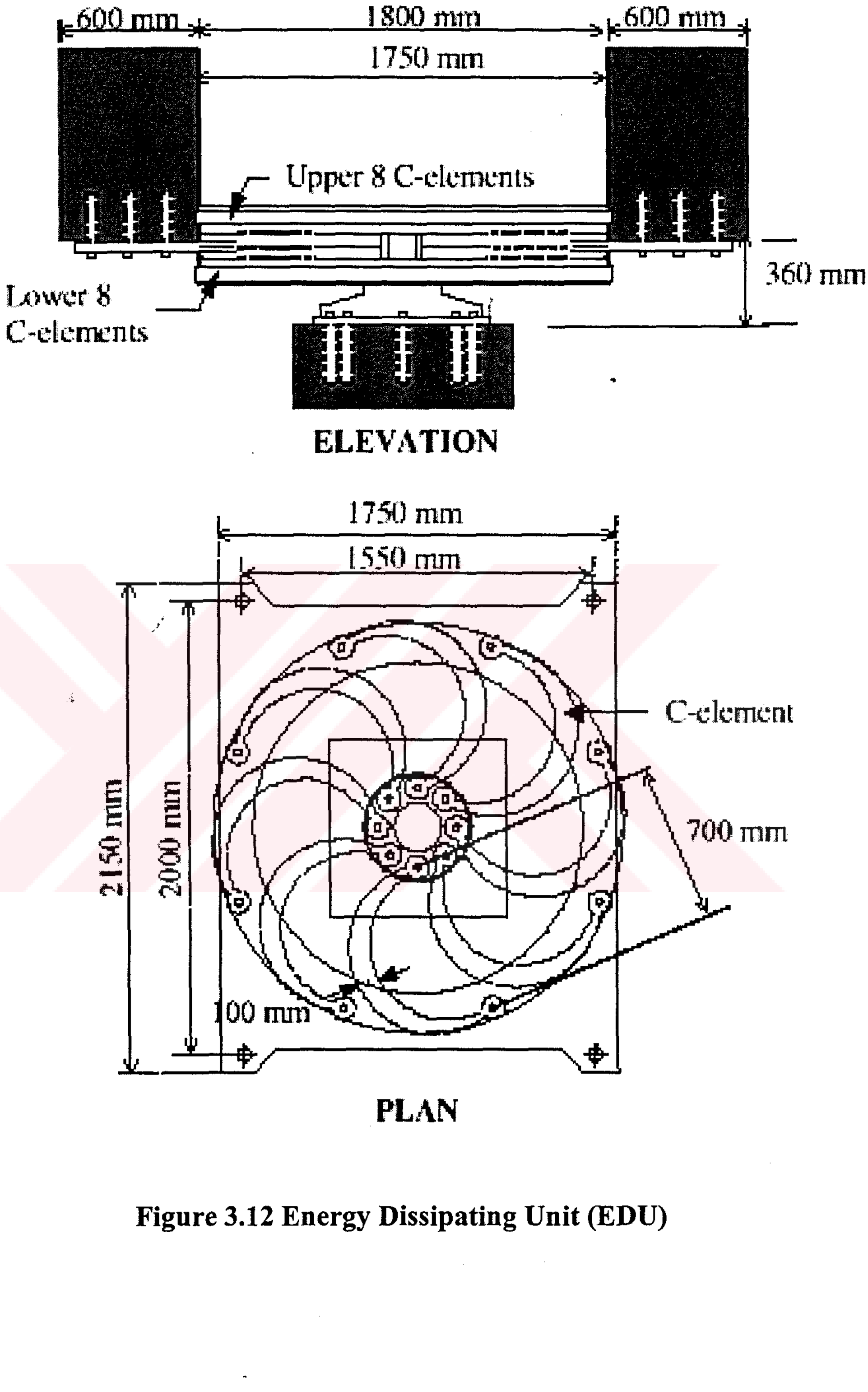


**Figure 3.12 Energy Dissipating Unit (EDU)**

**Figure 3.13 Multidirectional EP Device in Neutral Position and at Maximum Deflection**

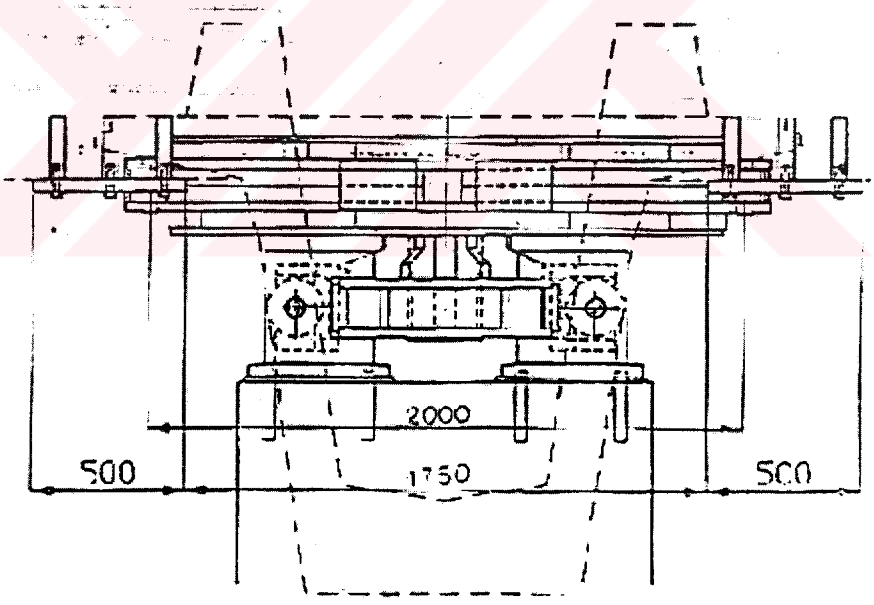


**Figure 3.14 VP Device (dimensions in mm)**

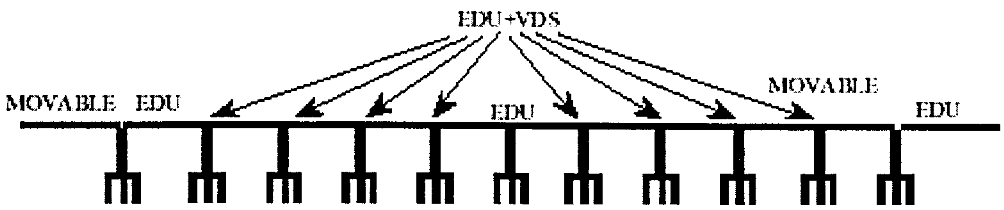


**Figure 3.15 Locations of EDU Devices**

The restraining system described above allows for free longitudinal movements of the superstructure due to creep, shrinkage and temperature (for which only the central pier is fixed) while preventing sudden relative displacements as those induced by dynamic forces. Under seismic loading condition, EDU's will start to function, providing an elasto-plastic connection of the superstructure to the piers [12].

Concrete shear blocks are also provided as seismic restrainers to the deck in order to limit the relative displacements between the pier and the deck to an upper value equal to the ultimate displacement of the EDU. Positive linkages composed of a number of cable restrainers are also provided at expansion joints to prevent span dropping due to unexpected larger displacements [12].

### 3.4 Structural Importance of the Bridge

As described in Section 3.2, Bolu Viaduct has special structural characteristics such as the total length of approximately 2.4 km, spans up to 40 m and pier heights up to 50 m. Moreover, the region on which the viaduct is located has very important seismological characteristics. Indeed, an active fault line passes through the viaduct as explained in Section 3.1, and it underwent extensive damage during the November 12,1999 Düzce earthquake. Energy Dissipating Units (EDU), as explained in Section 3.2, are of great importance in case of an earthquake.

# CHAPTER 4

# MODELING AND ANALYSIS

Modeling work can be divided into three main parts; (a) construction of the model geometry (nodal coordinates and member connection information), (b) definition of the section properties of the members and proper member angle, and (c) application of the seismic loading and analysis.

In this study, only right bridge is modeled since both bridges are similar. The modeling and analysis are performed by using SAP2000 Structural Analysis Program [3]. Shell and frame type of elements are used in the models. The first model, which is described in Section 4.1.3, is the main model and it is decided to be the best model to simulate actual behavior of the bridge among all generated models. The other models, Model 2, Model 3 and Model 4, are simpler than Model 1 and they are 3 dimensional models. Furthermore, two 2-dimensional models, Model 5 and Model 6 are constructed. All the models other than Model 1 are constructed in order to understand the effect of complexity in modeling works. In the main model, Model 1, the deck and box girders are modeled using shell elements, and piers are modeled using frame elements. The other models, especially Model 3 and Model 4, are almost composed of only frame type of elements. Furthermore, in all models rigid link elements are used between piers and the deck in order to simulate the non linear behavior of EDUs explained in Section 3.3.

Each model is also divided into two cases: Case (a) and Case (b). In case (a), the central piers for 10-span segments are fixed and all other piers are free to move in longitudinal direction. However, this case does not reflect the actual behavior of the bridge in case of an earthquake. There are "Lock-up Devices" on each pier cap and these devices restrain the movement of the piers during a strong excitation like in the case of an earthquake. Therefore, all models were run by taking this feature into account, and this case is called as Case (b).

It should be kept in mind that Model 1, 2, 3, 4, 5 and 6 in this study were run for two cases. The only difference is the restraints in pier deck connections (See Section 4.6). In Figure 4.1, the models are summarized.

### 4.1 Definition of Models

As mentioned in Section 2.1, a 2D analysis for Bolu Viaduct had already been carried out by Astaldi S.p.A. To understand whether Astaldi's 2D model successfully simulates the bridge behavior and response, it is intended to compare this existing model with the models generated in this thesis study. A general information related with the previous work done about bridge is given in Section 4.1.1.

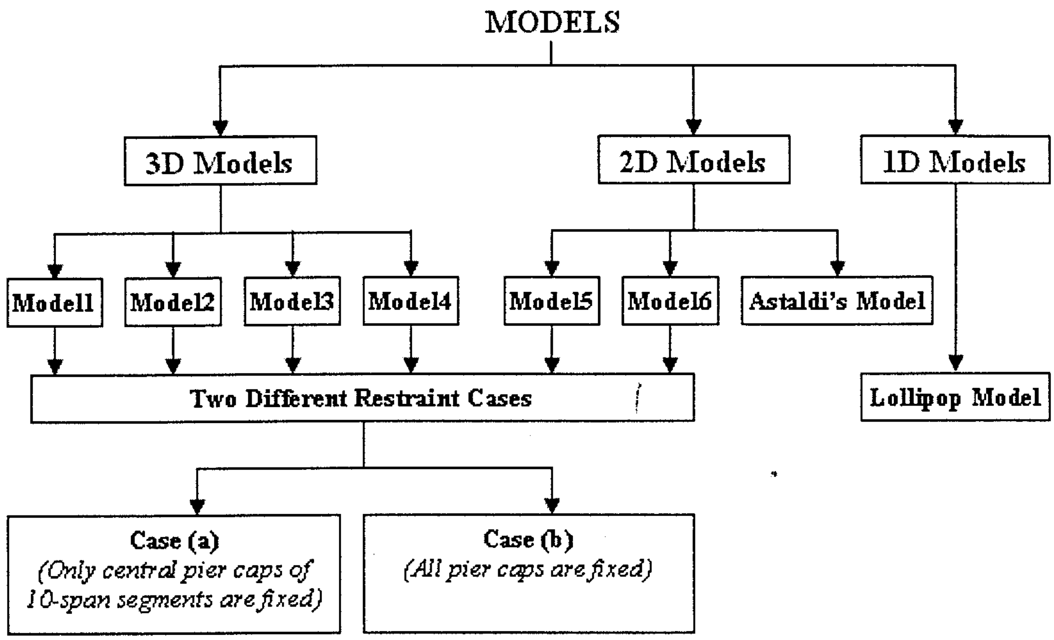


**Figure 4.1 Overlook to the Models Used in This Thesis Study**

In the scope of this thesis study, seven models with different complexity levels were planned to be constructed. However, the most complex model (largest of them all) had to be left out of the analysis, since the model became too large to be analyzed by the current personal computers technology and capacity. The models used in this study are listed below and briefly explained in the following sections.

"Most Complex Model" (Left out of the analysis)

Model 1, "3D Multiple Box Deck Model"

Model 2, "3D Flat Deck Model"

Model 3, "3D Frame Grid Model"

Model 4, "3D Lumped Beam Model"

Model 5, "2D Lumped Beam Model"

Model 6, "2D 10-Span Segment Model"

### *4.1.1 Two Dimensional Astaldi's Model*

Astaldi S.p.A., the main contractor of Gümüşova-Gerede Highway Project, analyzed the bridge using a computer program "ADINA" for seismic loading. Due to different behaviors of deck and supports, two different models were generated and analyzed for longitudinal and transverse earthquake loading cases for each continuous 10 spans. In Figure 4.2, the longitudinal model used between piers 10 and 20 is shown with the joint numbers used. As seen from the figure, last span is free to move in longitudinal direction due to boundary conditions. The transverse model is composed of 11 piers and 10 spans, and all spans are connected to the pier by Energy Dissipating Units (EDU). The continuity in transverse direction at the ends of a span in the transverse model is taken into account by using half of the pier and soil stiffness and including proper mass properties [12].

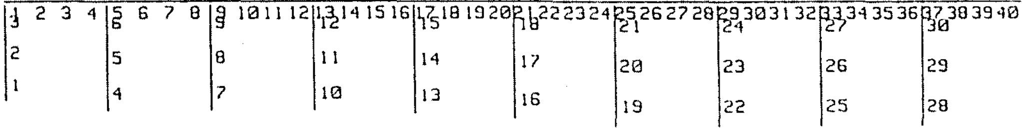


**Figure 4.2 Finite Element Model for Longitudinal Seismic Loading**

In both models, piers and the deck are divided into 3 and 4 beam elements, respectively. Pier top and the deck are connected by using rigid link elements. Pier and deck mass properties are assigned as distributed mass, and additional concentrated mass is added at the pier top. For modeling of Energy Dissipating Units, truss elements are used with elasto-plastic materials. The material properties used in the models are given in Table 4.1.

**Table 4.1 Properties of Structural Members Used in Astaldi's Model**

| Properties | Unit | Value |
|---|---|---|
| **PIERS:** | | |
| Cross-sectional area | $m^2$ | 14.30 |
| Moment of inertia in longitudinal direction | $m^4$ | 38.30 |
| Moment of inertia in transverse direction | $m^4$ | 106.30 |
| Modulus of Elasticity | $kN/m^2$ | 23,600,000.00 |
| Density | $kg/m^3$ | 2,502.00 |
| **DECK:** | | |
| Cross-sectional area | $m^2$ | 12.88 |
| Horizontal plane inertia | $m^4$ | 314.00 |
| Modulus of Elasticity | $kN/m^2$ | 31,200,000.00 |
| Density | $kg/m^3$ | 2,867.00 |
| **Concentrated mass at the each pier top** | kg | 428,135.00 |
| **EDU:** | | |
| Cross-sectional area | $m^2$ | 1.00 |
| Modulus of Elasticity | $kN/m^2$ | 60,000 |
| Yield stress | $kN/m^2$ | 1,480 |
| Ultimate Stress | $kN/m^2$ | 1,829 |
| *(In addition, kinematic hardening and Von Mises yield condition are utilized)* | | |

For the seismic analysis, seven different accelerograms matching AASHTO spectrum are generated by a computer program SIMQKE. A generated accelerogram and a comparison of the response spectrum for the acceleration and the AASHTO spectrum are shown in Figure 4.3 and Figure 4.4, respectively.

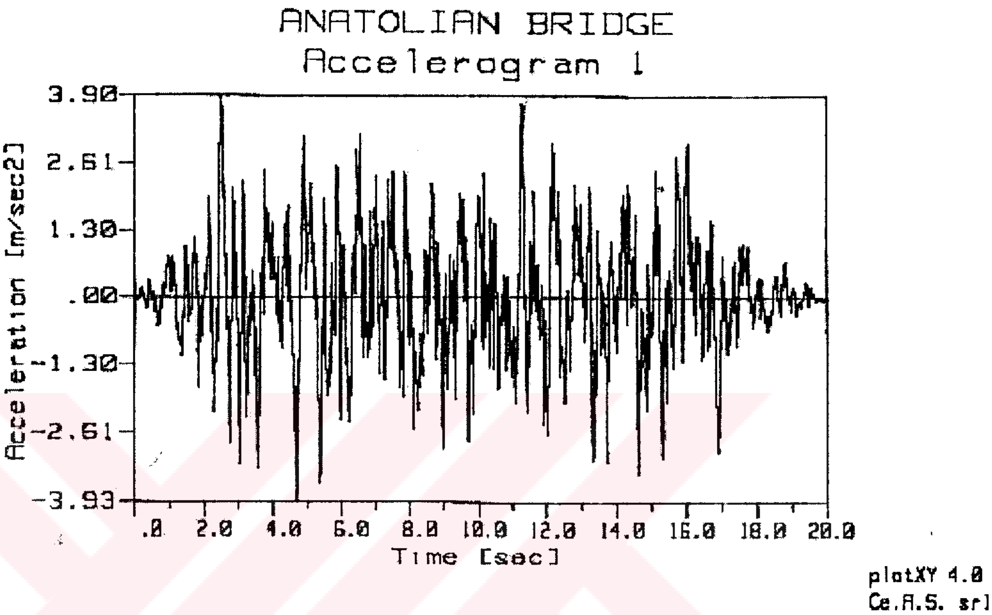


**Figure 4.3 SIMQKE Generated Accelerogram**

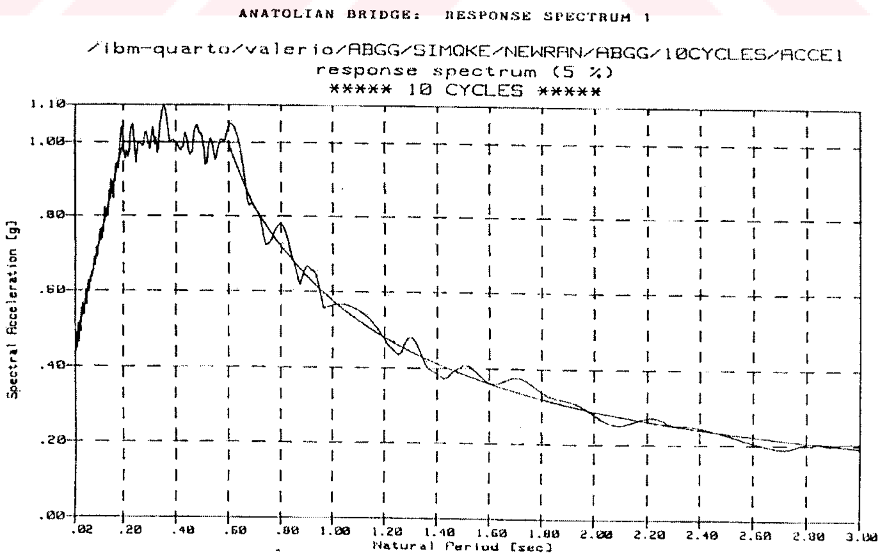


**Figure 4.4 AASHTO and Generated Acceleration Spectrum Comparison**

The finite element model has been solved fourteen times, seven in the longitudinal direction and seven in the transverse direction. ADINA computer code (Version 6.0.3) is used. Results are reported both in graphical form and in a listed form. In a similar manner the maximum displacements are provided in tabular or graphical form. (See Chapter 5 for the results.)

#### *4.1.2 "Most Complex Model"*

Although decided to be modeled at the beginning of the thesis study, "Most Complex Model" was left out of the analysis because of being too large to be analyzed by the current personal computers technology and capacity. It should not be ignored that this model, if generated and analyzed, is most probably the best one to simulate the actual behavior of the bridge during earthquake. However, there is also another point that the more complex the model the larger mathematical errors you will get. Therefore, it is not certain that Most Complex Model will simulate the behavior of the bridge under earthquake loading best.

The main complexity for Most Complex Model is coming from the mesh size of the deck in the model. Shell element size of approximately 0.40 x 0.60 m was used and thus, the number of degrees of freedom became over 500,000, which is very large. A view of finite element mesh sample of the deck, generated for Most Complex Model is shown in Figure 4.5.

**Figure 4.5 Finite Element Mesh Sample of the Deck (Most Complex Model)**

### *4.1.3 Model 1: "3D Multiple Box Deck Model"*

"3D Multiple Box Deck Model", as its name implies, is the most complicated model among analyzed ones since 3D geometry is used together with a large number of members in an attempt to model most of the major members of the bridge.

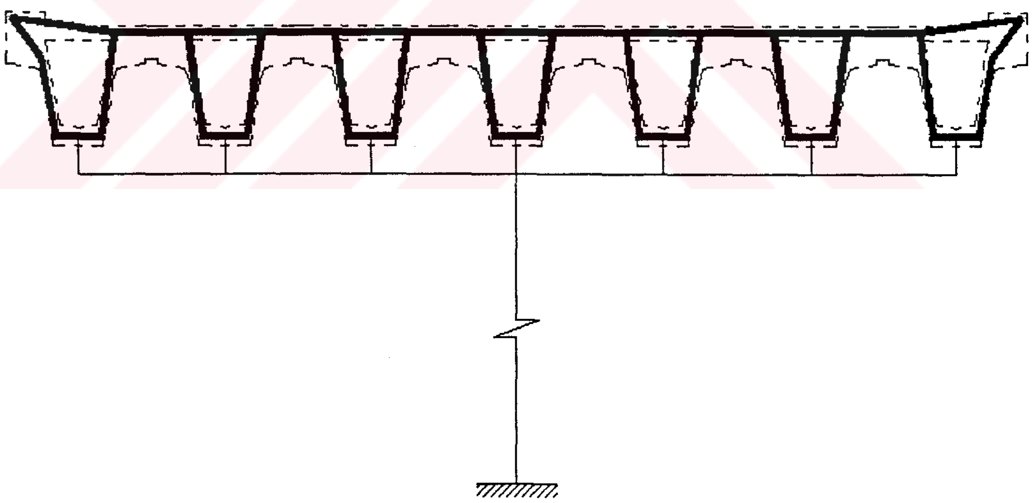

**Figure 4.6 Typical Cross Section of Model 1**

Both shell elements and frame elements are used in the model. Piers, as same in all models, are composed of frame elements. For deck, shell elements of various thicknesses with an average mesh size of 2 x 6 m are used. Total number of degrees of freedom is 140,196 (Figure 4.6).

### *4.1.4 Model 2: "3D Flat Deck Model"*

"3D Flat Deck Model" is composed of both shell elements and frame elements. Piers are composed of frame elements. For deck, shell elements and frame elements are used. Top slab layer is separated from the seven bottom wedges and defined by shell elements with an average mesh size of 2 x 6 m. The bottom wedges are lumped at the neutral axis of their own. Rigid links are used to connect the upper shell layer to these seven bottom beams. For the connection of these seven beams to the pier, again rigid links are used. Total number of degrees of freedom is 98,208 (Figure 4.7).

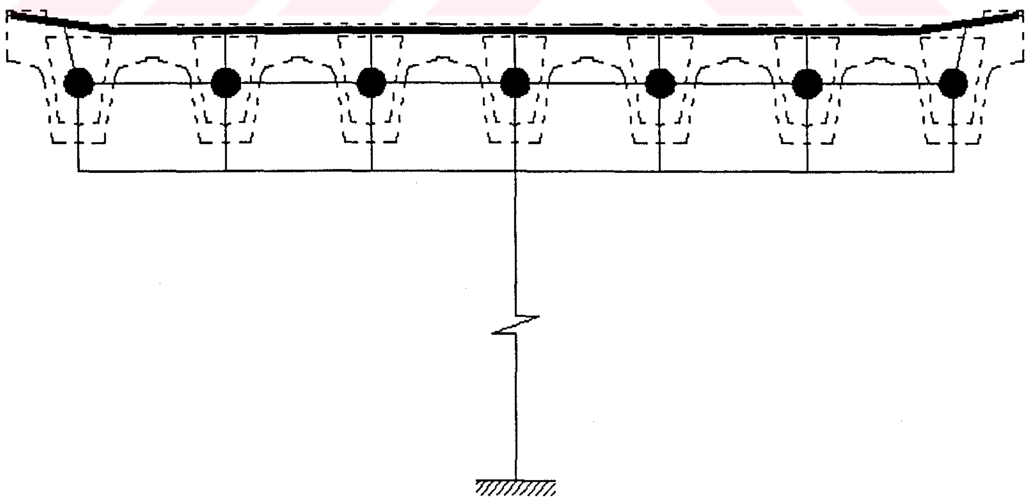

**Figure 4.7 Typical Cross Section of Model 2**

### *4.1.5 Model 3: "3D Frame Grid Model"*

"3D Frame Grid Model", as its name implies, has a frame grid deck. Piers are again same with other models and composed of frame elements. Different from Model 2, bottom wedges on the deck are taken together with the upper slab layer of a determined effective width and lumped at the neutral axis of the wedge with upper slab portion. Rigid links are used to connect these seven beams to the pier. Total number of degrees of freedom is 33,948 (Figure 4.8).

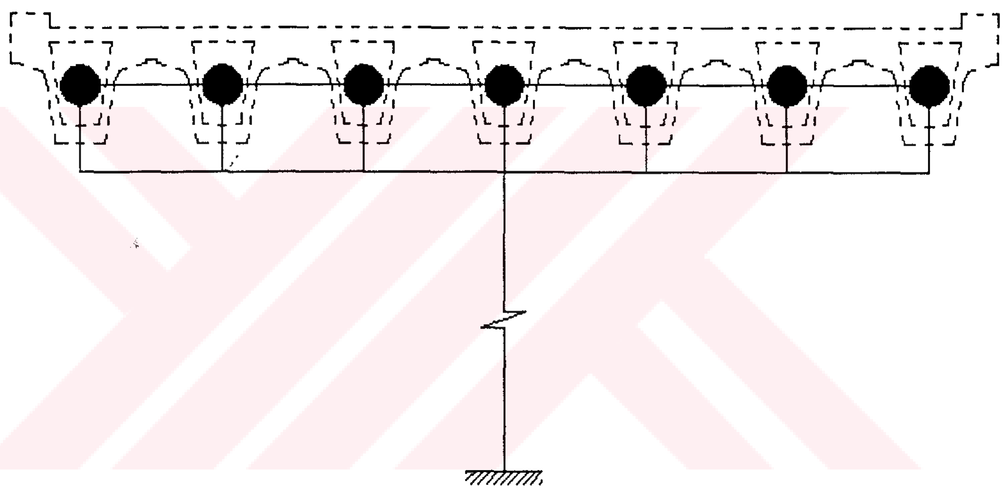

**Figure 4.8 Typical Cross Section of Model 3**

### *4.1.6 Model 4: "3D Lumped Beam Model"*

"3D Lumped Beam Model" is the simplest model and composed of only frame type of elements. Whole deck section of the bridge is lumped together at one point and connected to the pier by rigid links. Total number of degrees of freedom is 7,488 (Figure 4.9).

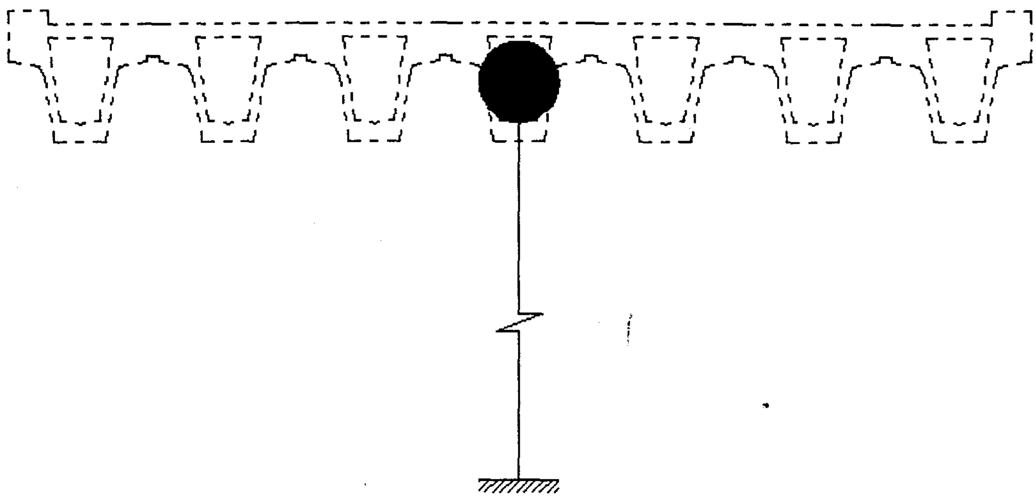

**Figure 4.9 Typical Cross Section of Model 4, Model 5, Model 6 and Lollipop Model**

### *4.1.7 Model 5: "2D Lumped Beam Model"*

This model is a two dimensional version of Model 4 (Figure 4.9). The curvature in plan is not included and the model is constructed on global X-Z plane (East-Vertical directions) only.

### *4.1.8 Model 6: "2D 10-Span Segment Model"*

This model is nothing but only a portion of Model 5 (Figure 4.9). In this model, the portion including the piers between Pier 20 and Pier 30 is modeled. Total number of degrees of freedom is 726 (Figure 4.9)

### *4.1.9 Lollipop Model*

This model is a very simple, lollipop like model and formed in order to compare correctness of the results of case (a) which was previously explained at the beginning of this chapter.

In this model, a 10-span segment of the bridge is lumped at a single point. This point represents the deck of 10 spans. Under this special joint, the same properties of a single pier are defined. Actually this is Pier 25 and it is a central fixed pier in case (a) (Figure 4.9).

## 4.2 Assumptions

On performing the modeling work, some assumptions are made in order to stay in the scope of the thesis study and to achieve the main objectives. These assumptions are listed in the following.

a) All models are analyzed for 1.0 DL + 1.0 EQ loading case. Live load is not taken into account. The study targets to see differences in pier demands (forces, moments, and displacements). No design related studies are aimed.
b) The support conditions of piers are idealized as fixed in all directions. (There are 12 piles located under each footing. The primary concern of this study is to evaluate the behavior of the superstructure.)
c) During an earthquake, as explained in Section 3.3, the force transfer between the deck and the piers is achieved by means of Energy

Dissipating Units (EDU) located between the piers and the deck. In this study the nonlinear behavior of the EDUs is not considered. Energy dissipating units (EDU) are assumed to be rigid. They are simulated by rigid links and all the forces occurred on the beams are assumed to be transferred to the piers. Their proper elastic (and plastic) behavior is left outside the scope of this study.

d) Linear type of analyses is performed for the generated models. The nonlinear analysis is left outside the scope of this thesis.

e) For simplicity, some parts of the pier and deck sections are simplified. (For example, the section of transverse beam at the top of piers is taken as rectangular although it is not exactly.)

## 4.3 Formation of the Geometry of Models

### *4.3.1 Formation of Pier Geometry*

Pier coordinates are taken from the data generated by Astaldi S.p.A, and these coordinates are used for the definition of pier joints. For all piers, specific pier reference points are defined. This point is the center of the rectangle formed with the points 15, 16, 27 and 28 shown in Figure 4.10. These reference points, are also used for the formation of deck geometry (See section 4.3.2). All piers are divided into 10 elements and the coordinates of these points are generated by using the pier reference points and the heights of the piers by the help of prepared Microsoft Excel – Visual Basic macros.

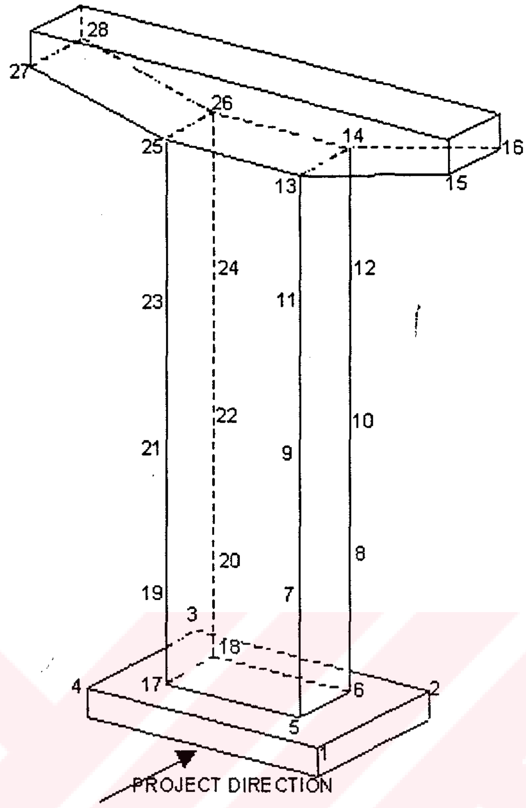


**Figure 4.10 Pier Joint Numbers Whose Coordinates Are Provided By Astaldi**

*4.3.2 Formation of Deck Geom etry*

The most difficult and time consuming part of the modeling work is the formation of the deck geometry, and mostly the formation of deck nodal coordinates, because the overall bridge length is approximately 2.4 kilometers, the bridge is curved or straight at different portions, and has a transverse and longitudinal variable slope. In order to overcome modeling related difficulties, a code, called as MESH, was written by using Fortran 77 programming language for mesh generation purpose. The program code of MESH is presented in Appendix A.

In MESH, a SAP90 based input file is generated as a program output file which is imported into SAP2000 [3] afterwards. There are two input files which were generated before running the main routine, MESH. One of them, which was named as REFJOINTS.txt, consists both the reference joint coordinates, which are x-, y- and z-coordinates of piers, and curves along highway. The input file REFJOINTS.txt has 57 rows corresponding to 57 piers, and each row has 8 number entries. First number is the pier number, and the following 6 numbers are x-, y- and z-coordinates of two selected points on the piers in an order. These two points are the mid point of joints 15 and 16 and mid point of joints 27 and 28 shown in Figure 4.10, respectively. Last number in file REFJOINTS.txt shows the curves of the highway on the related pier: 0 is for straight, 1 for curve to the right, 2 for curve to the left.

The second input file was named as D.txt and includes the relative distances of the points on the deck section shown in Figure 4.11 with respect to the upper middle point of the deck. As shown in Figure 4.11, there are 30 nodes on the deck of Model 1, and therefore, the number of rows in D.txt is 30. There are 3 number entries in each row. First number is the node number. Second and third numbers are the relative distances in x- and y- directions explained above, respectively.

There are three main jobs of MESH. First, it generates the nodal points of the deck using reference joints and relative distances, at the pier locations. Second, it modifies the coordinates by taking 4% curve slopes into account. Third, it generates the deck nodal points between piers.

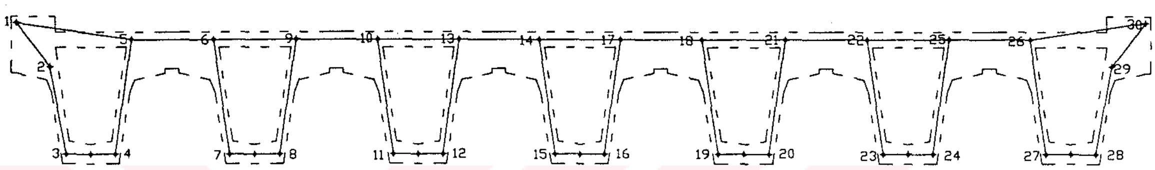


**Figure 4.11 Joint Numbers Assigned For Model 1**

After running MESH, an output file with the name COORD.txt is formed, which is the "JOINTS" input data block in SAP90 format. After adding other necessary data into this SAP90 input file, it is imported into SAP2000.

### 4.4 Section Properties

In SAP2000, cross-sectional properties are calculated automatically for defined common shapes. Since the deck is composed of shell elements in Model 1, it is easy to define deck section for this model. In the other models, however, cross-sectional properties are to be calculated, since some of or whole deck is lumped at some points, as explained in Section 4.1.4, 4.1.5 and 4.1.6, or the deck elements have not common geometrical shapes such as pier cross sections.

For that reason, the sections of deck elements for Model 2, Model 3, Model 4, Model 5 and Model 6, and the section of piers are defined as frame type and "general section" properties are selected and assigned for these elements. All the section properties are calculated separately by making acceptable assumptions and entered into the models generated in SAP2000. In SAP2000, there are 12 properties to be entered when "general section" is selected for a frame member. These are cross-sectional (axial) area, torsional constant, moment of inertia about 3 axis, moment of inertia about 2 axis, shear area in 2 direction, shear area in 3 direction, section modulus about 3 axis, section modulus about 2 axis, plastic modulus about 3 axis, plastic modulus about 2 axis, radius of gyration about 3 axis and radius of gyration about 2 axis. First six properties are calculated and last six properties, which are related with design considerations, are taken as 1. The calculated, assumed or assigned (e.g. for the case of rigid links) cross sectional properties are summarized in Table 4.2 and explained in the following sections.

### *4.4.1 Section Properties of Piers*

As the section of piers is not a common geometrical shape, all the pier sections are considered as frame and assigned as "general section" in SAP2000. All the section properties are calculated separately and entered to SAP2000.

**Table 4.2 Cross Sectional Properties of Structural Members**
*** I22 is taken as 0 for Case (a) and 1000 for Case (b)**

| MODEL NO | SECTION NAME | AREA ($m^2$) | TORSIONAL CONS. ($m^4$) | I33 ($m^4$) | I22 ($m^4$) | SHEAR AREA 22 ($m^2$) | SHEAR AREA 33 ($m^2$) | MATERIAL |
|---|---|---|---|---|---|---|---|---|
| MODEL1 | BEAM | 1.45 x 5.00 | | | | | | CONC |
| | CONNECT | 1000 | 100 | 1000 | 1000 | 1000 | 1000 | NONE |
| | PIER | 14.3 | 80.47 | 106.22 | 38.28 | 10.076 | 6.147 | CONC |
| | RIGIDLNK | 1000 | 100 | 1000 | 0* | 1000 | 1000 | NONE |
| | RIGIDMID | 1000 | 100 | 1000 | 1000 | 1000 | 1000 | NONE |
| MODEL2 | BEAM | 1.45 x 5.00 | | | | | | CONC |
| | C1 | 1000 | 100 | 1000 | 1000 | 1000 | 1000 | NONE |
| | C2 | 1000 | 100 | 1000 | 0* | 1000 | 1000 | NONE |
| | C2MID | 1000 | 100 | 1000 | 1000 | 1000 | 1000 | NONE |
| | GRIDLONG | 0.79 | 0.439 | 0.234 | 0.139 | 0.332 | 0.281 | CONC |
| | GRIDTRAN | 0.24 x 3.27 | | | | | | CONC |
| | PIER | 14.3 | 80.47 | 106.22 | 38.28 | 10.076 | 6.147 | CONC |
| | RIGIDLNK | 1000 | 100 | 1000 | 0* | 1000 | 1000 | NONE |
| | RIGIDMID | 1000 | 100 | 1000 | 1000 | 1000 | 1000 | NONE |
| MODEL3 | BEAM | 1.45 x 5.00 | | | | | | CONC |
| | GRIDLONG | 1.392 | 0.439 | 0.728 | 0.455 | 0.631 | 0.783 | CONC |
| | GRIDTRAN | 0.24 x 3.27 | | | | | | CONC |
| | PIER | 14.3 | 80.47 | 106.22 | 38.28 | 10.076 | 6.147 | CONC |
| | RIGIDLNK | 1000 | 100 | 1000 | 0* | 1000 | 1000 | NONE |
| | RIGIDMID | 1000 | 100 | 1000 | 1000 | 1000 | 1000 | NONE |
| MODEL4 (also for MODEL 5 & MODEL 6) | GRIDLONG | 13.5 | 3.063 | 5.1 | 335 | 4.417 | 5.481 | CONC |
| | PIER | 14.3 | 80.47 | 106.22 | 38.28 | 10.076 | 6.147 | CONC |
| | RIGIDLNK | 1000 | 100 | 1000 | 0* | 1000 | 1000 | NONE |
| | RIGIDMID | 1000 | 100 | 1000 | 1000 | 1000 | 1000 | NONE |

*(See Section 4.4.2 for the definitions of the section names.)*

Cross-sectional area is found as 14.3 $m^2$ by using the dimensions given in Figure 3.4.

For thin-walled hollow shafts, torsion is defined as,

$$T = \frac{4 \cdot @^2}{L \cdot \oint \frac{ds}{t}} \cdot G \cdot \phi \tag{4.1}$$

where @ is the area bounded by the center line of the wall cross section, L is the length of the shaft, t is wall thickness, G is shear modulus and $\phi$ is the angle of twist.

The torsional constant, j, is the term that is to be entered as input in SAP2000.

$$j = \frac{4 \cdot @^2}{\oint \frac{ds}{t}} \tag{4.2}$$

The pier cross section shown in Figure 3.4 is assumed to be approximately same as the cross section of a thin-walled hollow octagonal shaft as shown in Figure 4.12.

The area bounded by the center line of the wall cross section, @, is found as 25.7 $m^2$ by using the dimensions given in Figure 3.4 and the shape shown in Figure 4.12.

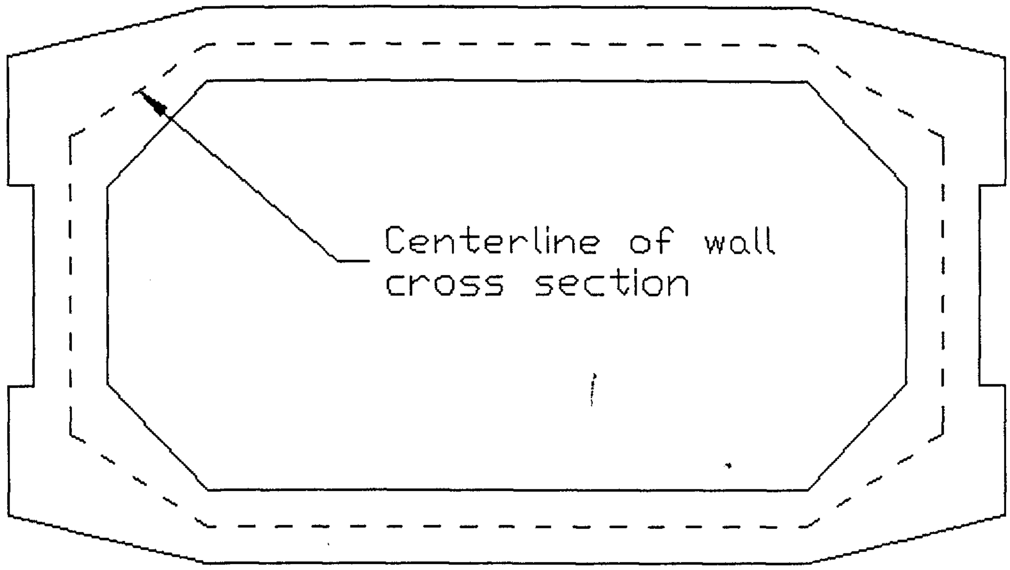


**Figure 4.12 Assumed Octagonal Cross Section for Torsional Constant Calculation**

The integral, $\oint \frac{ds}{t}$, is computed along the centerline of the wall section as shown in Figure 4.12. The thickness of the cross section is assumed to have constant thickness of 0.6 m.

$$\oint \frac{ds}{t} \cong \frac{Total \quad length \quad of \quad wall \quad center \quad line}{t} \tag{4.3}$$

Total length of wall centerline is calculated as 19.7 m. Since t is assumed to be 0.6 m;

$$\oint \frac{ds}{t} \cong \frac{19.7}{0.6} = 32.83 \tag{4.4}$$

From Eq. 4.4, torsional constant j is found as,

$$j = \frac{4 \cdot (25.7)^2}{32.83} = 80.47 \qquad (4.5)$$

Moment of inertia is found as 106.22 $m^4$ about 3-axis and 38.28 $m^4$ about 2-axis. Axes are shown in Figure 4.13.

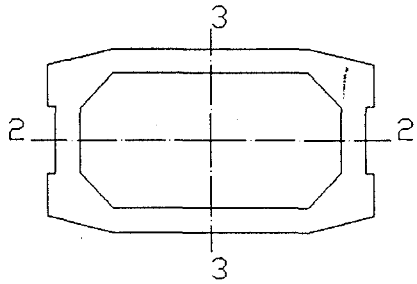


**Figure 4.13 Pier Axes**

Shear area is important for deep beams. In stiffness matrix, all the terms are modified by multiplying all the bending terms with a factor, called as β.

$$\beta := \frac{12 \cdot E \cdot I}{As \cdot G \cdot L} \qquad (4.6)$$

where As is the shear area, G is the shear modulus, E is modulus of elasticity, I is moment of inertia, and L is the length of the beam.

Shear area is defined, in Reference 1, as;

$$As = \frac{Ix^2}{\int_{y_b}^{y_t} \frac{Q^2(y)}{b(y)} dy} \qquad (4.7)$$

where shear forces are parallel to Y-direction shown in Figure 4.14, Ix is the moment of inertia of section about X-X, and Q(Y) is defined as,

$$Q(Y) = \int_{y}^{y_t} n \cdot b(n) \quad dn \tag{4.8}$$

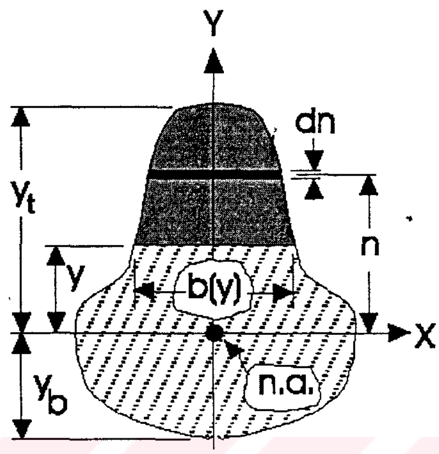


**Figure 4.14 Definitions of Variables Used in Eq. 4.7 and 4.8**

Shear area is found as 10.076 $m^2$ in 2-direction and 6.147 $m^2$ in 3-direction. Calculations for shear areas are carried out by using MathCAD Software [6] and shown in Appendix B.

### *4.4.2 Section Properties of the Deck*

In SAP2000, cross-sectional properties are calculated automatically for common shapes. Since the deck is composed of shell elements in Model 1, it is easy to define deck section for Model 1. In the other models, however, cross-sectional properties are to be calculated, since some of or whole deck is lumped at some points. Therefore, as done for piers, sections of deck elements for Model 2, Model 3, Model 4, Model 5 and Model 6 are considered as frame type and defined as "general section" in SAP2000, and effective sectional properties are calculated by making acceptable assumptions. Section names assigned in the generated models are defined one by one in the following.

Section Type "PIER" is used for piers and used in all generated models since piers are modeled in the same way in all models.

Section Type "BEAM" is used for the transverse beam sitting over each pier in order to bear the longitudinal deck beams as shown in Figure 3.5. Since the piers are modeled in the same way in each model, this section type is used in all the models.

Section Type "RIGIDLNK" is used for rigid links which simulate energy dissipating units. Rigid link elements located between each longitudinal deck beam and the beam sitting over the pier (BEAM). This section type is used in all generated models.

Section Type "RIGIDMID" is same as "RIGIDLNK" except that the frame members with "RIGIDMID" section type are located at the central pier of each continuous 10-span segments explained in Section 3.2, and only the central rigid link is of this type, i.e. the rigid link connecting the central longitudinal deck beam to the pier. This element or section type is used because EDU is directly fixed both to the pier and the deck at central pier of each continuous 10-span segments.

Section Types "CONNECT", "C1", "C2" and "C2MID" are used for the horizontal frame elements connecting shell type of elements to the rigid link elements. They are also rigid link elements, but named differently in order to be separated from vertical rigid link elements. Section Type "CONNECT" is used in Model 1 and other 3 type are used in Model 2. "C2MID" is used to connect the deck beam over the elements with "RIGIDMID" section type.

Section Types "GRIDLONG" and "GRIDTRAN" are used for the elements forming the deck in the shape of grid. Longitudinal deck beams have "GRIDLONG" section type. The elements having "GRIDLONG" section type are used in order to provide transversal continuity of the deck. "GRIDLONG" and "GRIDTRAN" section types are used for Model 2 and Model 3. In Model 4, only "GRIDLONG" is used since there is no grid. The sectional properties of "GRIDLONG" used in Model 2, in Model 3 and in Model 4 are obviously different. "GRIDLONG" elements simulate one seventh of the deck in Model 2, one seventh of the deck without slab in Model 3, and the whole deck in Model 4.

Properties of sections are summarized in Table 4.2. As mentioned at the beginning of this section, some of or whole deck is lumped at some points in

Model 2, Model 3 and Model 4, and cross sectional properties are calculated by making some acceptable assumptions. Calculations for the effective sectional properties of the lumped members are performed accordingly. The section types of lumped members are only "GRIDLONG" and "GRIDTRAN" defined above.

Section properties of Model 5 and Model 6 are same as Model 4. the only difference of Model 5 and Model 6 from Model 4 is that they are two dimensional.

In Model 4, only the section properties of GRIDLONG type are calculated. GRIDLONG consists of the whole deck, and therefore it simulates the whole deck behavior (Figure 4.9). The value of Lw in Figure 4.15 is 17.5 m.

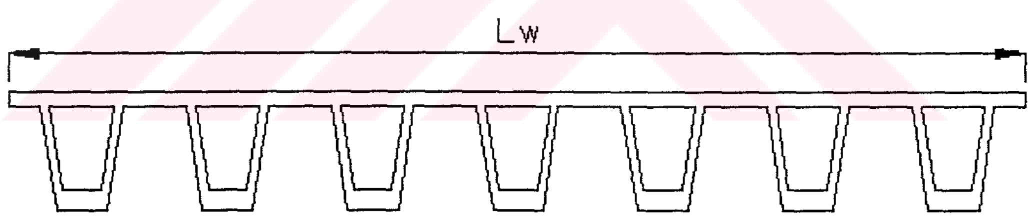


**Figure 4.15 Deck Width**

In Model 2, both GRIDLONG and GRIDTRAN type of elements are used. GRIDLONG consists of one seventh of the whole deck (Figure 4.7).

Calculations for GRIDLONG section type:

The definitions of variables used for the calculations are shown in Figure 4.16. In Figure 4.16, b1 is the one seventh of the transversal length of the deck. The values of the variables are b1 = 2.508 m, b2 = 0.88 m, h = 1.45 cm, t1 = 0.24 m, t2 = 0.16 m, t3 = 0.35 m.

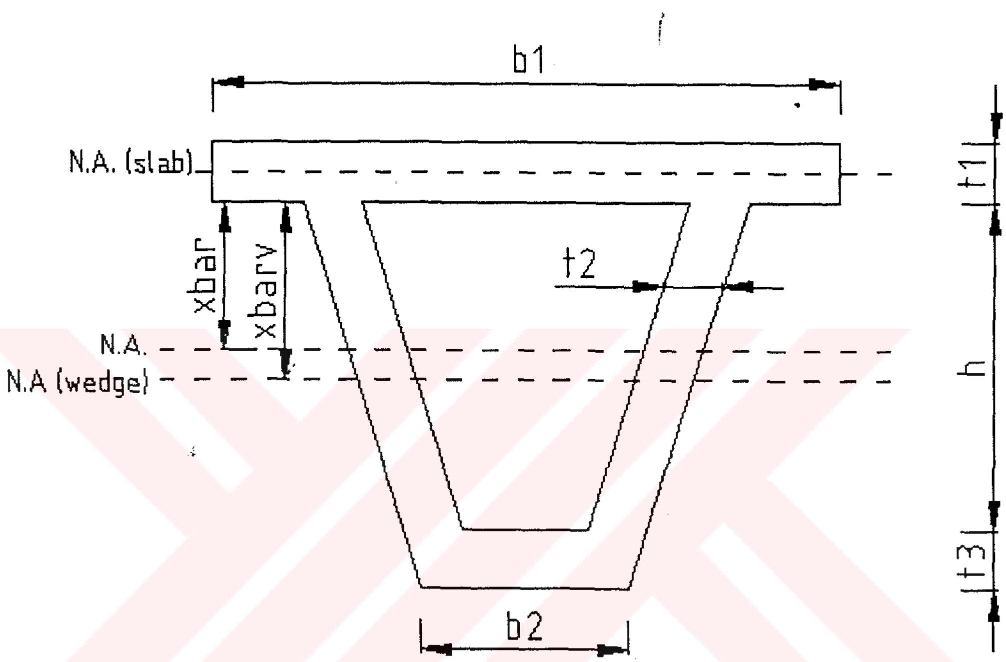


**Figure 4.16 Definition of Variables in Used in the Girder Section for the Calculations of Sectional Properties**

Cross-sectional area is found as 14.3 $m^2$ by using the dimensions given in Figure 3.4.

For Model 2, moment of inertia, shear area and torsional constant are calculated separately.

Moment of inertia is calculated as follows. Definitions of variables are shown in Figure 4.16.

Neutral axis for the whole section is found as xbar = 0.557 cm.

$$I33 := \frac{b1\cdot t1^3}{12} + \frac{h^3\cdot t2\cdot 2}{12} + \frac{b2\cdot t3^3}{12} + b1\cdot t1\cdot\left(xbar + \frac{t1}{2}\right)^2 + t2\cdot 2\cdot h\cdot\left(xbar - \frac{h}{2}\right)^2 + b2\cdot t3\cdot\left(h + \frac{t3}{2} - xbar\right)^2 \quad (4.9)$$

Using above formula (Eq. 4.9), I33 is found as 0.728 $m^4$.

Moment of inertia for the slab is calculated by the formula $Is := \frac{b1\cdot t1^3}{12}$ and found as $2.899*10^{-3}$ $m^4$.

Neutral axis for the wedge (lower U shape) is found by using the formula:

$$xbarv := \frac{h\cdot 2\cdot t2\cdot\frac{h}{2} + b2\cdot t3\cdot\left(h + \frac{t3}{2}\right)}{Av} \quad , xbarv = 1.084 \text{ m} \quad (4.10)$$

where $Av := (b2\cdot t3 + 2\cdot h\cdot t2)$

Finally, Iveff in 3 direction is found by the formula

$$Iveff := I33 - Is - b1\cdot t1\cdot\left(xbar + \frac{t1}{2}\right)^2 - Av\cdot(xbarv - xbar)^2 \text{ , } Ieff = 0.234 \text{ m}^4 \quad (4.11)$$

In the same way, Ieff in 2 direction can be found as 0.139 $m^4$.

### 4.5 Material Properties

For dead load calculations the properties of concrete [3] are used:

| | | |
|---|---|---|
| Mass per unit volume | : | 2.4007 t/m³ |
| Weight per unit volume | : | 23.5616 kN/m³ |
| Modulus of Elasticity | : | 24821130 kN/m² |
| Poisson's Ratio | : | 0.2 |
| Coeff. Of Thermal Expansion | : | $9.9 \times 10^{-6}$ |

### 4.6 Restraints

Fixed supports are assigned at the bottom of each pier. That is, all degrees of freedom for very bottom joints of the piers are fixed. All other points are free to move with 6 degree of freedoms except the central piers for 10-span segments. These central piers are also fixed. In case of a strong excitation, all the other piers are also restrained by lock up devices explained in Chapter 4. This is included in the case (b) and not included in case (a) of the models.

### 4.7 Loading

Dead Load (DL) and Earthquake Load (EQ) are defined for analyses. 1.0 DL + 1.0 EQ load combination is used for the analyses of the bridge models. Dead Load (DL) is the self weight of the structure and Earthquake Load (EQ) is the measured time history data.

The earthquake data for 12 November 1999 Bolu-Düzce Earthquake are used for the time-history analysis. East-West, North-South, and vertical components of Düzce station records of the earthquake are applied simultaneously to the bridge models. Time history data are shown in graphical form in Figure 4.17.

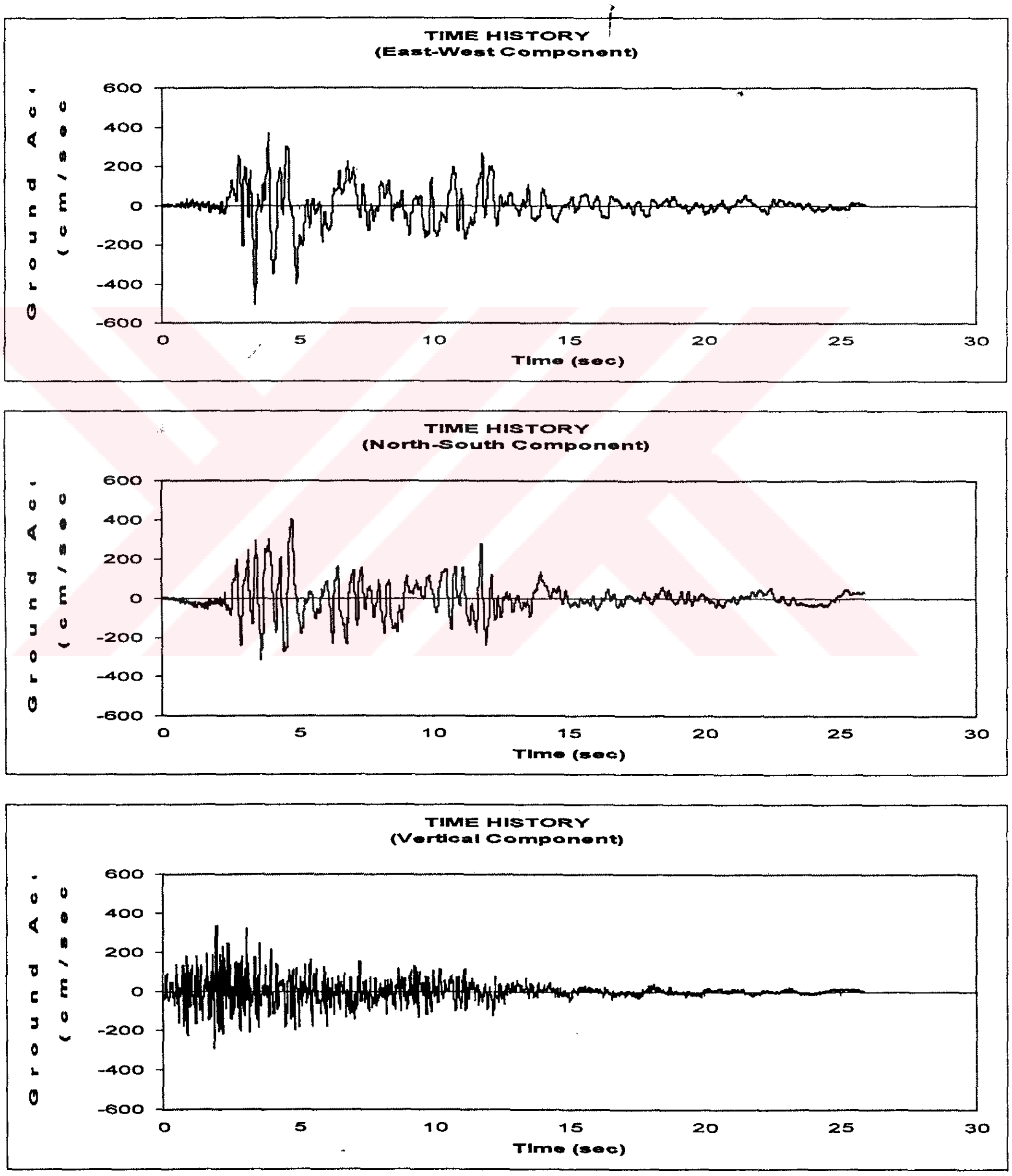


**Figure 4.17 Time History Data of 12 November 1999 Düzce Earthquake (Düzce Recording Station, EW, NS, and Vertical Components)**

## 4.8 Dynamic Analysis

For the dynamic analysis, there are two analysis methods: Eigenvector Analysis and Ritz-vector Analysis. In this study, Ritz-vector Analysis method is selected to be used, since they are considered to be more effective in dynamic loading. Ritz vectors are load dependent and such dynamic analyses based on a special set of Ritz vectors yield more accurate results than the use of the same number of natural mode shapes [4]. The reason why the Ritz vectors yield excellent results is that they are generated by taking into account the spatial distribution of the dynamic loading, whereas the direct use of the natural mode shapes neglects this very important information. A total of 200 modes are used in Ritz vector analysis for simulation and time history analysis of all analytical models.

When eigen vectors are used, it is more likely to find the self excitations of the piers in the lower modes, which is not useful for these complex models. Using Ritz vectors greatly enhances the modal shapes to occur in lower modes.

Earthquake simulation is done by using November 1999 Düzce Earthquake data. For the dynamic analysis, a constant damping ratio of 5% is used for all modes of analyses. For the results of maximum internal forces and displacements, envelope property is used in SAP2000.

Total assembled joint masses in global coordinates and modal load participation ratios for each model is summarized in Table 4.3 and 4.4 respectively. As seen from Table 4.3, almost all participating total mass amount are very close to 100% for the number of modes taken into account for the dynamic analysis.

**Table 4.3 Modal Load Participation Ratios**

| MODEL | ACC UX (%) (Dynamic) | ACC UY (%) (Dynamic) | ACC UZ (%) (Dynamic) |
|---|---|---|---|
| Model1A | 99.9092 | 99.8837 | 99.3324 |
| Model2A | 99.4785 | 99.3207 | 97.6543 |
| Model3A | 99.8818 | 99.8426 | 99.2234 |
| Model4A | 99.9227 | 99.8980 | 99.4379 |
| Model5A | 99.9899 | 99.9579 | 99.9291 |
| Model6A | 100.0000 | 100.0000 | 100.0000 |
| Model1B | 99.9677 | 99.9599 | 99.7387 |
| Model2B | 99.8447 | 99.7930 | 99.0328 |
| Model3B | 99.9727 | 99.9654 | 99.7659 |
| Model4B | 99.9800 | 99.9743 | 99.8544 |
| Model5B | 99.9962 | 99.9852 | 99.9605 |
| Model6B | 100.0000 | 100.0000 | 100.0000 |

**Table 4.4 Total Assembled Joint Masses (in Global Coordinates)**

| MODEL | Total UX (Tons) | Total UY (Tons) | Total UZ (Tons) |
|---|---|---|---|
| Model1A | 166468.124 | 166468.124 | 166468.124 |
| Model2A | 166448.772 | 166448.772 | 166448.772 |
| Model3A | 166494.374 | 166494.374 | 166494.374 |
| Model4A | 166437.004 | 166437.004 | 166437.004 |
| Model5A | 166493.740 | 166493.740 | 166493.740 |
| Model6A (only 10 spans) | 33125.894 | 33125.894 | 33125.894 |
| Model6A (x~5) | ~165629.47 | ~165629.47 | ~165629.47 |
| Model1B | 166468.124 | 166468.124 | 166468.124 |
| Model2B | 166448.772 | 166448.772 | 166448.772 |
| Model3B | 166494.374 | 166494.374 | 166494.374 |
| Model4B | 166437.004 | 166437.004 | 166437.004 |
| Model5B | 166493.740 | 166493.740 | 166493.740 |
| Model6B (only 10 spans) | 33125.894 | 33125.894 | 33125.894 |
| Model6B (x~5) | ~165629.47 | ~165629.47 | ~165629.47 |

Response spectrum curves in both East (X) and North (Y) directions are drawn using the time history data. The magnitudes are normalized using (a) peak ground acceleration and (b) 0.4 times gravitational acceleration (0.4*g) in Figures 4.18 and 4.19, respectively, to have a general idea of the variations from the spectrum curve formed from the criteria in Turkish Seismic Code [7 & 10].

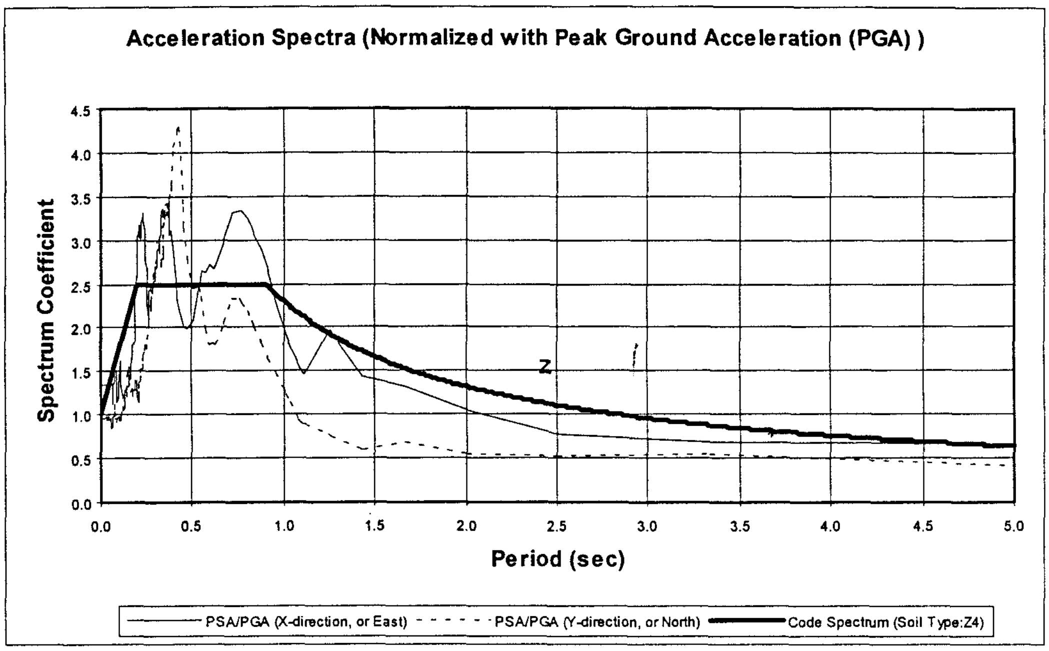


Figure 4.18 Acceleration Spectra Normalized with Peak Ground Acc. (PGA)

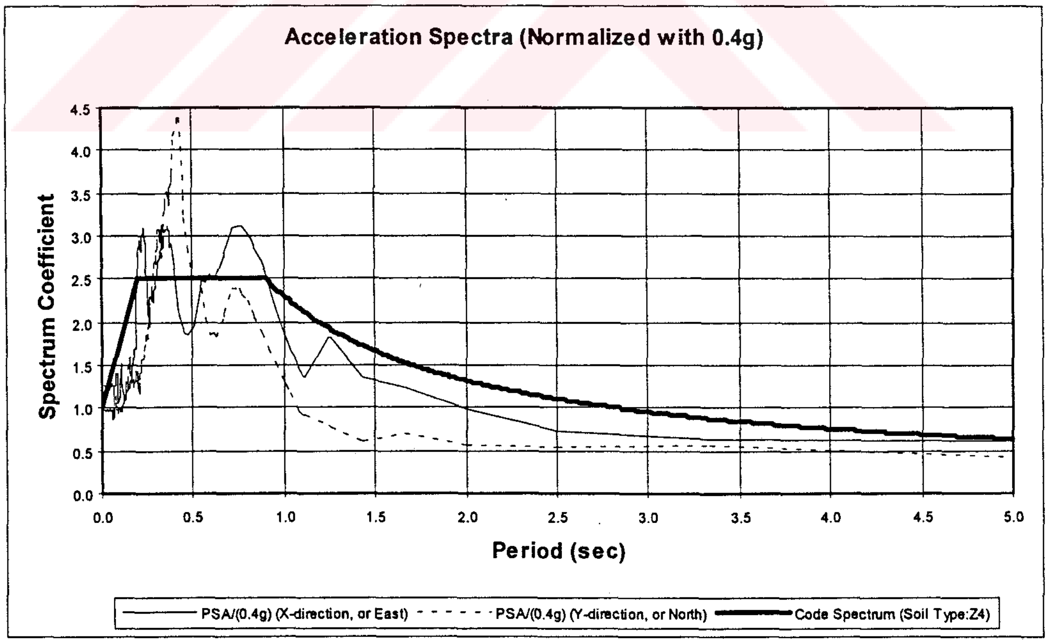


Figure 4.19 Acceleration Spectra Normalized with 0.4g

# CHAPTER 5

# COMPARISON AND DISCUSSION OF RESULTS

As indicated in Section 2.2, the comparison of the results obtained from each different model and investigation of the effect of model complexity on the results are of great importance. In this Chapter, the internal forces at pier bases, maximum displacements at pier caps, mode shapes, and modal periods of each bridge model analysis are presented, compared against each other, and discussed. Furthermore, additional comparisons and discussions are made referring to Astaldi's non-linear analysis results. The internal forces used for comparison are the shear and bending moments in longitudinal and transverse directions. Likewise, maximum horizontal displacements (drifts) are compared in longitudinal and transverse directions.

## 5.1 Mode Shapes and Modal Periods

The modeling works in this study were conducted under two major branches as explained in Chapter 4: Case (a) term is used for models allowing longitudinal relative deformations between pier caps and deck except central fixed piers of each 10-span segments. Case (b) term is used for models where all pier-to-deck connections are fixed. Mode shape and period comparison of Case (a) revealed irrelevant results and not presented here. Case (b) results are presented in Table 5.1 and Figure 5.1 for first 3 longitudinal and first 15 transverse mode shapes. Vertical modes are not included in Table 5.1 since they usually appeared at very low periods compared to the transverse and longitudinal modes.

**Table 5.1 Modal Periods**

| Mode Shape | Model 1B | | Model 2B | | Model 3B | | Model 4B | | Model 5B | | Model 6B | |
|---|---|---|---|---|---|---|---|---|---|---|---|---|
| | Mode No | Period (sec.) | Mode No | Period (sec.) | Mode No | Period (sec.) | Mode No | Period (sec.) | Mode No | Period (sec.) | Mode No | Period (sec.) |
| 1st Longitudinal | 1 | 1.2424 | 1 | 1.1914 | 1 | 1.1024 | 3 | 1.0517 | 3 | 1.0542 | 1 | 1.2309 |
| 2nd Longitudinal | 12 | 0.8227 | 69 | 0.7825 | 14 | 0.7532 | 14 | 0.7371 | 14 | 0.7429 | 8 | 0.3117 |
| 3rd Longitudinal | 18 | 0.6002 | 75 | 0.5628 | 20 | 0.5525 | 19 | 0.5445 | 19 | 0.5441 | 11 | 0.2031 |
| 1st Transverse | 2 | 1.1065 | 2 | 1.0955 | 2 | 1.0892 | 1 | 1.0801 | 1 | 1.0799 | 2 | 1.0358 |
| 2nd Transverse | 3 | 1.0795 | 3 | 1.0708 | 3 | 1.0696 | 2 | 1.0618 | 2 | 1.0574 | 3 | 0.9658 |
| 3rd Transverse | 4 | 1.0633 | 4 | 1.0538 | 4 | 1.0537 | 4 | 1.0407 | 4 | 1.0395 | 4 | 0.8719 |
| 4th Transverse | 5 | 1.0352 | 5 | 1.0279 | 5 | 1.0279 | 5 | 1.0147 | 5 | 1.0146 | 5 | 0.7264 |
| 5th Transverse | 6 | 1.0131 | 6 | 1.0058 | 6 | 1.0058 | 6 | 0.9924 | 6 | 0.9934 | 6 | 0.5439 |
| 6th Transverse | 7 | 0.9902 | 7 | 0.9852 | 7 | 0.9860 | 7 | 0.9719 | 7 | 0.9728 | 7 | 0.3943 |
| 7th Transverse | 8 | 0.9549 | 8 | 0.9548 | 8 | 0.9568 | 8 | 0.9407 | 8 | 0.9411 | 9 | 0.2972 |
| 8th Transverse | 9 | 0.9144 | 10 | 0.9113 | 9 | 0.9121 | 9 | 0.9003 | 9 | 0.9026 | 10 | 0.2366 |
| 9th Transverse | 10 | 0.8759 | 56 | 0.8650 | 10 | 0.8788 | 10 | 0.8611 | 10 | 0.8617 | 12 | 0.2000 |
| 10th Transverse | 11 | 0.8417 | 66 | 0.8383 | 11 | 0.8494 | 11 | 0.8310 | 11 | 0.8327 | 21 | 0.1785 |
| 11th Transverse | 13 | 0.7986 | 68 | 0.8003 | 12 | 0.8119 | 12 | 0.7907 | 12 | 0.7926 | 22 | 0.1677 |
| 12th Transverse | 14 | 0.7565 | 70 | 0.7587 | 13 | 0.7741 | 13 | 0.7508 | 13 | 0.7532 | | |
| 13th Transverse | 15 | 0.7122 | 71 | 0.7174 | 15 | 0.7367 | 15 | 0.7094 | 15 | 0.7132 | | |
| 14th Transverse | 16 | 0.6701 | 72 | 0.6710 | 16 | 0.6942 | 16 | 0.6698 | 16 | 0.6754 | | |
| 15th Transverse | 17 | 0.6126 | 73 | 0.6284 | 17 | 0.6546 | 17 | 0.6149 | 17 | 0.6183 | | |

In general, finite element models become more flexible when finer meshing and larger number of members are used (for the same structure). Higher flexibility causes the periods to become larger. In this study, the number of members used for modeling increased for more complicated models, which caused modal periods to get slightly larger as the model complexity increased (Figure 5.1).

Modal periods of Model 5 are generally greater than those of Model 4, which does not comply with the previous generalization. However, the complexity of Model 4 over Model 5 is not due to finer element meshing, but due to 2D – 3D geometry effect. Both Model 4 and Model 5 are composed of frame elements for the deck (lumped beam model), but the latter one is a straight 2D model and ignores the curves in plan.

On the other hand, modal periods of Modal 3B is greater than those of Model 1B and 2B, in higher-degree-mode shapes (e.g. $9^{th}$, $10^{th}$, $11^{th}$, $12^{th}$, $13^{th}$, $14^{th}$, $15^{th}$ transverse mode shapes). Model 3B is composed of frame elements only and in order to provide the transversal continuity of the section, transverse direction frame elements are defined, and these elements most probably affected the modal periods.

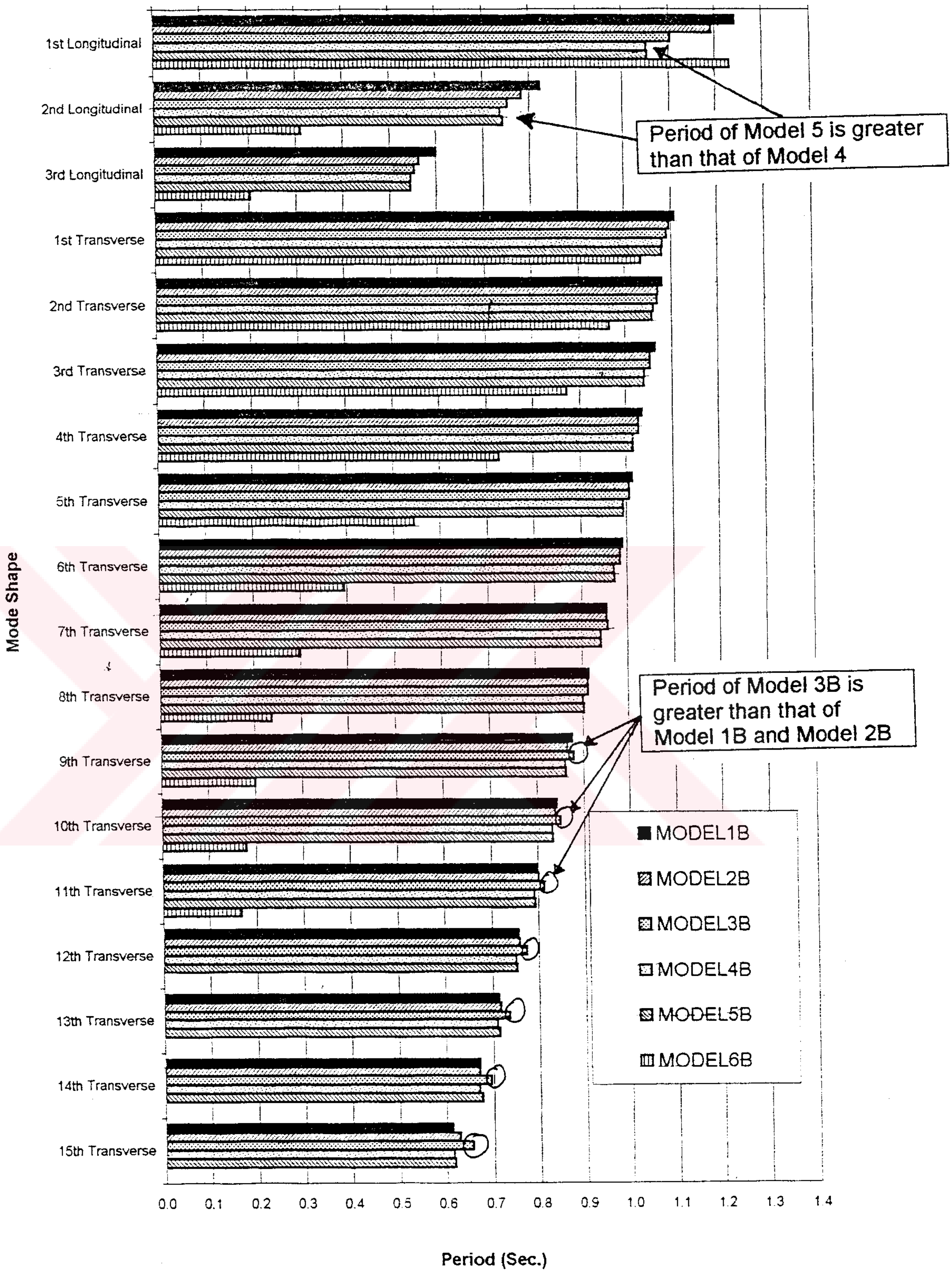


**Figure 5.1 Modal Periods**

The modal periods for Model 6 are very low except 1st longitudinal mode, because it is only a model of 10-span segment. The 10-span segment cannot simulate the behavior of the whole bridge since a fraction of the whole length is considered (see Appendix C, transverse mode shapes).

In Table 5.1, it can be seen that the "mode numbers" of lower degree mode shapes for Model 2B are very high (e.g. 69 in 2nd longitudinal, 56 in 9th transverse). This is because Model 2 has vertical modes in lower mode numbers which are located between the longitudinal and transverse modes. The high period content of vertical modes for Model 2B might be due to increase in vertical flexibility.

## 5.2 Internal Forces

As only central pier caps of 10-span segments are fixed in case (a), longitudinal shear forces and moments are gathered in these central piers. Models can be grouped for these peak values. Model 1A, 2A, and 3A has closer shear force and moment values in longitudinal direction. Also, Model 4A and Model 5A has closer values for these internal forces (Figure 5.2, 5.3). This grouping can be seem more clearly seen in Table 5.2 (e.g. Pier 5, $|M_{22}|_{MAX}$ : Model 1A, 2A, 3A is around 1.5E6 kN.m and Model 4A, 5A is around 1.0E6 kN.m). The reason for this to happen is most probably because of the fact that first three models fully considers the inertial dynamic contribution of the deck width whereas Model 4A and 5A have only wire frames with the sectional properties imposed on the sections. The total shear force and moment in longitudinal direction gathered in the central fixed piers increased due to the transverse dimension that exists in Models 1A, 2A, and 3A.

**Table 5.2 Forces at the Bases of Central Fixed Piers (CASE A)**

| | FORCE | UNIT | MODEL1A | MODEL2A | MODEL3A | MODEL4A | MODEL5A | MODEL6A |
|---|---|---|---|---|---|---|---|---|
| PIER 5 | $\lvert V22\rvert_{MAX}$ (Tran.) | kN | 12,859.96 | 10,370.94 | 10,851.36 | 9,676.57 | 10,315.91 | N/A |
| | $\lvert V33\rvert_{MAX}$ (Long.) | kN | 133,823.60 | 125,949.90 | 126,560.40 | 98,805.21 | 99,918.72 | N/A |
| | $\lvert M22\rvert_{MAX}$ (Long.) | kN.m | 1,494,631.00 | 1,501,888.00 | 1,478,002.00 | 1,090,641.00 | 1,079,061.00 | N/A |
| | $\lvert M33\rvert_{MAX}$ (Tran.) | kN.m | 172,174.40 | 120,020.60 | 142,100.10 | 109,724.90 | 117,384.00 | N/A |
| PIER 15 | $\lvert V22\rvert_{MAX}$ (Tran.) | kN | 13,438.32 | 14,294.98 | 15,446.60 | 15,812.62 | 15,055.54 | N/A |
| | $\lvert V33\rvert_{MAX}$ (Long.) | kN | 32,462.73 | 31,244.98 | 27,240.92 | 24,099.61 | 26,327.05 | N/A |
| | $\lvert M22\rvert_{MAX}$ (Long.) | kN.m | 1,449,492.00 | 1,323,146.00 | 1,089,242.00 | 823,452.90 | 899,193.90 | N/A |
| | $\lvert M33\rvert_{MAX}$ (Tran.) | kN.m | 586,507.40 | 625,592.50 | 650,759.90 | 677,418.00 | 640,770.40 | N/A |
| PIER 25 | $\lvert V22\rvert_{MAX}$ (Tran.) | kN | 8,433.95 | 9,069.08 | 9,855.65 | 10,929.27 | 10,575.98 | 12,800.74 |
| | $\lvert V33\rvert_{MAX}$ (Long.) | kN | 37,890.68 | 35,817.14 | 32,890.41 | 25,273.19 | 26,765.28 | 26,775.80 |
| | $\lvert M22\rvert_{MAX}$ (Long.) | kN.m | 1,747,111.00 | 1,583,994.00 | 1,388,359.00 | 900,537.80 | 955,738.10 | 956,112.60 |
| | $\lvert M33\rvert_{MAX}$ (Tran.) | kN.m | 422,311.80 | 426,923.20 | 447,561.80 | 476,116.00 | 454,699.90 | 553,172.00 |
| PIER 35 | $\lvert V22\rvert_{MAX}$ (Tran.) | kN | 9,748.53 | 8,981.59 | 9,010.49 | 9,906.28 | 9,664.15 | N/A |
| | $\lvert V33\rvert_{MAX}$ (Long.) | kN | 38,573.00 | 38,750.31 | 36,034.23 | 27,241.85 | 27,362.55 | N/A |
| | $\lvert M22\rvert_{MAX}$ (Long.) | kN.m | 1,827,589.00 | 1,743,477.00 | 1,549,791.00 | 994,579.10 | 982,363.60 | N/A |
| | $\lvert M33\rvert_{MAX}$ (Tran.) | kN.m | 445,505.50 | 408,064.40 | 389,675.80 | 423,231.30 | 429,744.90 | N/A |
| PIER 45 | $\lvert V22\rvert_{MAX}$ (Tran.) | kN | 8,632.61 | 9,266.83 | 9,433.90 | 9,694.48 | 10,604.72 | N/A |
| | $\lvert V33\rvert_{MAX}$ (Long.) | kN | 33,323.11 | 33,019.79 | 28,319.76 | 28,335.15 | 26,322.55 | N/A |
| | $\lvert M22\rvert_{MAX}$ (Long.) | kN.m | 1,476,630.00 | 1,432,551.00 | 1,153,657.00 | 988,544.40 | 899,398.10 | N/A |
| | $\lvert M33\rvert_{MAX}$ (Tran.) | kN.m | 411,388.40 | 430,301.80 | 406,055.00 | 447,514.50 | 487,031.30 | N/A |
| PIER 54 | $\lvert V22\rvert_{MAX}$ (Tran.) | kN | 16,313.77 | 15,446.75 | 16,654.13 | 15,797.46 | 16,520.73 | N/A |
| | $\lvert V33\rvert_{MAX}$ (Long.) | kN | 20,419.42 | 20,700.27 | 20,894.11 | 23,813.74 | 22,314.23 | N/A |
| | $\lvert M22\rvert_{MAX}$ (Long.) | kN.m | 831,886.80 | 802,293.20 | 778,765.60 | 755,274.80 | 698,075.40 | N/A |
| | $\lvert M33\rvert_{MAX}$ (Tran.) | kN.m | 653,035.30 | 614,936.70 | 660,322.60 | 614,622.90 | 635,472.40 | N/A |

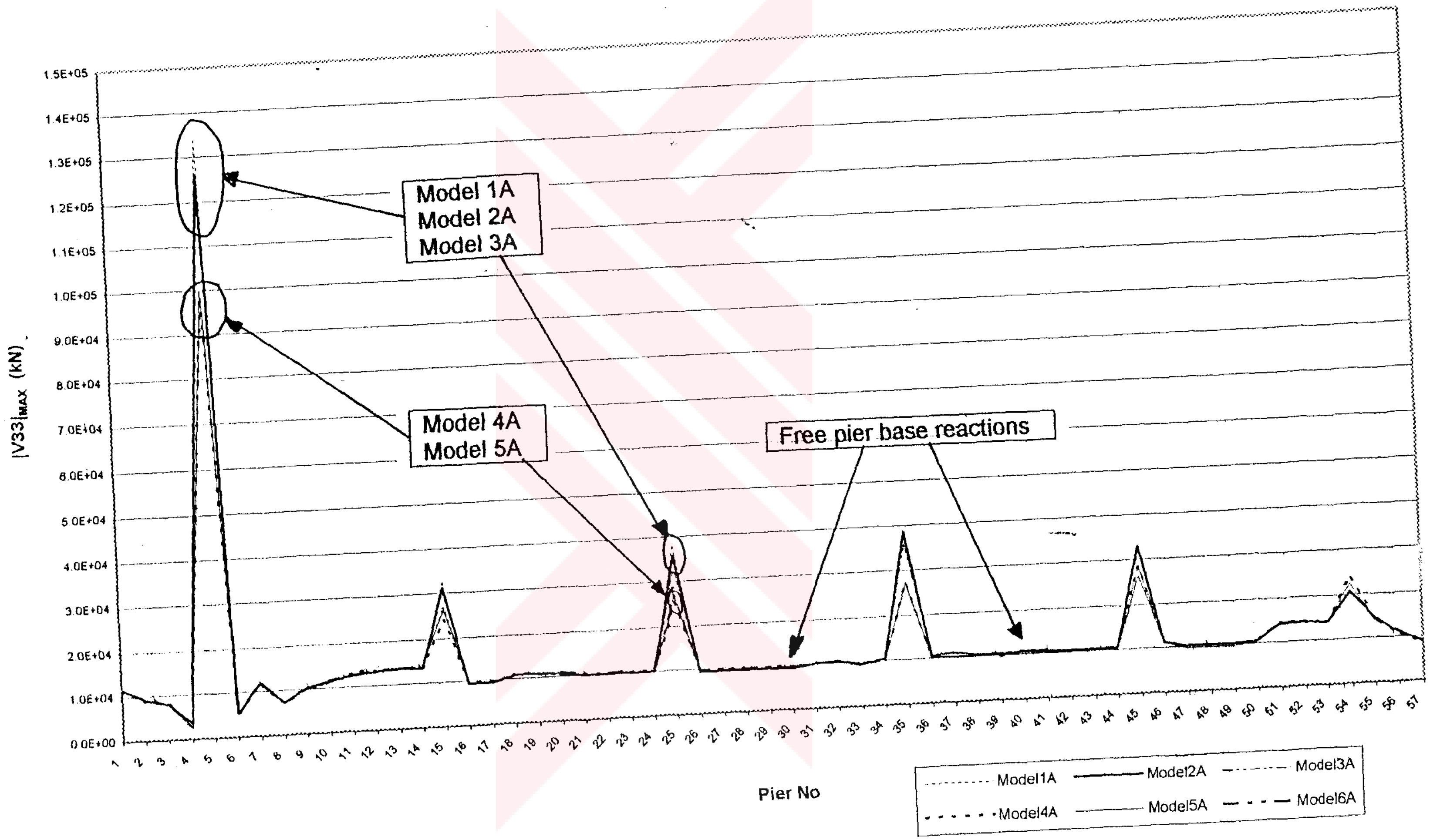


Figure 5.2 Absolutely Maximum Shear Force in Longitudinal Direction (CASE A)

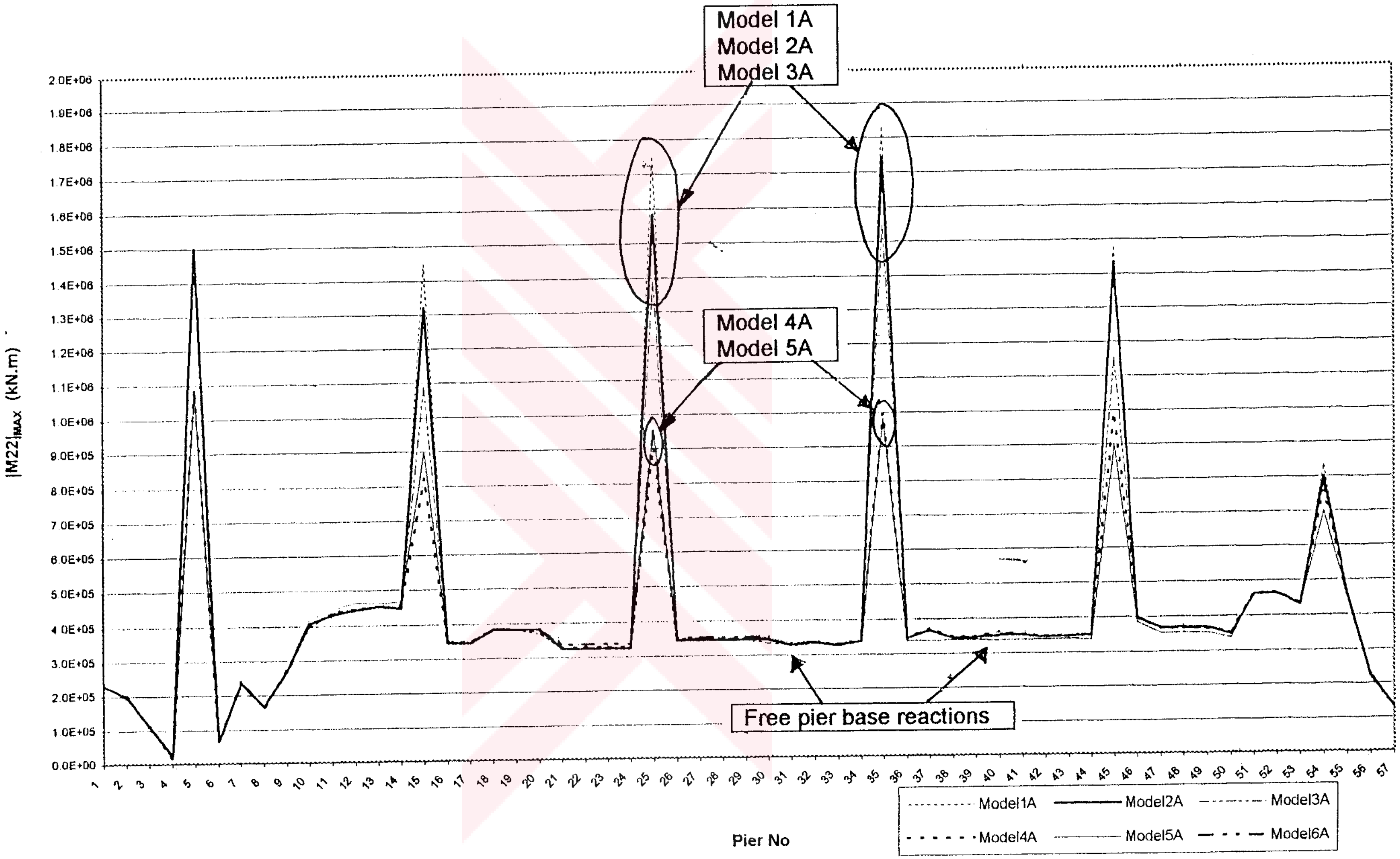


**Figure 5.3 Absolutely Maximum Moment in Longitudinal Direction (CASE A)**

As in the ideal case, it is expected that there will be no moment or shear force in longitudinal direction of the base of piers which do not have fixed caps. However, there are some shear forces and moments developing in those pier bases. This is simply because of the self excitation of piers independent from the bridge superstructure. (Free pier base reactions). As shown in Figure 5.2 and 5.3, these values are almost same for all models.

In case (b), the situation is quite different. There are no peaks at central piers for longitudinal internal forces, since these central piers are not fixed. The load more or less evenly distributes throughout the bridge (Figure 5.4, 5.5). On the other hand, for piers 4, 5, 6, 56, and 57, which are very short compared to other piers, there are large values (peaks) for both in shear and moment values (Figure 5.4, 5.5). This is an expected situation; because, usually short members are stiffer compared to long ones and attracts more forces.

Since there are no peak values of longitudinal internal forces and the load more or less evenly distributes throughout the bridge, it is better to look at the sum of the forces at piers rather than individual central piers. In Table 5.3, these values (sum of forces) are summarized in detail. In Figures 5.6 and 5.7, a smooth increase or decrease is not seen in longitudinal direction. Although there is an increase in longitudinal shear force values as complexity of the modeling decreases, there are both decreasing and increasing patterns for the moment case. This may happen in certain cases since moment also depends on the moment arm.

If the shear value increases while the member height decreases (at a larger scale) the moment might also decrease. Therefore, increase in shear together with decrease in moment is possible and logical.

The percentage variations in sums of the forces at pier bases, normalized according to Model 1B and 6B, are shown in Table 5.4. As the complexity changes, the percentage differences between moment and shear sums in transverse and longitudinal directions change, too (Figure 5.8, Figure 5.9). The largest difference is 16.9% in Model 4 normalized according to Model 1, for shear in longitudinal direction.

As seen in relevant figures of transverse direction for both Case (a) and Case (b) (Figure 5.10, 5.11, 5.12, and 5.13), all generated models give closer shear force and moments. However, there is a big amount of decrease in transverse shear and moment in Pier 4, 5, 6, 56, and 57, the shortest central fixed piers, which is not an expected situation. Usually, short members are stiffer and attract more shear force compared to long ones. Possible explanation of small shear is due to the fact that natural periods of such stiff structures are outside the frequency content of the seismic excitation. After this point on, shear and moment values immediately increase (Figure 5.10, 5.11, 5.12, 5.13).

Because Model 6 is only 10-span segment model, it will be compared with Astaldi's Model in Section 5.2.1, in more detail.

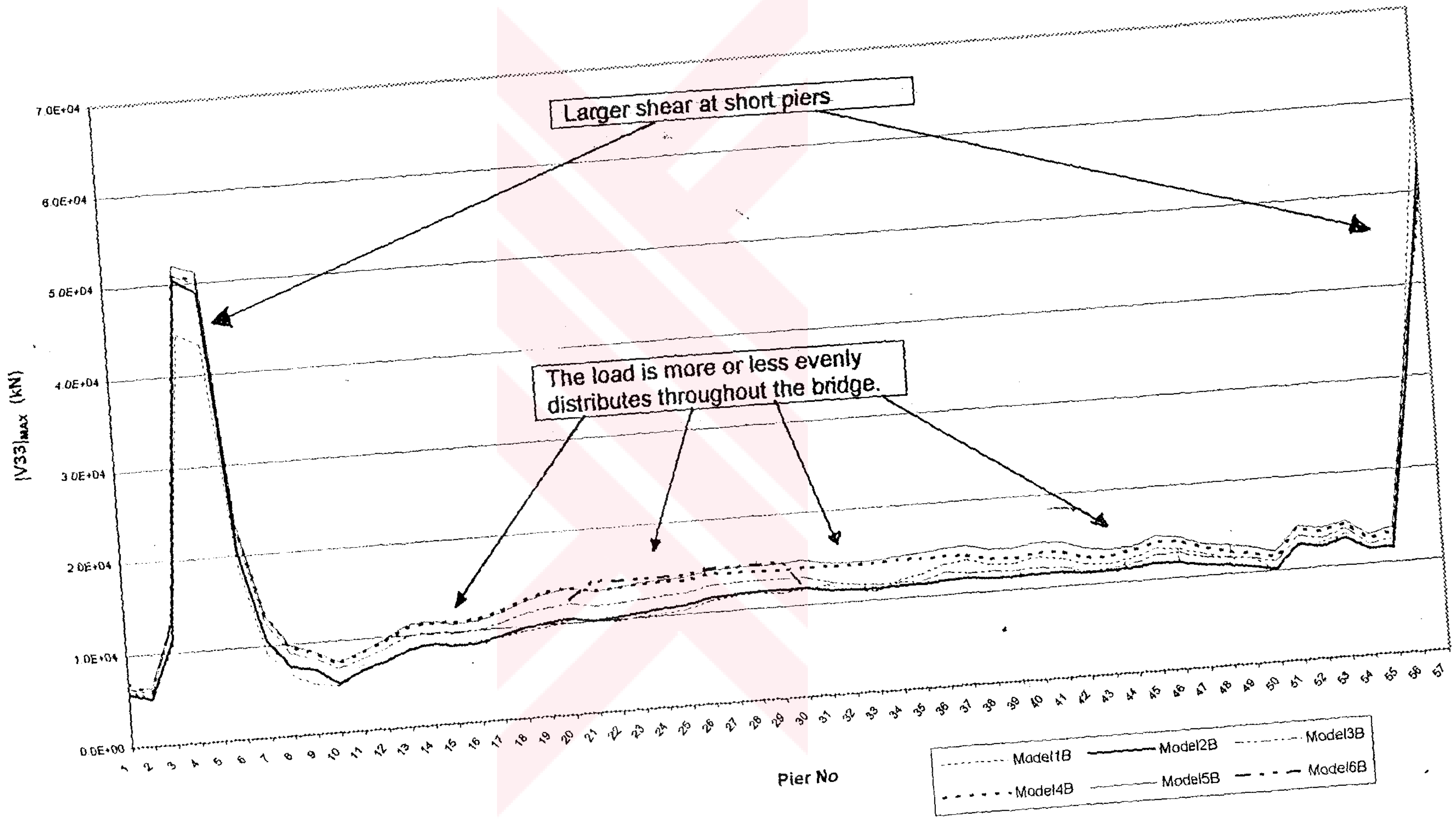


Figure 5.4 Absolutely Maximum Shear Force in Longitudinal Direction (CASE B)

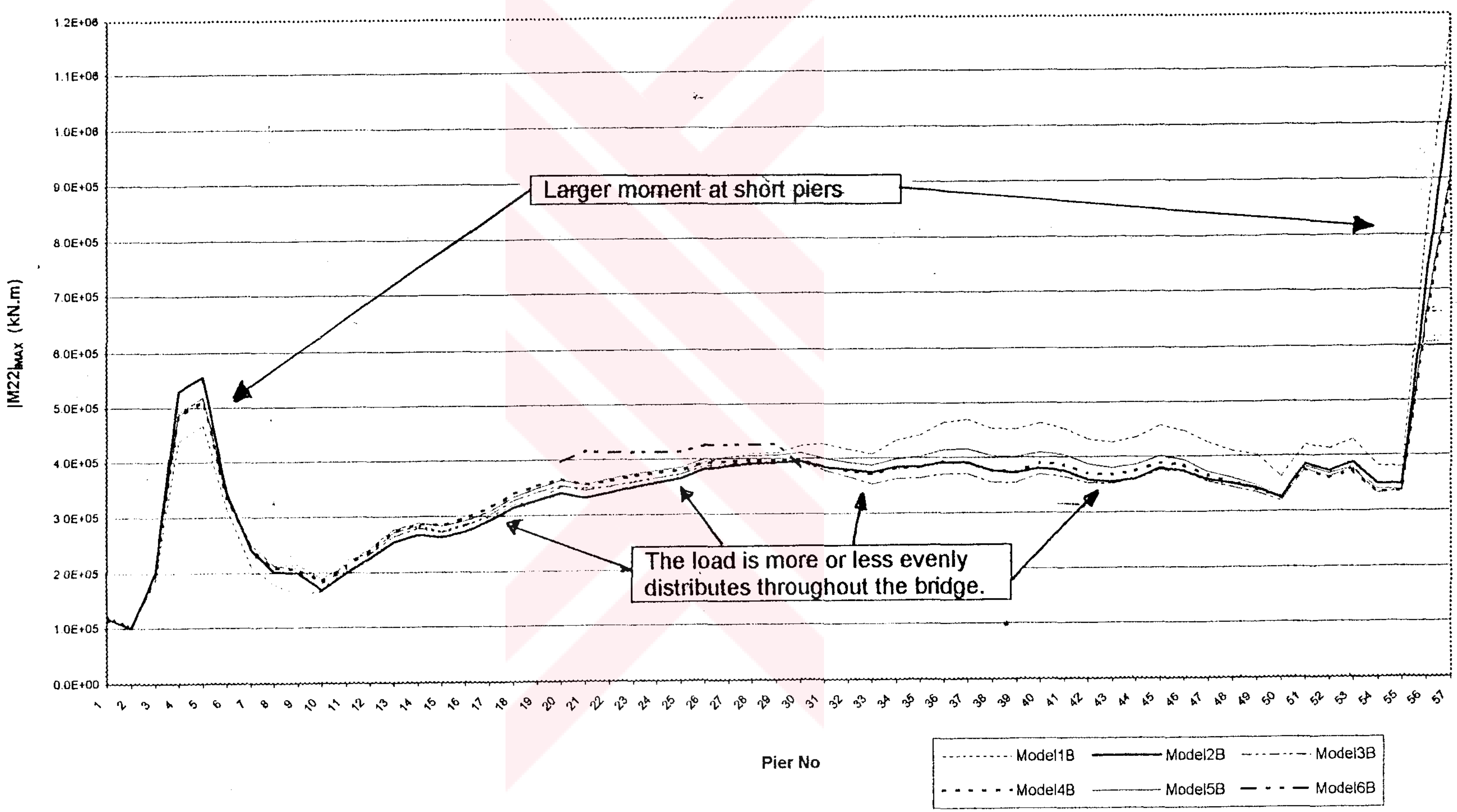


**Figure 5.5 Absolutely Maximum Moment in Longitudinal Direction (CASE B)**

**Table 5.3 Sums of Forces at Pier Bases (CASE B)**

| FORCE | MODEL1B | MODEL2B | MODEL3B | MODEL4B | MODEL5B | MODEL6B | ASTALDI'S MODEL |
|---|---|---|---|---|---|---|---|
| Shear Force, $\|V33\|_{MAX}$ **(Long. Direction)** | 755,832.61 | 745,299.10 | 798,281.33 | 861,043.88 | 883,772.17 | 154,139.95 | 125,760.00 |
| Shear Force, $\|V22\|_{MAX}$ **(Tran. Direction)** | 714,008.35 | 750,565.58 | 757,178.98 | 806,891.06 | 777,496.68 | 134,753.38 | 139,844.00 |
| Moment, $\|M22\|_{MAX}$ **(Long. Direction)** | 21,774,285.60 | 20,137,650.35 | 19,778,274.50 | 20,181,936.60 | 20,636,301.40 | 4,559,594.40 | 2,362,600.00 |
| Moment, $\|M33\|_{MAX}$ **(Tran. Direction)** | 27,904,134.40 | 28,856,856.70 | 29,101,740.27 | 30,518,044.20 | 29,622,113.20 | 5,879,864.60 | 2,959,600.00 |

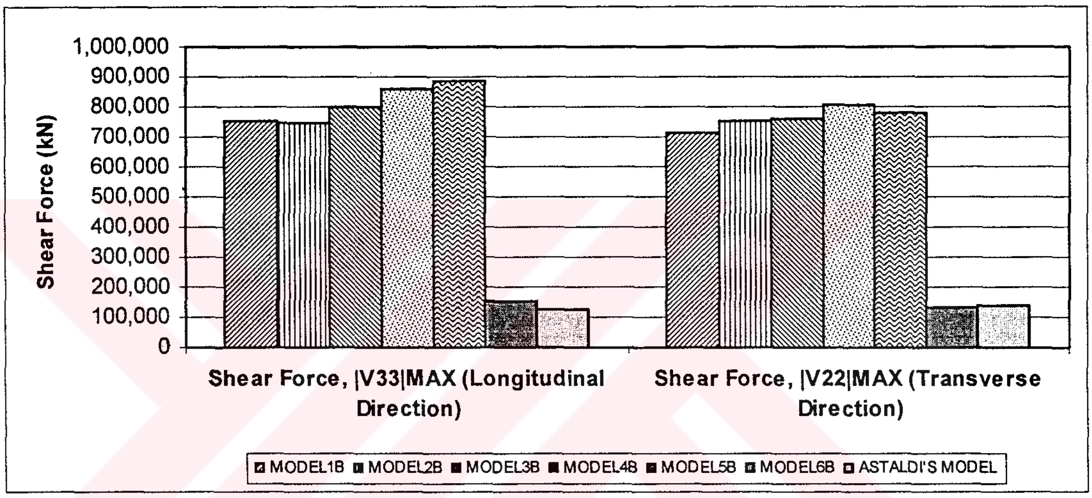


**Figure 5.6 Sums of Shear Forces at Pier Bases (CASE B)**

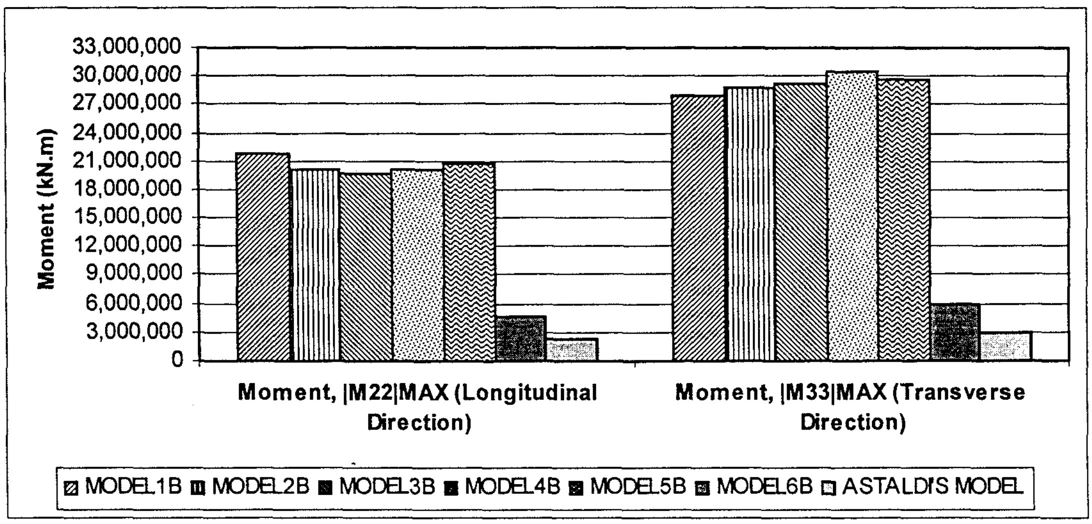


**Figure 5.7 Sums of Moments at Pier Bases (CASE B)**

**Table 5.4 Percentage Variations in Sums of the Forces at Pier Bases (CASE B)**
***(Normalized according to Model1B & Model 6B)**

| FORCE | MODEL1B* | MODEL2B | MODEL3B | MODEL4B | MODEL5B | MODEL6B* | ASTALDI'S MODEL |
|---|---|---|---|---|---|---|---|
| Shear Force, $\lvert V33 \rvert_{MAX}$ **(Long. Direction)** | 0.000 | -0.014 | 0.056 | 0.139 | 0.169 | 0.000 | -0.184 |
| Shear Force, $\lvert V22 \rvert_{MAX}$ **(Tran. Direction)** | 0.000 | 0.051 | 0.060 | 0.130 | 0.089 | 0.000 | 0.038 |
| Moment, $\lvert M22 \rvert_{MAX}$ **(Long. Direction)** | 0.000 | -0.075 | -0.092 | -0.073 | -0.052 | 0.000 | -0.482 |
| Moment, $\lvert M33 \rvert_{MAX}$ **(Tran. Direction)** | 0.000 | 0.034 | 0.043 | 0.094 | 0.062 | 0.000 | -0.497 |

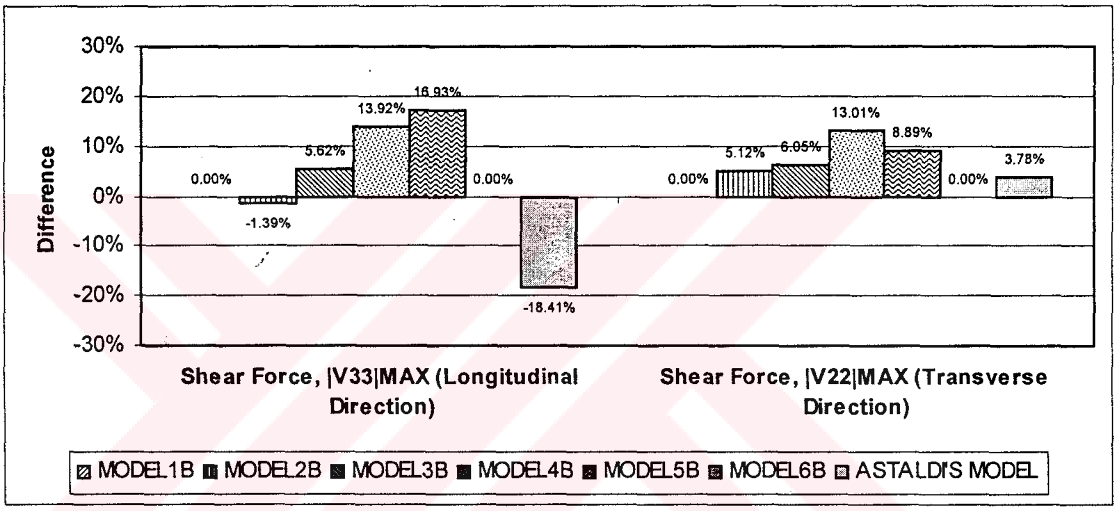


**Figure 5.8 Percentages of Variations in Sums of Shear Forces at Pier Bases (CASE B) (Normalized According To Model 1B & Model 6B)**

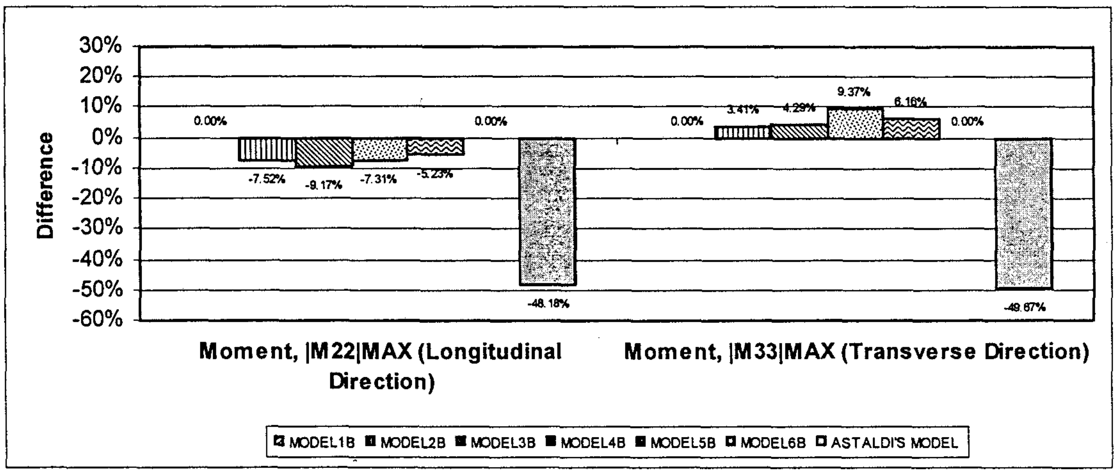


**Figure 5.9 Percentages of Variations in Sums of Moments at Pier Bases (CASE B) (Normalized According To Model 1B & Model 6B)**

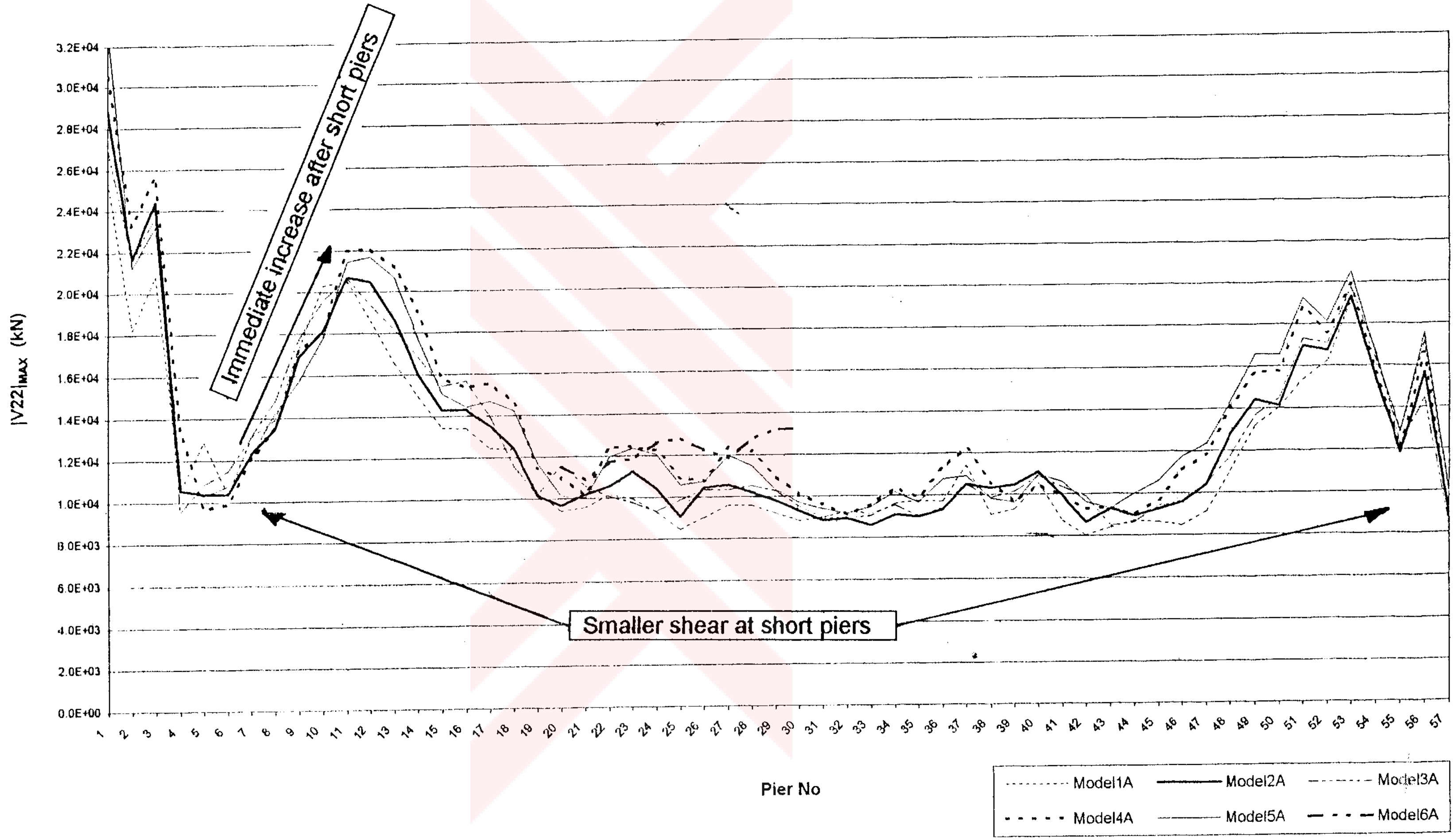


**Figure 5.10 Absolutely Maximum Shear Force in Transverse Direction (CASE A)**

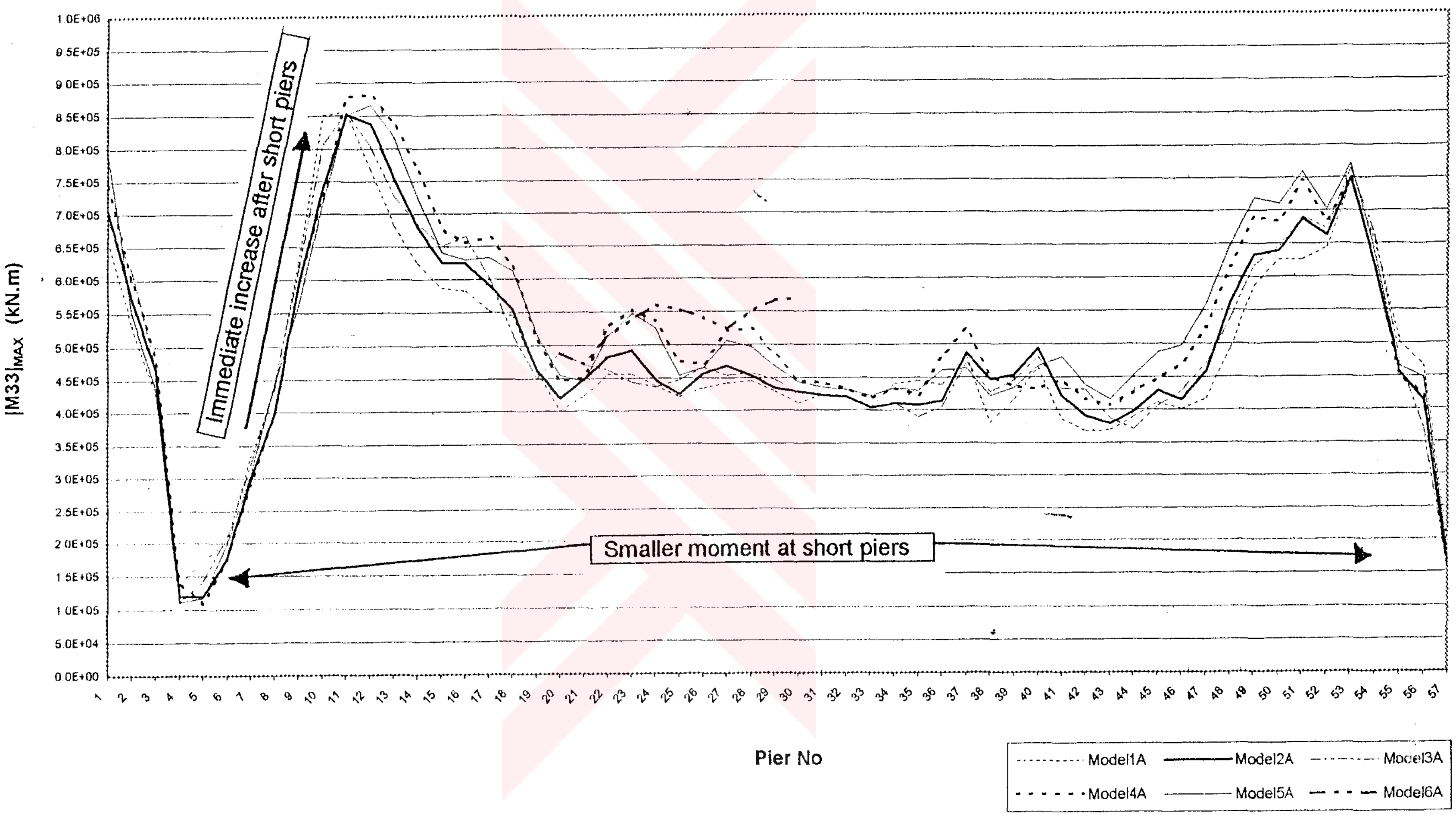


**Figure 5.11 Absolutely Maximum Moment in Transverse Direction (CASE A)**

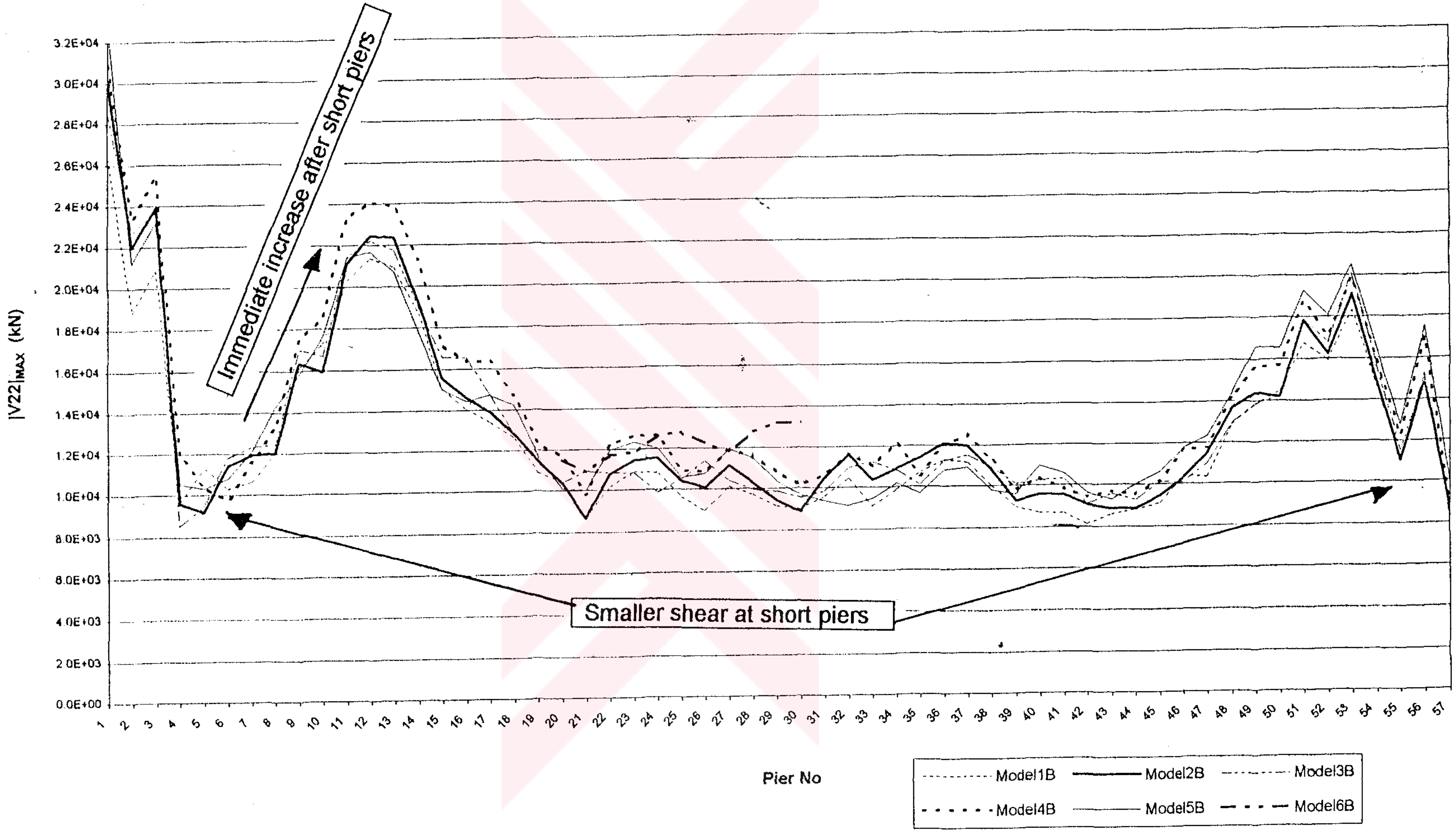


Figure 5.12 Absolutely Maximum Shear Force in Transverse Direction (CASE B)

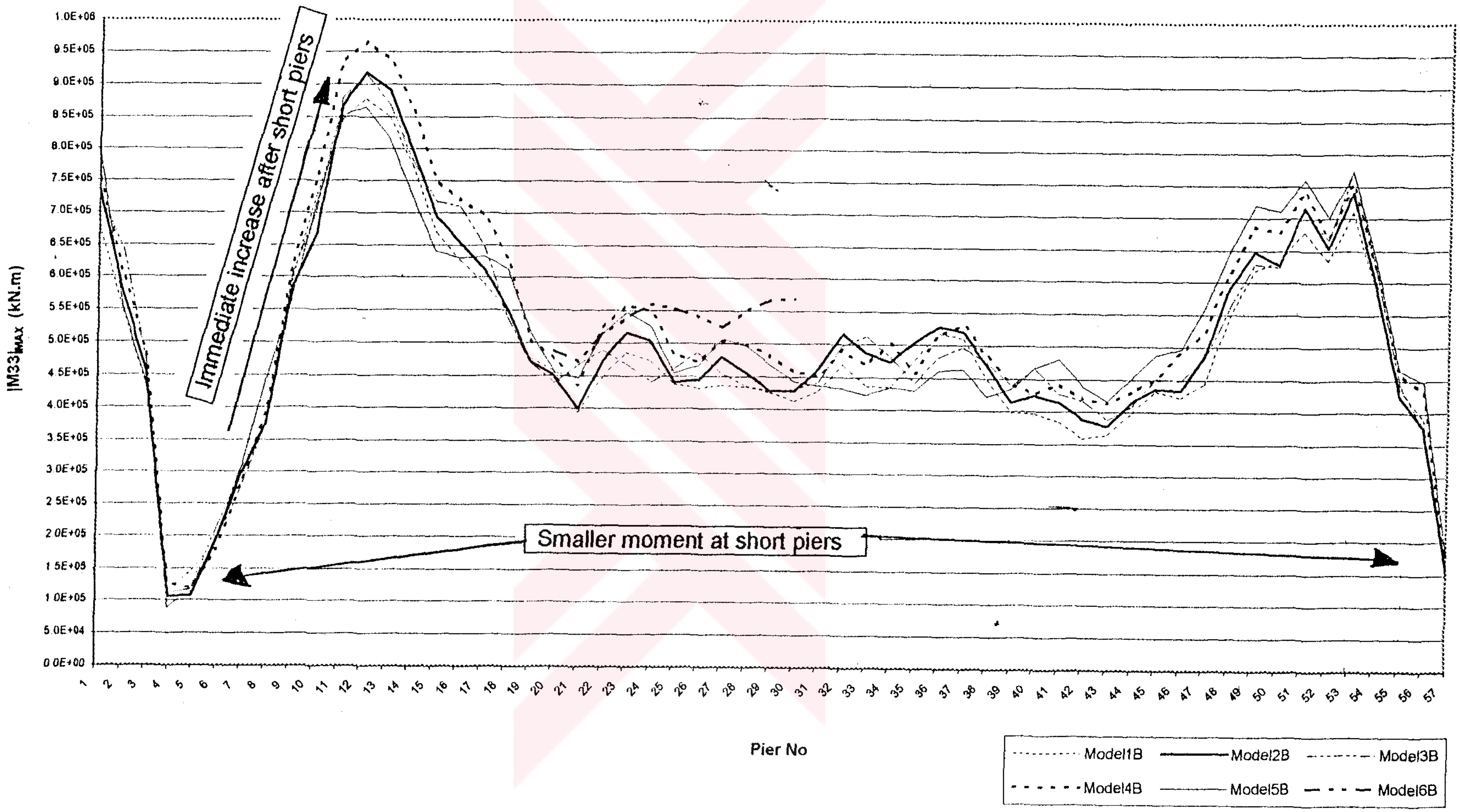


Figure 5.13 Absolutely Maximum Moment in Transverse Direction (CASE B)

### *5.2.1 Model 6 and Astaldi's Model*

Astaldi's Model may only be compared with case (b) of Model 6, because Astaldi's Model is relevant to Model 6B in geometry and complexity level. However, there are differences between these two models. Astaldi's Model represents the bridge portion between Piers 10 and 20, whereas Model 6B represents the bridge portion between Piers 20 and 30. Furthermore, Astaldi constructed this model before the major earthquakes explained in Section 2.1 occurred. That is, the earthquake data used for the two analyses are also different. Another difference is that Astaldi's Model is non-linear while Model 6 uses linear analysis. The overall difference in responses can be clearly seen in the percentage values given in Figure 5.8 and 5.9, for shear force and moment, respectively. (Approximately 50% difference can be observed for moment in both longitudinal and transverse directions.)

In Figures 5.14, 5.15, 5.16, and 5.17, absolutely maximum internal forces (shear, moment) in longitudinal and transverse directions are shown for Astaldi's Model and Model 6B. A major observation for figures both in longitudinal and transverse directions is that shear is same for both models whereas moment for Model 6B is almost two times more than moment for Astaldi's Model.

This is simply because the pier heights in each model are different. This difference in pier heights leads the differences in the moment values for Astaldi's

Model and Model 6B. However, for the case of shear, pier heights do not significantly affect the values of shear forces.

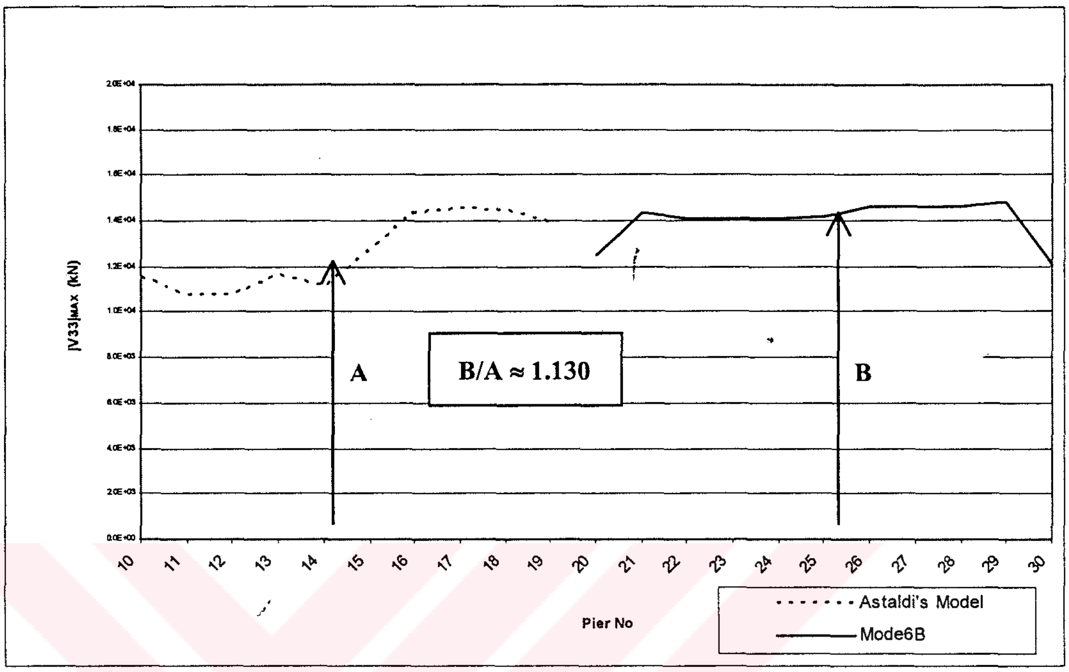


**Figure 5.14 Absolutely Maximum Shear Force in Longitudinal Direction (Comparison of Astaldi's Model and Model 6B)**

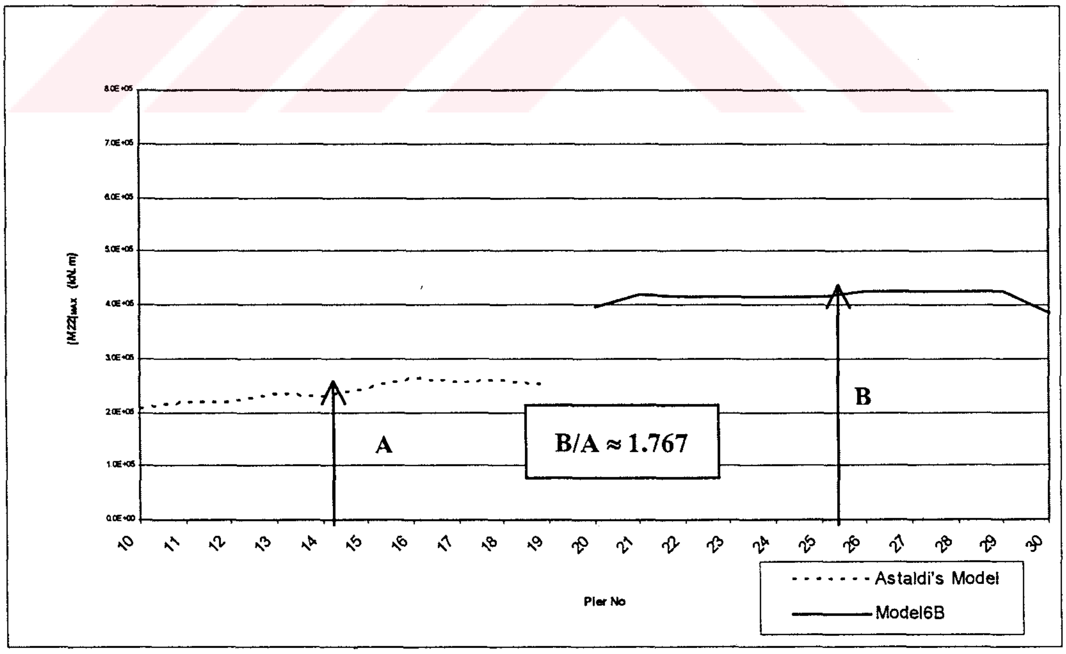


**Figure 5.15 Absolutely Maximum Moment in Longitudinal Direction (Comparison of Astaldi's Model and Model 6B)**

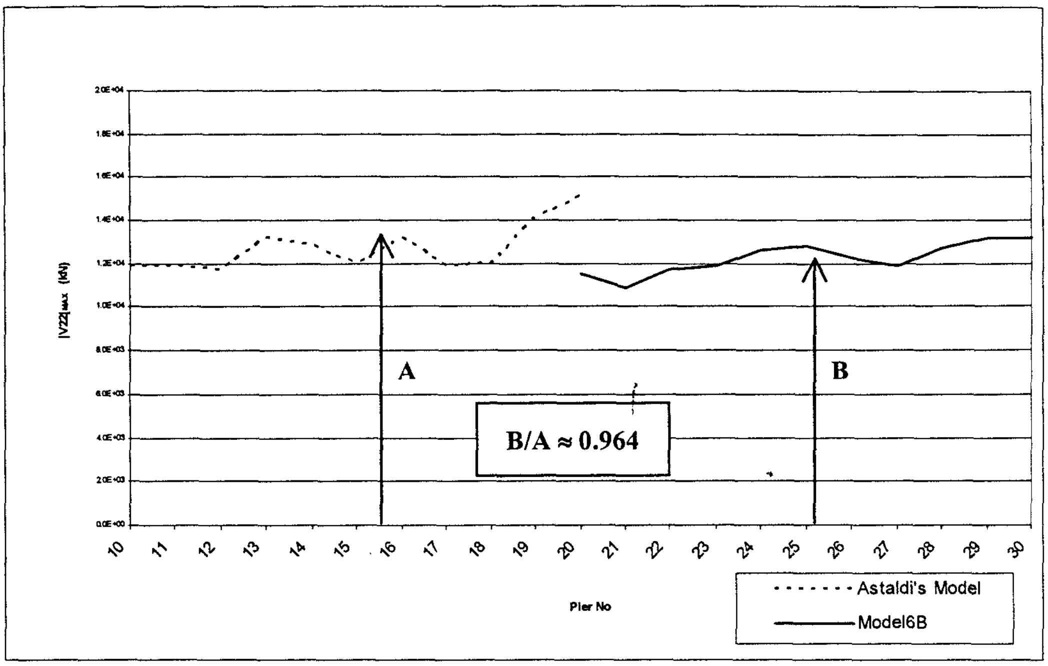


**Figure 5.16 Absolutely Maximum Shear Force in Transverse Direction (Comparison of Astaldi's Model and Model 6B)**

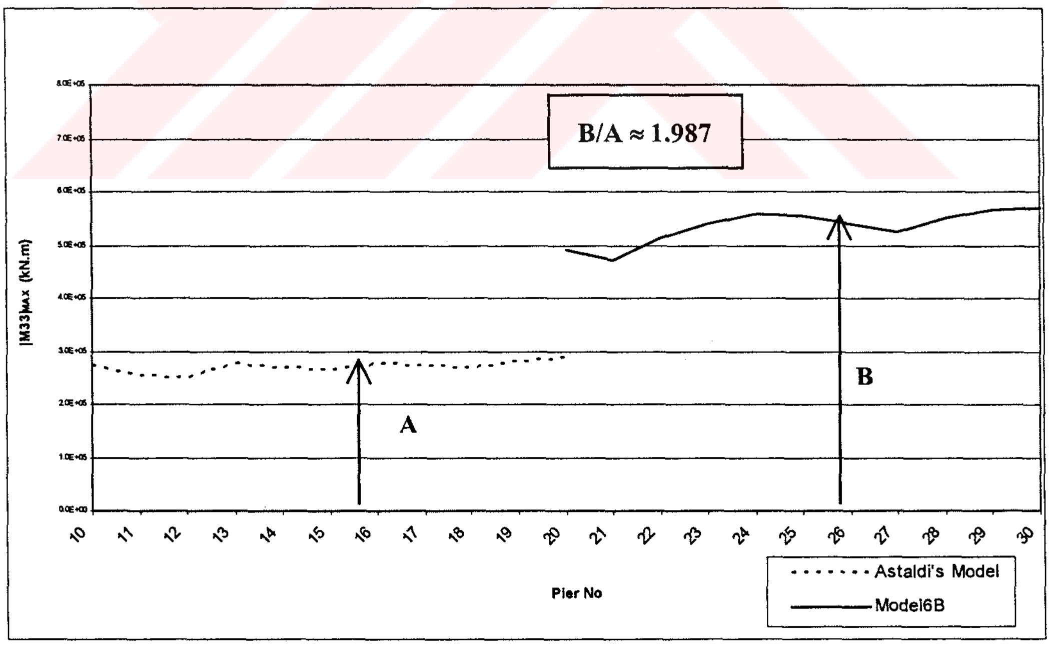


**Figure 5.17 Absolutely Maximum Moment in Transverse Direction (Comparison of Astaldi's Model and Model 6B)**

The envelopes for shear forces and moments for two dimensional Astaldi's Model are tabulated in Figures 5.18 and 5.19

SHEAR [kN]

| PIER | P10 | P11 | P12 | P13 | P14 | P15 | P16 | P17 | P18 | P19 |
|---|---|---|---|---|---|---|---|---|---|---|
| Shear | 7783 | 7265 | 7287 | 7817 | 7439 | 8336 | 9624 | 9446 | 9359 | 8955 |
| Shear | 6681 | 6156 | 6166 | 6786 | 6675 | 6668 | 7233 | 7130 | 6959 | 6703 |
| Shear | 11520 | 10730 | 10770 | 11610 | 11120 | 12780 | 14970 | 14520 | 14420 | 13920 |
| H [m] | 37 | 41 | 41 | 41 | 42 | 44 | 47 | 47 | 47 | 47 |
| Moment | 983 | 1017 | 1020 | 1094 | 1067 | 1247 | 1532 | 1500 | 1481 | 1423 |
| Moment | 1390 | 1469 | 1473 | 1550 | 1474 | 1571 | 1679 | 1695 | 1679 | 1656 |
| Moment | 2099 | 2183 | 2188 | 2330 | 2288 | 2413 | 2629 | 2537 | 2572 | 2451 |

MOMENT x $10^{-2}$ [kNm]

**Figure 5.18 Pier Forces - Longitudinal Earthquake P10-P20 Section**

SHEAR [kN]

| PIER | P10 | P11 | P12 | P13 | P14 | P15 | P16 | P17 | P18 | P19 | P20 |
|---|---|---|---|---|---|---|---|---|---|---|---|
| Shear | 3898 (x2) | 8447 | 8403 | 9043 | 8891 | 8178 | 9001 | 8401 | 8189 | 9993 | 5300 (x2) |
| Shear | 4136 (x2) | 7171 | 6935 | 7295 | 7036 | 6731 | 6562 | 6526 | 6186 | 6393 | 3386 (x2) |
| Shear | 5936 (x2) | 11910 | 11750 | 13150 | 12800 | 12020 | 13190 | 11920 | 12000 | 14120 | 7556 (x2) |
| H [m] | 37 | 41 | 41 | 41 | 42 | 44 | 47 | 47 | 47 | 47 | 47 |
| Moment | 490 (x2) | 1174 | 1167 | 1258 | 1264 | 1211 | 1434 | 1341 | 1308 | 1591 | 845 (x2) |
| Moment | 891 (x2) | 1755 | 1746 | 1818 | 1824 | 1817 | 1967 | 1885 | 1912 | 2026 | 1071 (x2) |
| Moment | 1355 (x2) | 2535 | 2505 | 2742 | 2666 | 2631 | 2737 | 2731 | 2662 | 2802 | 1428 (x2) |

MOMENT x $10^{-2}$ [kNm]

**Figure 5.19 Pier Forces - Transverse Earthquake P10-P20 Section**

Despite the differences between Astaldi's Model and Model 6B mentioned above, two different charts are formed to have a general idea about the approximate value of Earthquake Load Reduction Factor, which will be called as "R Factor". The values of shear forces and the values of moments at pier bases are shown separately in these charts (Figure 5.16, 5.17). The values for Model 6B are entered in horizontal axis (abscissa), and the values for Astaldi's Model are entered in vertical axis (ordinate). Both longitudinal and transverse values are entered in the same figure and the averages of each set are connected to the origin. The proportion of ordinate to abscissa gives the R Factor (Figure 5.20 and Figure 5.21).

This factor can also be calculated by dividing the sum of the values of internal forces (shear force, moment) at pier bases for Model 6B to the sum of the values of internal forces (shear force, moment) at pier bases for Astaldi's Model, both in longitudinal and transverse direction. On that case, two different R Factors can be found for each separate chart: $R_{LONG}$ and $R_{TRAN}$. However, the values are close to each other:

$R_{LONG}$=1.130, $R_{TRAN}$=0.964 (using shear force values).

$R_{LONG}$=1.767, $R_{TRAN}$=1.987 (using moment values).

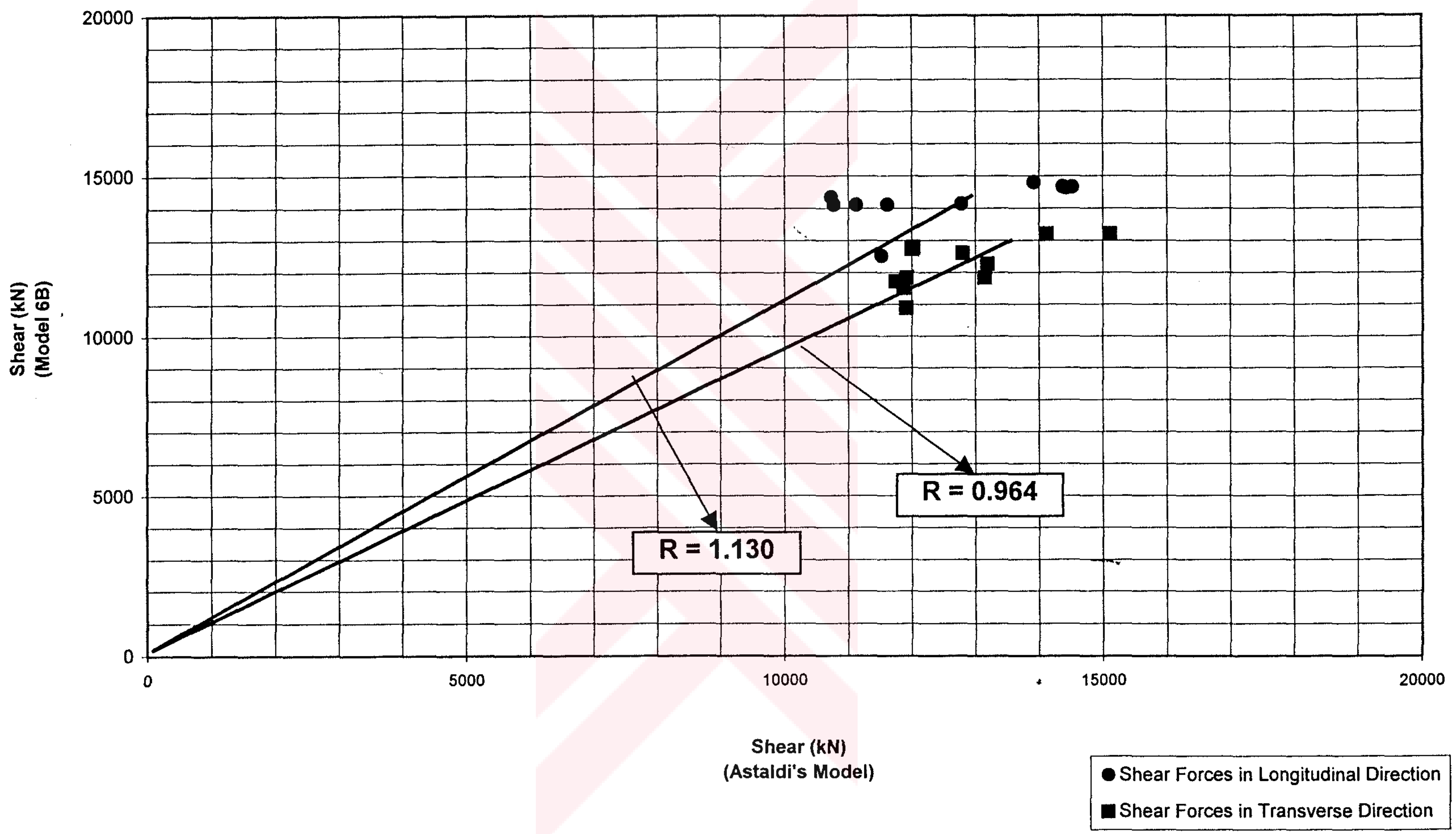


**Figure 5.20 Earthquake Load Reduction Factor (R Factor)**
**(Shear Force Values)**

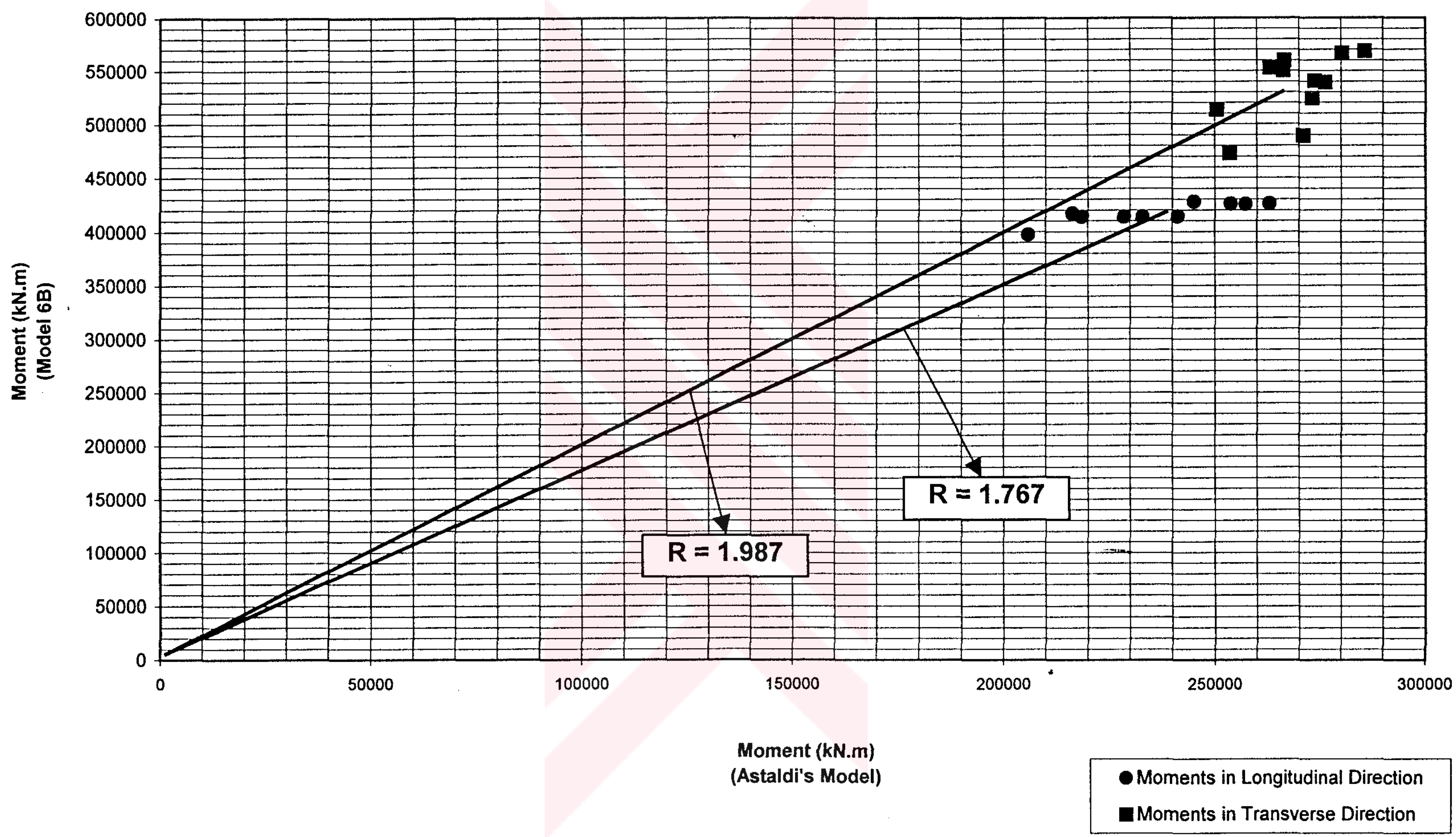


**Figure 5.21 Earthquake Load Reduction Factor (R Factor)**
**(Moment Values)**

The R Factor calculated for pier moments are in fact due to the height differences of piers used in two different models (i.e. Astaldi's Model and Model 6B). These two models are formed for different bridge portions (i.e. Pier 10 to 20 for Astaldi's Model, and Pier 20 to 30 for Model 6B). Because of this fact, the R Factor chart for shear force values is more logical to comment on. In Figure 5.14, 5.15, 5.16, and 5.17, the differences in both models can be seen. Astaldi's Model was used to simulate major earthquake recordings. Although the R Factor is found to be close to 1 (Figure 5.20) and shear values are close (Figure 5.14 and 5.16), the actual response of Model 6B would have been much lower if Energy Dissipating Units (EDU) were non-linearly modeled. That shows the anticipated earthquake loads for Astaldi were much larger than measured earthquake response of Düzce.

### *5.2.2 Comparison with Lollipop Model*

As explained in Section 4.1.9, a lollipop like model is formed in order to make a reality check and compare against all models constructed so far. This can be done only for case (a), since in case (b) all piers are transferring shear in longitudinal direction. In case (a), all the loads gather in the central fixed pier. In Table 5.5, a comparison is shown between Model 1A to 6A and Lollipop Model.

**Table 5.5 Comparison of the Internal Forces in Longitudinal Direction with Simple Lollipop Model**

| MODEL | $\|V33\|_{MAX}$ (Long.) (kN) | $\|M22\|_{MAX}$ (Long.) (kN.m) |
|---|---|---|
| **Lollipop Model (Pier 20-30 lumped at Pier 25)** | 39,139 | 1,911,690 |
| **Model 1A - Pier 25** | 37,891 | 1,747,111 |
| **Model 2A - Pier 25** | 35,817 | 1,583,994 |
| **Model 3A - Pier 25** | 32,890 | 1,388,359 |
| **Model 4A - Pier 25** | 25,273 | 900,538 |
| **Model 5A - Pier 25** | 26,765 | 955,738 |
| **Model 6A - Pier 25** | 26,776 | 956,113 |

As it can be seen from Table 5.5, the values of shear forces and moments in longitudinal direction calculated for Lollipop Model are close to Model 1A. However, it should not be forgotten that all the dimensional features are ignored in Lollipop Model. For example, moments coming from the width of the deck are ignored and it is assumed that the whole mass is on top of the pier. Although Model 6A is more close to Lollipop Model when simplicity is concerned, it cannot be said that Lollipop Model completely represents the correct behavior of a bridge in case of an earthquake.

### 5.3 Displacements

In case (a), it can be said that first three models (Model 1A, 2A, and 3A) give larger displacements at central fixed piers than the other models in both directions (global X-direction (East) and global Y-direction (North)) (Figure 5.22, 5.23). This is more clearly seen in global X-direction, because global X-direction is close to the longitudinal direction of the bridge. (There is approximately an angle of 31 degrees between longitudinal direction of the bridge and global X-direction). The displacement values at these specific locations (central fixed piers) are also tabulated in Table 5.6.

**Table 5.6 Peak Displacements at Central Fixed Pier Caps (CASE A)**

| | DISPLACEMENT | UNIT | MODEL1A | MODEL2A | MODEL3A | MODEL4A | MODEL5A | MODEL6A |
|---|---|---|---|---|---|---|---|---|
| PIER 5 | $\|UX\|_{MAX}$ (East) | m | 0.0608 | 0.0609 | 0.0600 | 0.0443 | 0.0475 | N/A |
| | $\|UY\|_{MAX}$ (North) | m | 0.0477 | 0.0485 | 0.0476 | 0.0349 | 0.0022 | N/A |
| | $\|U\|_{MAX}$ | m | 0.0773 | 0.0779 | 0.0766 | 0.0564 | 0.0476 | N/A |
| PIER 15 | $\|UX\|_{MAX}$ (East) | m | 0.8244 | 0.7427 | 0.6113 | 0.4371 | 0.4799 | N/A |
| | $\|UY\|_{MAX}$ (North) | m | 0.6675 | 0.5901 | 0.4803 | 0.3474 | 0.1440 | N/A |
| | $\|U\|_{MAX}$ | m | 1.0542 | 0.9399 | 0.7509 | 0.5142 | 0.4809 | N/A |
| PIER 25 | $\|UX\|_{MAX}$ (East) | m | 1.0710 | 0.9706 | 0.8591 | 0.4389 | 0.4004 | 0.4005 |
| | $\|UY\|_{MAX}$ (North) | m | 0.8675 | 0.7699 | 0.6416 | 0.3774 | 0.1115 | 0.1347 |
| | $\|U\|_{MAX}$ | m | 1.3772 | 1.2226 | 1.0437 | 0.6093 | 0.5498 | 0.5535 |
| PIER 35 | $\|UX\|_{MAX}$ (East) | m | 1.3422 | 1.2355 | 1.0727 | 0.6070 | 0.5848 | N/A |
| | $\|UY\|_{MAX}$ (North) | m | 0.7822 | 0.7244 | 0.6152 | 0.3824 | 0.1138 | N/A |
| | $\|U\|_{MAX}$ | m | 1.5068 | 1.4000 | 1.2096 | 0.7013 | 0.5862 | N/A |
| PIER 45 | $\|UX\|_{MAX}$ (East) | m | 1.0038 | 0.9586 | 0.7142 | 0.5499 | 0.4800 | N/A |
| | $\|UY\|_{MAX}$ (North) | m | 0.4463 | 0.4384 | 0.3620 | 0.2974 | 0.1114 | N/A |
| | $\|U\|_{MAX}$ | m | 1.0716 | 1.0285 | 0.8007 | 0.6236 | 0.6236 | N/A |
| PIER 54 | $\|UX\|_{MAX}$ (East) | m | 0.3097 | 0.2990 | 0.2903 | 0.2556 | 0.2665 | N/A |
| | $\|UY\|_{MAX}$ (North) | m | 0.2378 | 0.2145 | 0.2063 | 0.1630 | 0.1187 | N/A |
| | $\|U\|_{MAX}$ | m | 0.5062 | 0.4776 | 0.4533 | 0.3981 | 0.3121 | N/A |

The fact that larger displacements occur in first three models means that the third dimension (width factor) affects the displacement values. About 56% difference in both directions is observed (Figure 5.22, 5.23). In Figure 5.24, maximum displacements at central fixed pier caps are calculated by using the square root of sum of squares of displacement values at each time step in both directions. It is observed that large differences occur at the Piers 15. 25, 35, and 45, which are high central piers; and small differences occur at the Piers 5 and 54, which are short central piers.

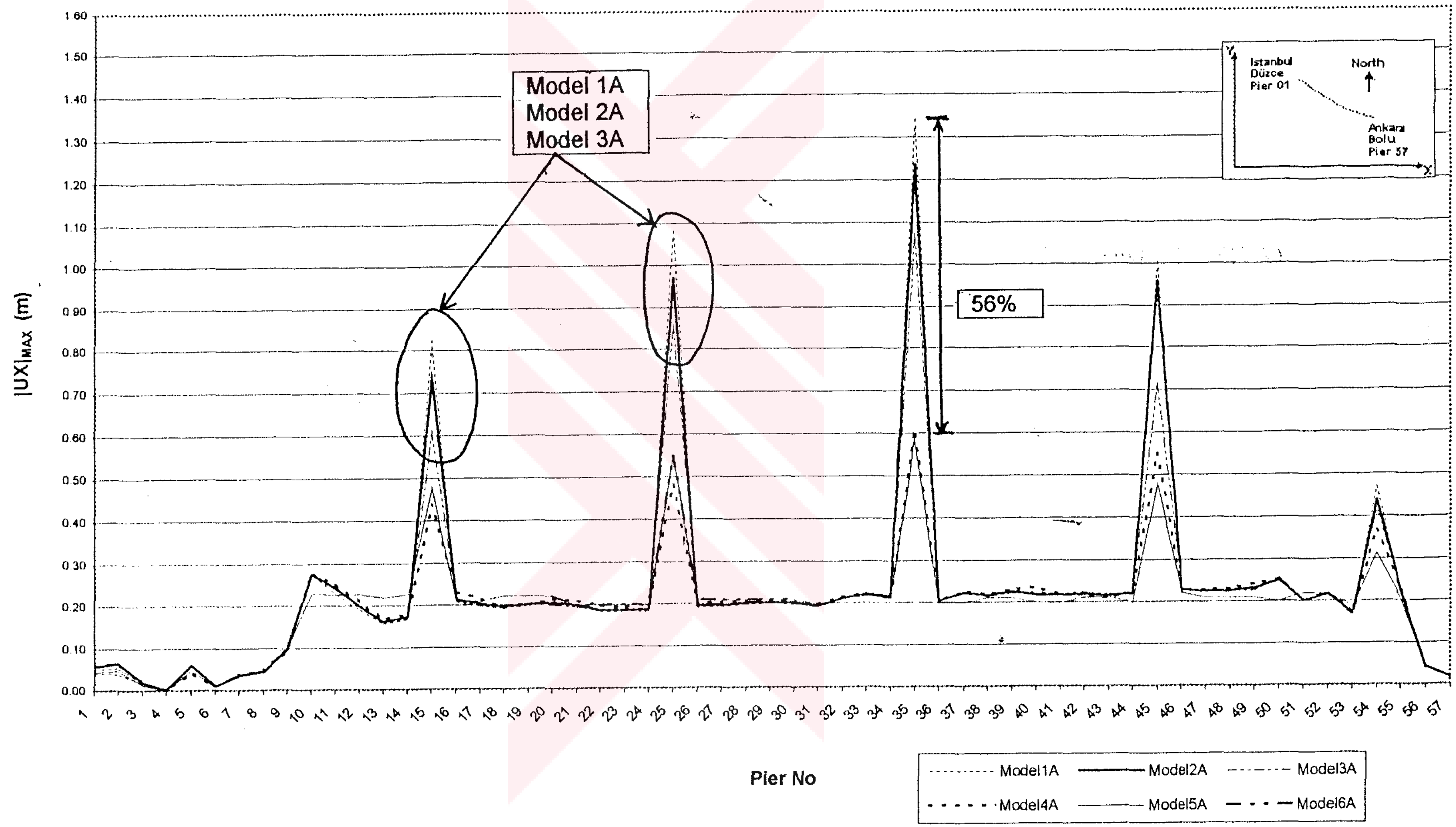


Figure 5.22 Absolutely Maximum Displacements at Pier Caps in Global X-Direction (East) (CASE A)

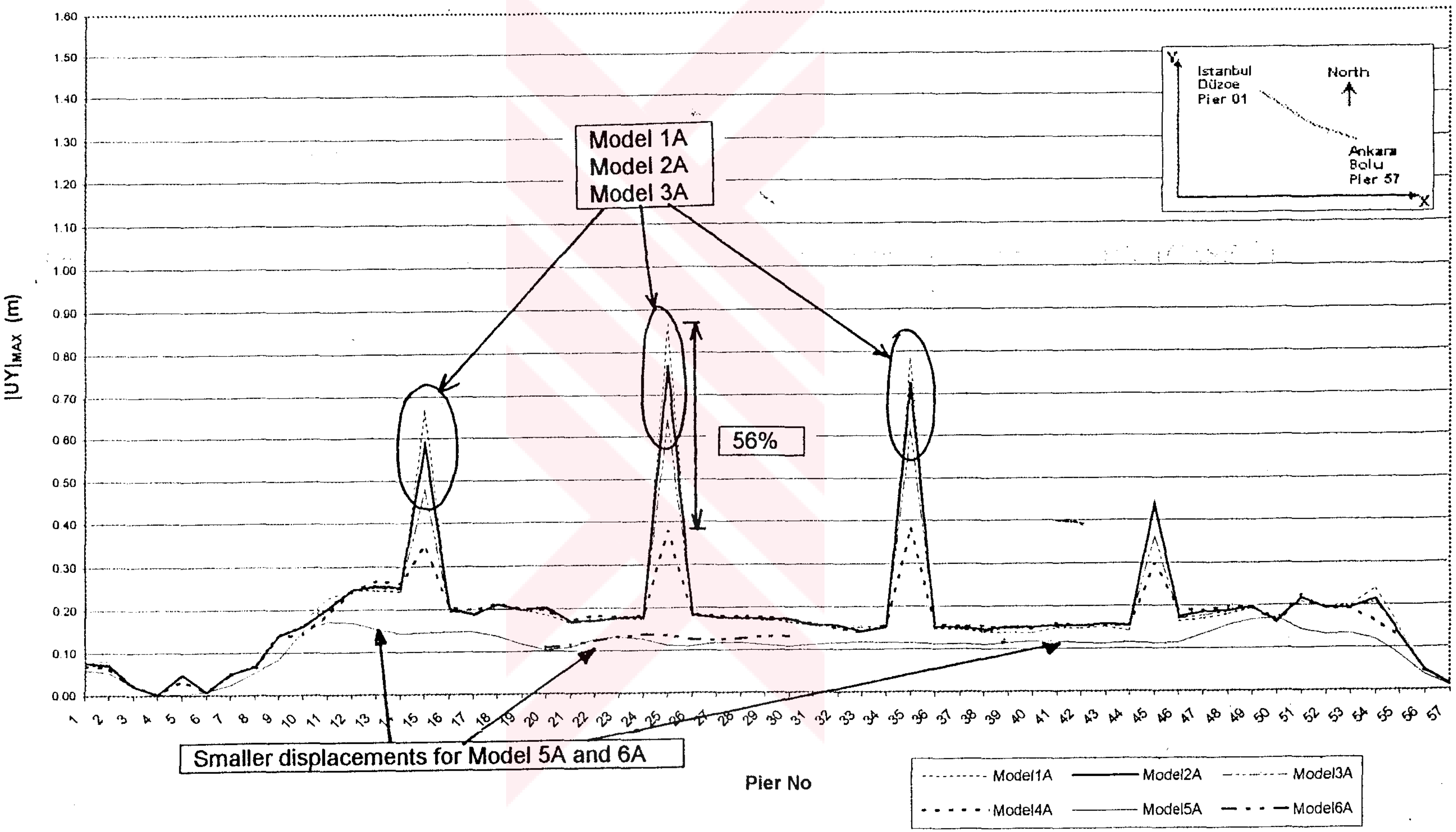


Figure 5.23 Absolutely Maximum Displacements at Pier Caps in Global Y-Direction (North) (CASE A)

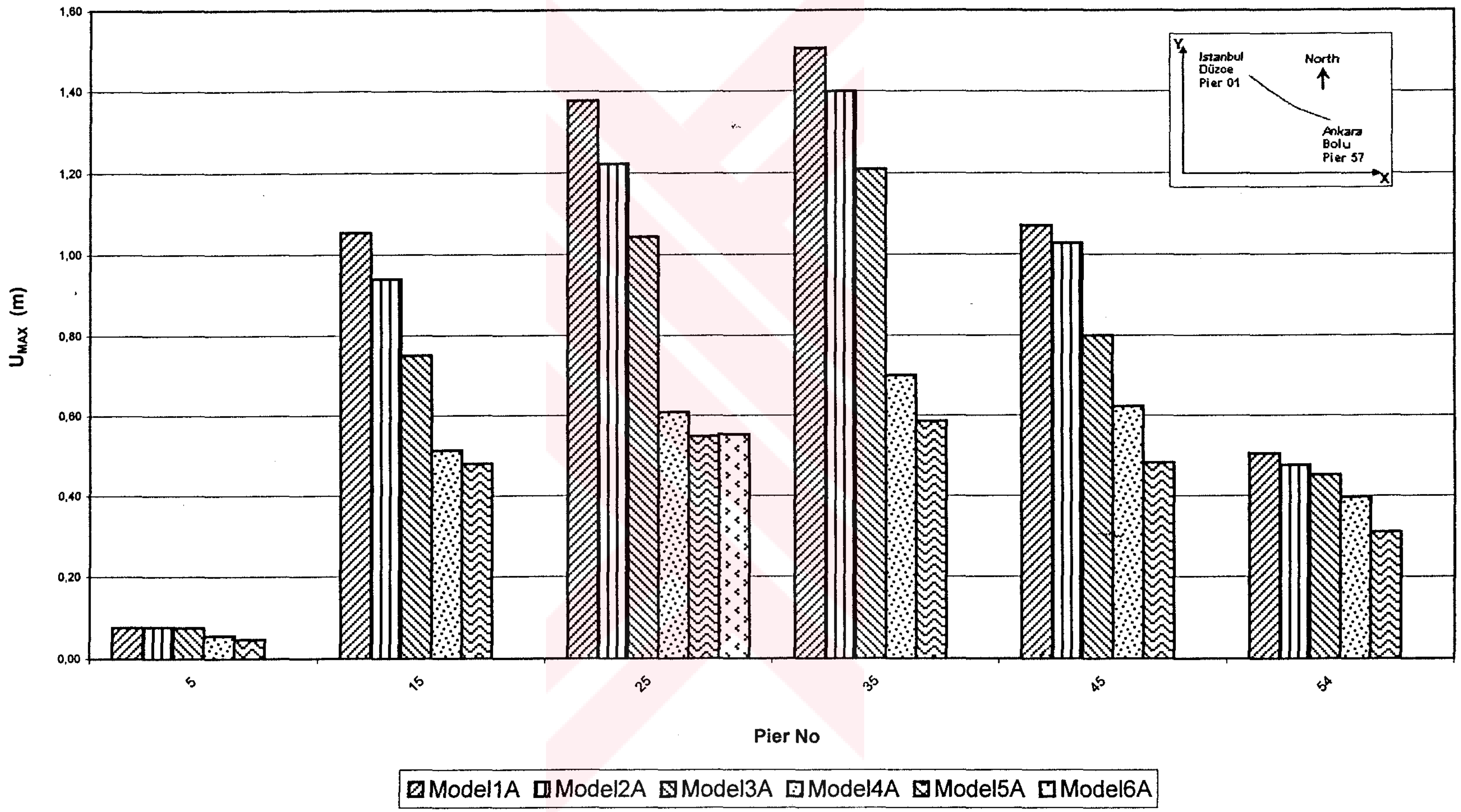


**Figure 5.24 Modified Maximum Displacements at Central Fixed Pier Caps**
**$[U_{MAX} = (|UX|_{MAX}^2 + |UY|_{MAX}^2)^{1/2}]$ (CASE A)**

The displacements for Model 5A and Model 6A in global Y-direction (North) are smaller than values of the other models (Figure 5.23), since the orientation of the bridge in Model 5 and Model 6 is not same as in the other models. In order to make the models 2 dimensional, approximately an angle of 31 degrees from global X-direction is ignored in these models; and this leads the difference in the displacement values.

In case (b), there are no peak displacement values, since there are no specific central fixed piers. The deformation is more or less evenly distributes throughout the bridge (Figure 5.25, 5.26). On the other hand, for Piers 4, 5, 6, 56, and 57, which are very short compared to other piers, there are small displacement values for both in global X- and Y-directions. The decrease in the vicinity of Pier 5 demonstrates the general short column behavior very well (Figure 5.25, 5.26).

For the absolutely maximum displacements at pier caps in global X-direction, it is interesting that Model 5 gives a smooth line and Model 3B and 4B are almost equal (Figure 5.25). Model 1B makes large deviations in the middle portions of the whole bridge. Model 2B behaves as an average of Model 1B and Model 3B (or Model 4B).


**Figure 5.25 Absolutely Maximum Displacements at Pier Caps in Global X-Direction (East) (CASE B)**

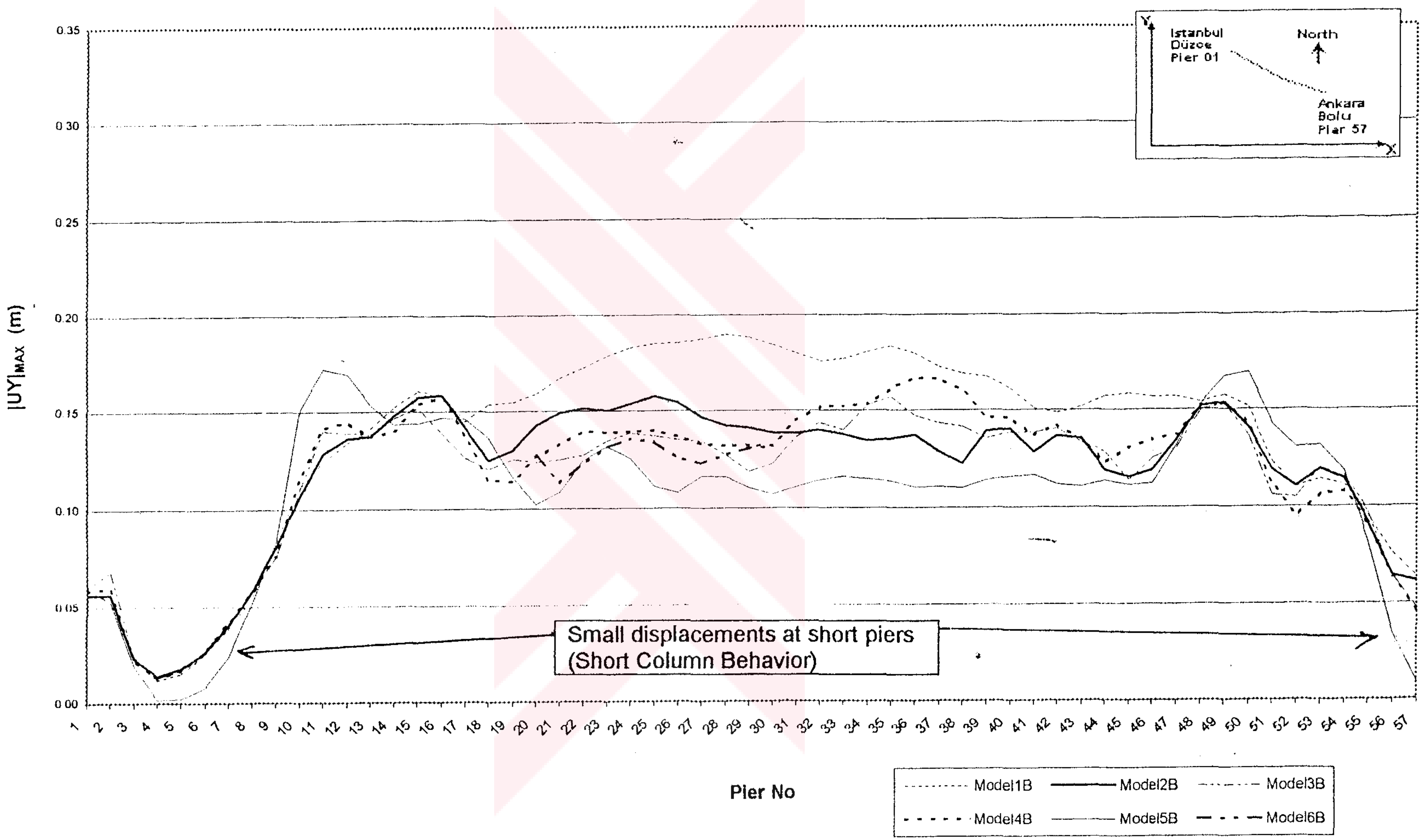


**Figure 5.26 Absolutely Maximum Displacements at Pier Caps in Global Y-Direction (North) (CASE B)**

The maximum displacements in both directions (global X-direction (East) and global Y-direction (North)) is summarized in Table 5.7. As it is seen in this table, maximum of the maximum displacements is in Model 1B.

**Table 5.7 Maximum Displacements for Case B**

| MODEL | $\|UX\|_{MAX}$ (m) (Global X-direction, or East) | $\|UY\|_{MAX}$ (m) (Global Y-direction, or North) |
|---|---|---|
| Model 1B | 0.3136 | 0.1898 |
| Model 2B | 0.2528 | 0.1586 |
| Model 3B | 0.2275 | 0.1586 |
| Model 4B | 0.2357 | 0.1670 |
| Model 5B | 0.2011 | 0.1723 |
| Model 6B | 0.2206 | 0.1361 |
| Astaldi's Model | 0.2970 (in longitudinal direction of the bridge) | |

*Note: There is an angle of approximately 31 degrees between the longitudinal direction of the bridge and global X-direction (East).*

In Figure 5.27, maximum displacements at the caps of selected piers (the same pier numbers as central fixed piers in case (a)) are calculated by using the square root of sum of squares of displacement values at each time step in both directions. It is observed that the smallest displacements occur at Pier 5, which is the shortest of them. Furthermore, the modified "maximum displacements for all models at this short pier (Pier 5) are slightly different (almost same). However, some large differences can be observed at the other high piers (Figure 5.27).

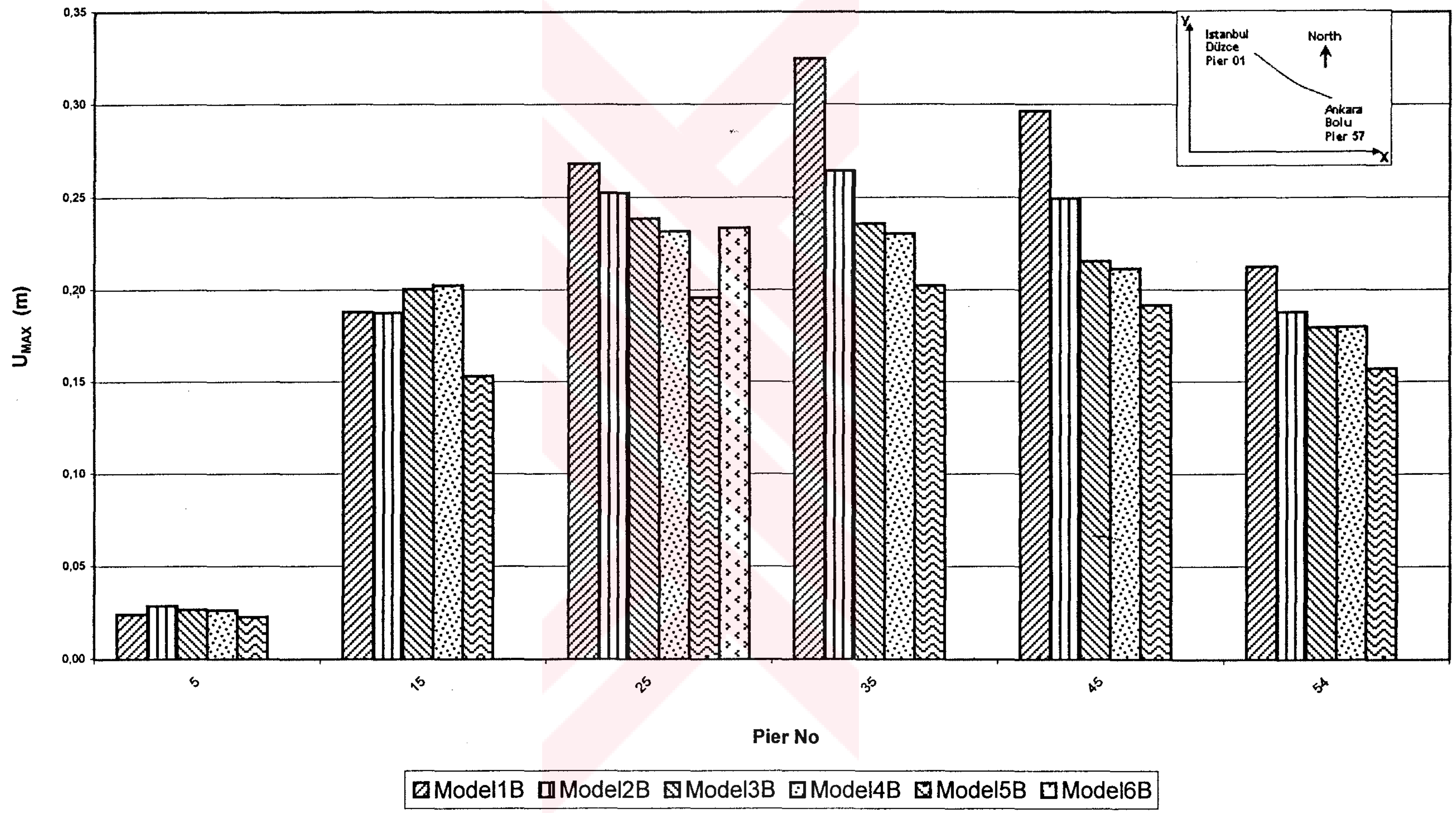


**Figure 5.27 Modified Maximum Displacements at Selected Pier Caps**
**[$U_{MAX} = (|UX|_{MAX}^2 + |UY|_{MAX}^2)^{1/2}$] (CASE B)**

Pier 25 is selected as an example for comparison of whole time history traces of pier cap displacements. Results for Case (a) are shown in Figures 5.28, 5.29 and 5.30 in global X-direction, global Y-direction, and modified maximum values, respectively. For Case (b), similar Figures are obtained and shown in Figures 5.31, 5.32, and 5.33.

There are significant differences between the time history traces of groups of models for case (a). It is observed that Model 1A, 2A, and 3A have similar behavior. Similarly, Model 4A, 5A, and 6A have also similar responses. The differences and similarities are mainly due to modeling techniques used for those models. The first thee models have third dimensional effect whereas others are mostly wire frame models. This result highlights the importance of fully considering third dimensional shape in modeling. On the other hand, for case (b), this grouping is not observed; however, it can be said that the behaviors of all models in case (b) are similar.

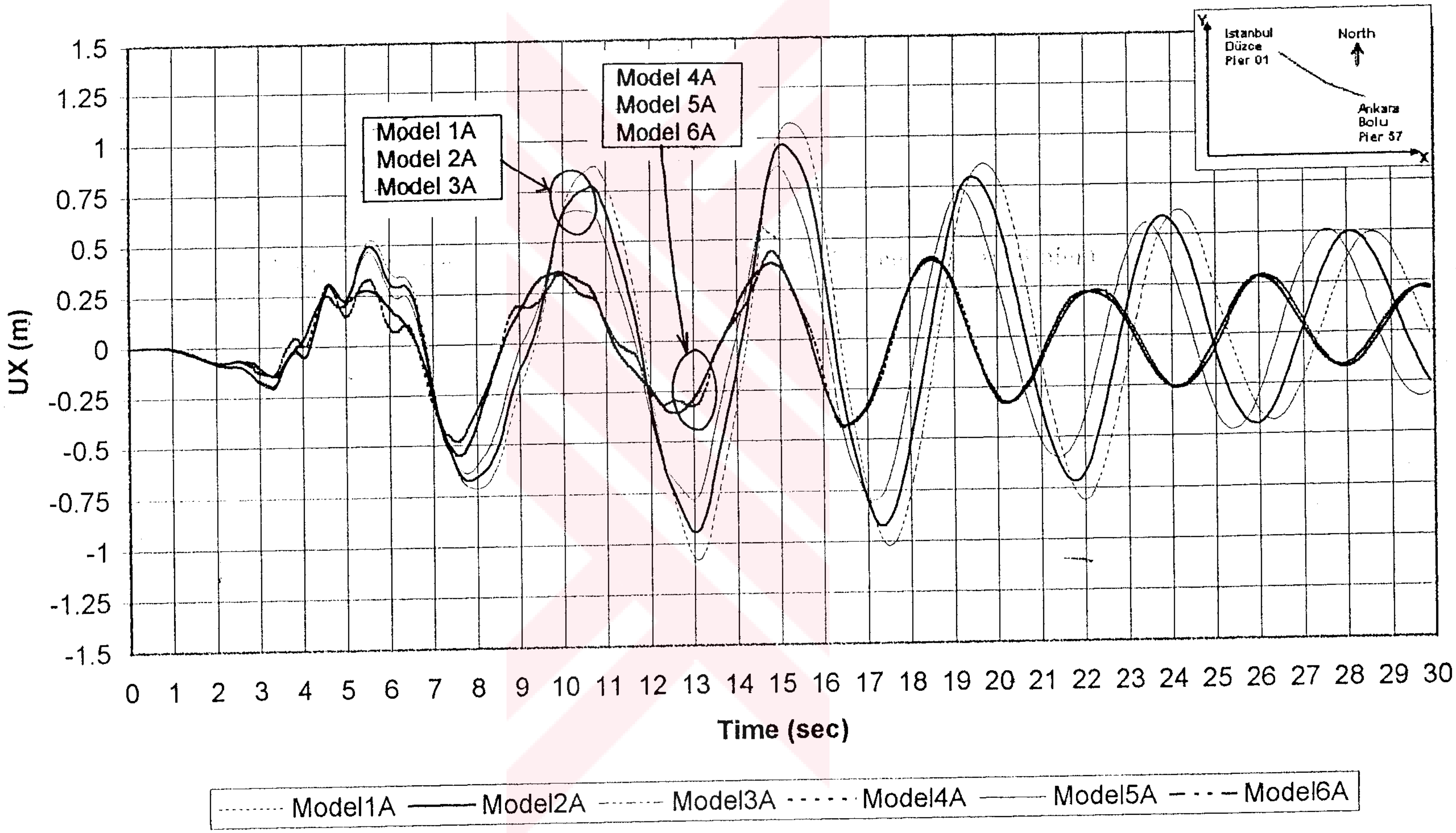


**Figure 5.28 Displacements at Pier Cap of Pier25 (a central fixed pier) in Global X-Direction (East) (CASE A)**

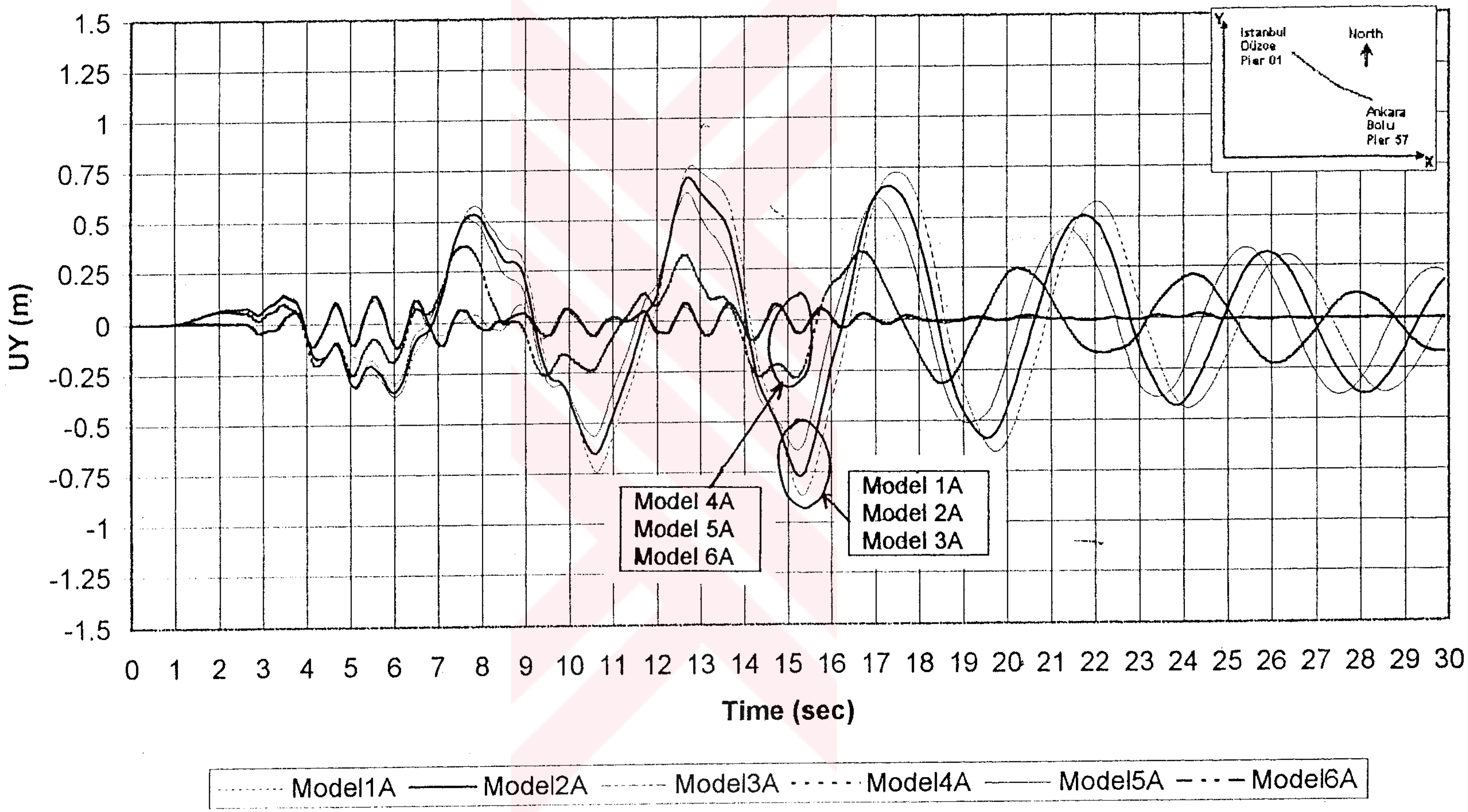


**Figure 5.29 Displacements at Pier Cap of Pier25 (a central fixed pier) in Global Y-Direction (North) (CASE A)**

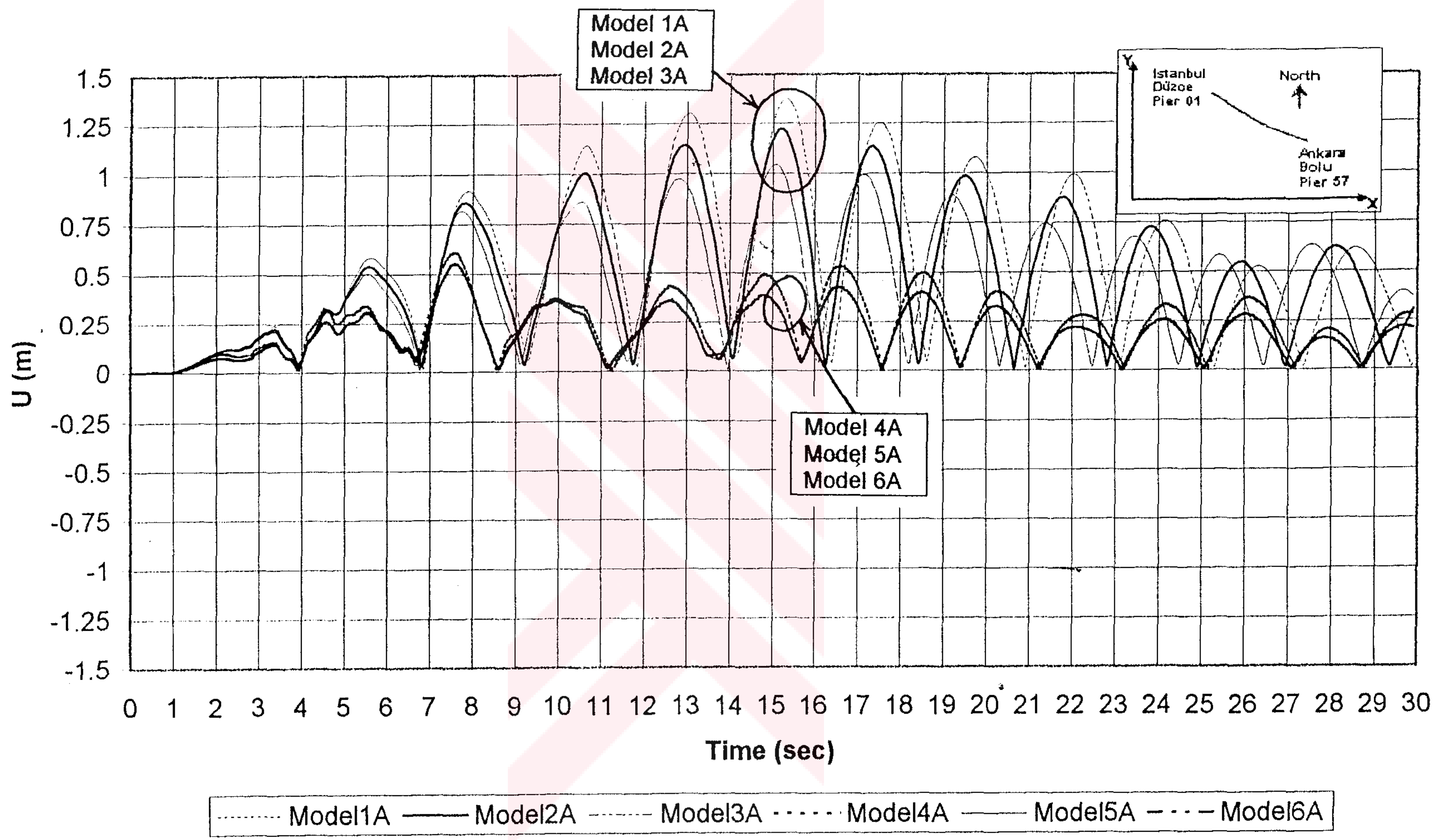


**Figure 5.30 Modified Displacements at Pier Cap of Pier25 (a central fixed pier)**
**$[U=(UX^2+UY^2)^{1/2}]$ (CASE A)**

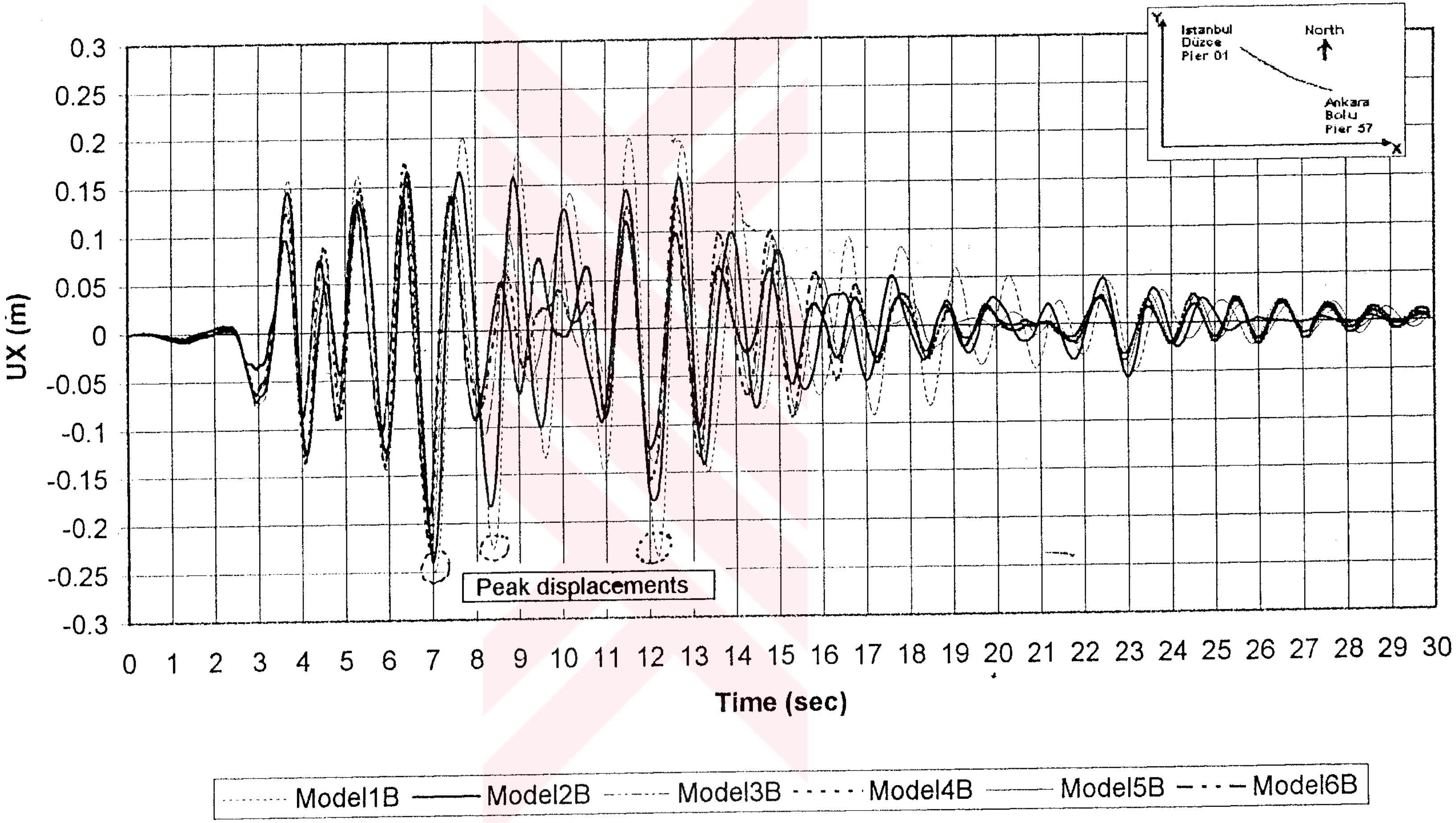


Figure 5.31 Displacements at Pier Cap of Pier25 (a selected pier) in Global X-Direction (East) (CASE B)

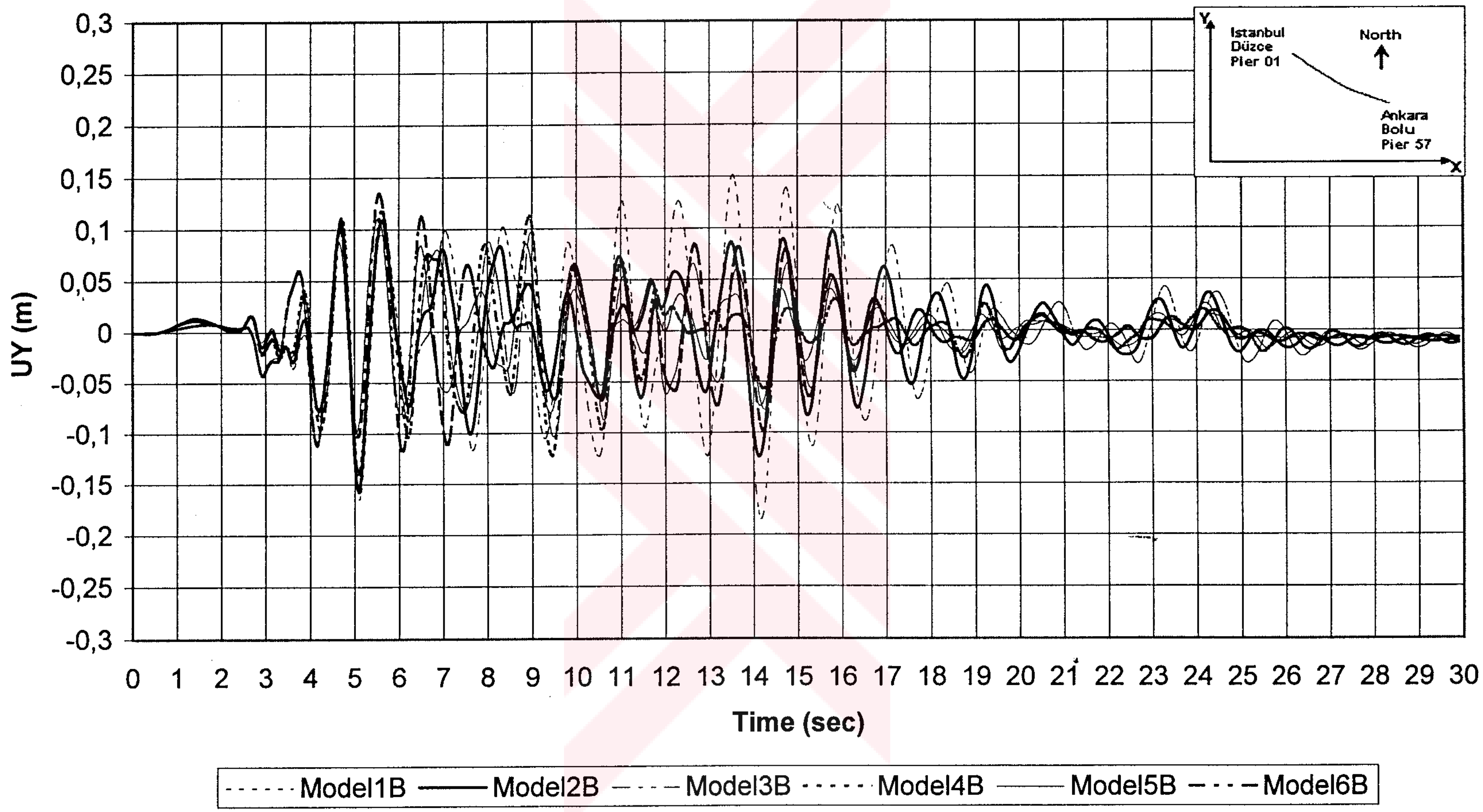


Figure 5.32 Displacements at Pier Cap of Pier25 (a selected pier) in Global Y-Direction (North) (CASE B)

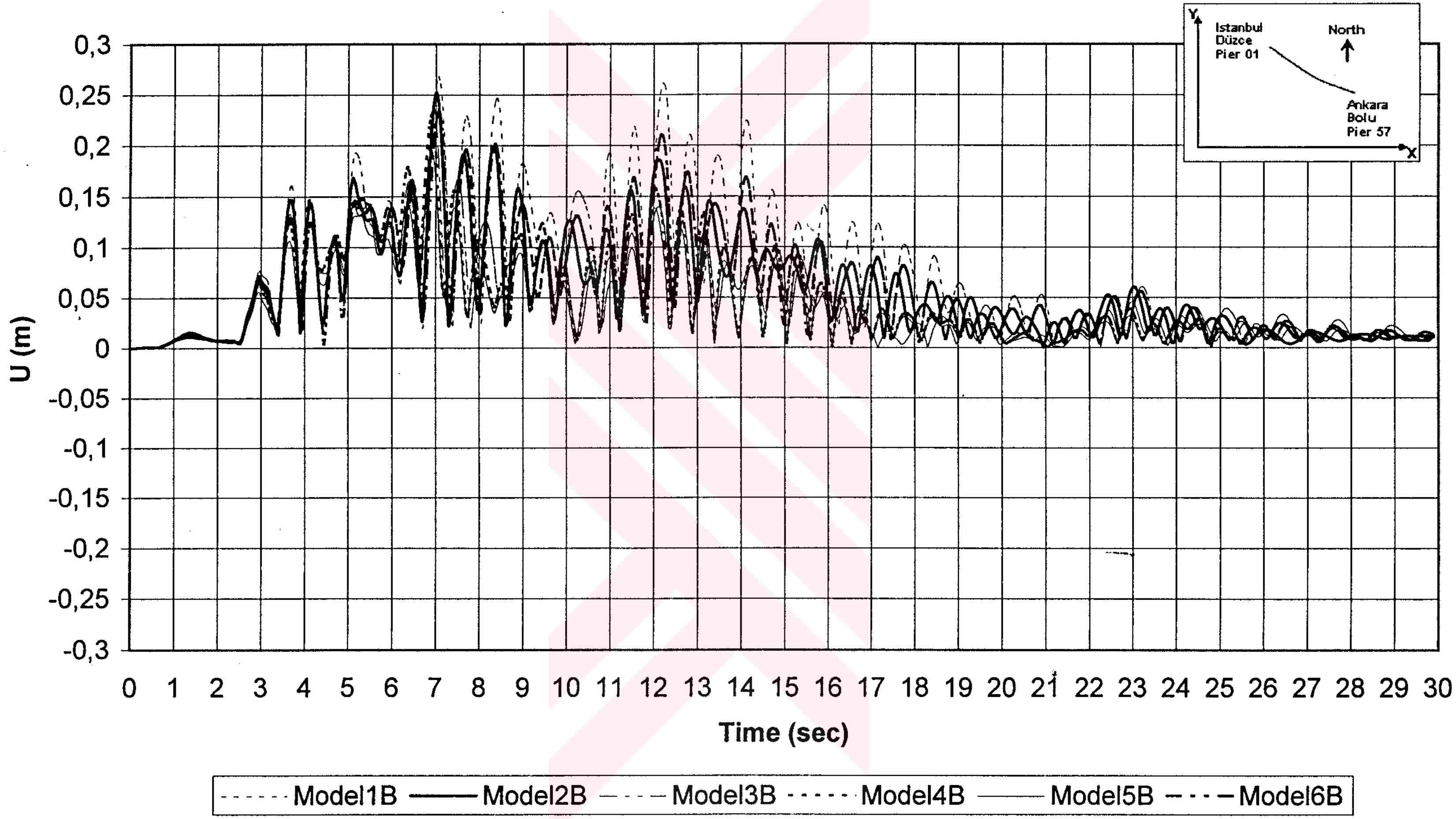


**Figure 5.33 Modified Displacements at Pier Cap of Pier25 (a selected pier)**
**$[U=(UX^2+UY^2)^{1/2}]$ (CASE B)**

The displacements at the top of pier in Astaldi's Model for accelerogram 1 in longitudinal direction is shown in Figure 5.34.

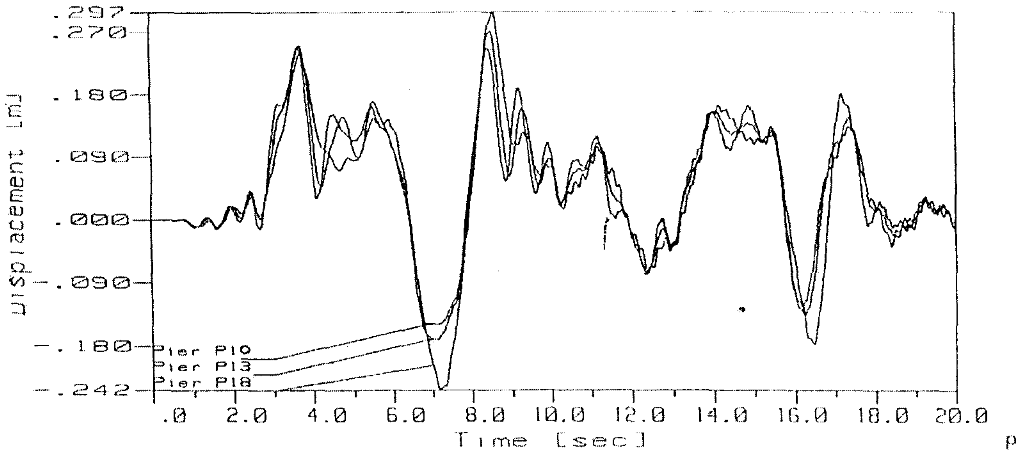


**Figure 5.34 Pier Top Displacements due to Accelerogram 1 in Longitudinal Direction**

Although the calculated displacements are in different directions, it is possible to compare Figure 5.31 and 5.34 in marginal view. Figure 5.34 shows the displacements in longitudinal direction of the bridge; and Figure 5.31 shows the displacements in global X-direction, which makes an angle of approximately 31 degrees with the longitudinal direction of the bridge.

Despite this difference, the peak displacement values are observed at the 3rd, 7th, 8th, and 12th seconds from the beginning of the seismic excitation. Maximum displacement values are around 0.3 m and 0.22 m for Astaldi's Model and Model 6B, respectively. The fact that Astaldi's Model had greater displacement values reveals the effect of non-linear analysis on displacement results.

# CHAPTER 6

## SUMMARY AND CONCLUSIONS

Bolu Viaduct was affected by August 17, 1999 Kocaeli-Gölcük Earthquake and underwent an extensive damage during November 12, 1999 Düzce Earthquake. The main contractor for the Bolu Mountain Project, Astaldi S.p.A, analyzed the bridge by two dimensional computer models in two perpendicular directions. In this master thesis, a 3D computer modeling and 3D time history analysis of the bridge were examined. Four 3D and two 2D new computer models were constructed to simulate the behavior of the bridge. Although there are major differences in analysis methods and modeling between Astaldi's Model and new generated models, the results of Astaldi's 2D models were also useful to be compared against different modeling techniques that are used in this thesis.

The bridge has special characteristics, therefore this fact led to carry out an academically interesting subject and a real life application. The main work load of this study consists:

- Generation of models with different levels of complexity,
- Simulation of earthquake loading measured during Düzce Earthquake, and
- Comparison of results.

Using the combination of the computer programs (SAP2000, Excel, Visual Basic, and Fortran 77) made it easier to achieve the objectives of modeling and result comparison. The written Fortran 77 and Excel – Visual Basic macros were useful for forming the geometry of the whole bridge and post-process of analyses outputs.

Because the general geometry and cross-section of Bolu Viaduct are very complicated, the sectional properties of the structural members needed to be calculated separately, which was a great deal of time consuming work. During the development of analytical models, numerous runs and troubleshooting were necessary to detect and correct errors related with the modeling. Due to the unusually large size of the "complicated" models, it sometimes took almost a whole day to conduct a single run to find out a single error. At the end, all modeling related errors are detected and corrected.

Comparison of the results obtained from each different model and investigation of the effect of model complexity on the results were other aspects to be considered for the thesis study. Internal forces at pier bases and the displacements (drifts) at pier caps were determined and compared against each other and with the existing Astaldi's model.

The maximum of the maximum displacements calculated for case (b) of generated models (Model 1B, 2B, 3B, 4B, 5B, and 6B) is 0.3136 meters, which belongs to the most fine meshed (refined) model (Model 1B). Usually, refined finite element meshing causes models to converge towards a more flexible state. Maximum displacements calculated for each model become larger as the model complexity increases. This concludes that displacements increase as the complexity of the modeling increases.

Another conclusion on displacements can be drawn for Astaldi's Model and Model 6B although there are major differences. These differences can be categorized under "modeling" (linear vs. non-linear) and "earthquake data" (measured Düzce EQ vs. generated and recorded major earthquake's data). The values of maximum displacements in Astaldi's Model are greater than those in Model 6B, which shows the combined effect of non-linear analysis and different earthquake data on displacement results.

Although Astaldi's Model was non-linear, it had potential weaknesses to simulate the 3D effects of the structure and response to earthquake. This conclusion is drawn from the fact that 2-dimensional Model 6B failed to simulate global lateral modes of the whole bridge. Furthermore, longitudinal modes are affected by the different pier heights and bridge curves in plan, which are not possible to model with Model 6B or Astaldi's Model.

The "most complex" model results in a very large number of degrees of freedom, which is unsuitable for the solutions with current computer technology.

Moreover, as the model size gets larger and depending on the solution method, numerical errors due to the round-off and matrix inversion may build up.

Although results (shear, moment, displacement, mode shapes, periods) obtained from all models are different at most two times, there is a general grouping of models 1,2,3 and 4,5,6 based on their response to earthquake excitation. The major differences between these two groups come from modeling of the third dimension in transverse direction. It is concluded that wire frame models (i.e. Models 4, 5, and 6) fail to successfully simulate the dynamic behavior of deck rotation and deck rotational inertia in transverse bending modes.

The scope of the thesis regarding the different model type generations has been extended from what was initially planned. The initial 3-dimensional models have been extended to 2-dimensional and 1-dimensional models for a total of 7 models. There are still some additional issues in this subject that might be improved and implemented as future studies. A non-linear time history analysis might be successfully performed as a future study. The non- linear behavior of Energy Dissipating Units (EDU) would greatly affect the seismic response of this bridge. A full non-linear analysis of complex models may not be feasible; however, semi-linear hybrid models (i.e. linear bridge + non-linear EDU) can also be used. An additional study can be conducted using different earthquake records to see and compare response and behavior of linear or non-linear models. A comparison between the analysis results of linear time history and response spectrum curves may also bring interesting results into consideration.

**REFERENCES**


1. Chopra, A.K., *Dynamics of Structures Theory and Applications to Earthquake Engineering*, Prentice Hall, New Jersey, 1995.

2. Clough, R.W., Penzien, J., Dynamics of Structures, Second Edition, McGraw-Hill Inc., Singapore, 1993.

3. Computers and Structures, Inc., Berkeley, California, USA, *SAP2000 Non- Linear Version 6.11 Structural Analysis Program*.

4. Computers and Structures, Inc., Berkeley, California, USA, *SAP2000 Integrated Finite Element Analysis and Design of Structures, Analysis Reference,* Version 6.1, Revised September 1997.

5. Digital Equipment Corporation, *Visual Fortran Professional Edition 6.0.0.*

6. MathSoft, Inc, *Mathcad 2000 Professional*, Industry Standard Calculation Software.

7. Ministry of Public Works and Settlement, *Specification for Structures to be Built in Disaster Areas Part III*, Issued on September 2, 1997, Official Gazette No.23098, Amended on July 2, 1998, Official Gazette No.23390, (English Translation Prepared Under The Direction of Aydınoğlu, M. N., İstanbul).

8. Roussis, P. C., *Assessment of Performance of Bolu Viaduct in the 1999 Düzce Earthquake*, Department of Civil, Structural & Environmental Engineering, University of Buffalo.

9. SAP2000, Structural Analysis Program, Computers and Structures Inc., Berkeley, California.

10. T.C. Bayındırlık ve İskan Bakanlığı, *Afet Bölgelerinde Yapılacak Yapılar Hakkında Yönetmelik*, 02/09/1997 tarih ve 23098 sayılı Resmi Gazete, 02/07/1998 tarih ve 23390 sayılı Resmi Gazete ile değiştirilmiş.

11. Xiao, Y., Yaprak, T.T., Tokgözoğlu F., *Observations of the November 12, 1999, Düzce Earthquake.*

12. Yılmaz, Ç., *Paper: Design Philosophy and Criteria For Viaduct No:1 (Bolu Viaduct)*, METU, Ankara.

## APPENDIX A

## "MESH" - FORTRAN 77 CODE WRITTEN FOR MESH GENERATION

```
      REAL*8 X(20000),Y(20000),Z(20000),DPLAN(20000),DELEV(20000),
     *COORD(600000,5),DDPLAN(20000),DDELEV(20000)
      REAL*8 X1(20000),Y1(20000),Z1(20000)
      REAL*8 X2(20000),Y2(20000),Z2(20000)
      REAL VERTC1,VERTC2,onder
      INTEGER SECNO,CURVE(120),NN,CCURVE
      REAL*8 COORDX(30),COORDY(30),COORDZ(30)
      REAL*8 COORDXX,COORDYY,COORDZZ
      REAL*8 DELX1(60000,30),DELY1(60000,30),DELZ1(60000,30)

      OPEN(1,STATUS='OLD',FILE='REFJOINTS.TXT')
    1 READ(1,*,END=5) SECNO,X1(SECNO),Y1(SECNO),Z1(SECNO),
     *X2(SECNO),Y2(SECNO),Z2(SECNO),CURVE(SECNO)
      Z1(SECNO)=Z1(SECNO)+0.9
      Z2(SECNO)=Z2(SECNO)+0.9
      Z(SECNO)=Z1(SECNO)+2.04
      X(SECNO)=(X1(SECNO)+X2(SECNO))/2
      Y(SECNO)=(Y1(SECNO)+Y2(SECNO))/2
      GOTO 1
    5 CLOSE(1)
      OPEN(2,STATUS='OLD',FILE='D.TXT')
    2 READ(2,*,END=6) NO,DPLAN(NO),DELEV(NO)
      GOTO 2
    6 CLOSE(2)

      K=0
      DO 20 I=1,(SECNO-1)*14+1,14
      K=K+1
      DX=X2(K)-X1(K)
      DY=Y2(K)-Y1(K)
      DO 20 J=0,13,1
C Joint Number:
      COORD(I+J,1)=I+J
C **********X Coordinate**********
C
C ADDING %4 SLOPE IN CURVES...
C
C CURVE=1: turn to the right;
C CURVE=2: turn to the left;
C CURVE=0: Straight
C
      IF(CURVE(K).EQ.1) THEN
C VERTC1: Vertical slope coefficient for X & Y coordinates
modification
```

```
      VERTC1=(DPLAN(J+1)*COS(-0.06981317)-DELEV(J+1)*SIN(-
0.06981317))
     */DPLAN(J+1)
      ELSEIF(CURVE(K).EQ.2) THEN
      VERTC1=(DPLAN(J+1)*COS(0.06981317)-
DELEV(J+1)*SIN(0.06981317))
     */DPLAN(J+1)
      ELSE
      VERTC1=1.0
      ENDIF

COORD(I+J,2)=X(K)+VERTC1*((DPLAN(J+1)/(DX**2+DY**2)**(0.5)*DX))
C **********Y Coordinate**********

COORD(I+J,3)=Y(K)+VERTC1*((DPLAN(J+1)/(DX**2+DY**2)**(0.5)*DY))

C **********Z Coordinate**********
      IF(CURVE(K).EQ.1) THEN
C Z coordinates modification
       VERTC2=DPLAN(J+1)*SIN(-0.06981317)+DELEV(J+1)*COS(-
0.06981317)
     *-DELEV(J+1)
      ELSEIF(CURVE(K).EQ.2) THEN

VERTC2=DPLAN(J+1)*SIN(0.06981317)+DELEV(J+1)*COS(0.06981317)
     *-DELEV(J+1)
      ELSE
       VERTC2=0.0
      ENDIF
C
      COORD(I+J,4)=Z(K)+DELEV(J+1)+VERTC2
   20 CONTINUE
  100 FORMAT(I7,1X,'X=',F11.6,' Y=',F11.6,' Z=',F10.6)


      OPEN(3,STATUS='UNKNOWN',FILE='COORD.TXT')
  101 FORMAT(I7,1X,F11.6,1X,F11.6,1X,F10.6)

      K=1
      DO 30 I=1,(SECNO-1)*14+1,14
      DO 40 J=0,13,1
      DELX1(K,J+1)=COORD(I+J+14,2)-COORD(I+J,2)
      DELY1(K,J+1)=COORD(I+J+14,3)-COORD(I+J,3)
      DELZ1(K,J+1)=COORD(I+J+14,4)-COORD(I+J,4)

   40 CONTINUE
      K=K+1
   30 CONTINUE

C FORMATION OF SLABS BETWEEN PIER SECTIONS
      K=1
      NN=0
      DO 50 I=1,(SECNO-1)*14+1,14
      DO 60 J=0,13,1
      NN=NN+1
      WRITE(3,100) NN,COORD(I+J,2),COORD(I+J,3),COORD(I+J,4)
```

```
      IF(I+J.EQ.SECNO*14) GOTO 70

      COORDX(J+1)=COORD(I+J,2)
      COORDY(J+1)=COORD(I+J,3)
      COORDZ(J+1)=COORD(I+J,4)
   60 CONTINUE


      DO 31 I1=1,12
      DO 31 I2=1,14
      NN=NN+1

      COORDXX=COORDX(I2)+DELX1(K,I2)/13.0*I1
      COORDYY=COORDY(I2)+DELY1(K,I2)/13.0*I1
      COORDZZ=COORDZ(I2)+DELZ1(K,I2)/13.0*I1

   31 WRITE(3,100) NN,COORDXX,COORDYY,COORDZZ
      K=K+1
   50 CONTINUE

   70 WRITE(3,*) ' '
      CLOSE(3)


      STOP
      END
```

## APPENDIX B

## SHEAR AREA CALCULATIONS FOR MODEL 2

$h := 1.45$ $t1 := 0.24$ $t2 := 0.16$ $t3 := 0.35$ $b1 := 2.508$ $b2 := 0.88$

$a1 := 0.7$ $a2 := 2.9333$ $a3 := 0.665$ $a4 := 0.2175$ $xbarv := 1.084$

X – DIRECTION

************************************************************************************************************************************

$$Q1X(y) := \int_{y}^{4} n \cdot (2.05 - 0.25n)\, dn$$

$$Q2X(y) := \int_{y}^{3.8} n \cdot (5.7 - 0.5n)\, dn + \int_{3.8}^{4} n \cdot (2.05 - 0.25n)\, dn$$

$$Q3X(y) := \int_{y}^{3.2} n \cdot (-2.7 + 1.625n)\, dn + \int_{3.2}^{3.8} n \cdot (5.7 - 0.5n)\, dn + \int_{3.8}^{4} n \cdot (2.05 - 0.25n)\, dn$$

$$Q4X(y) := \int_{y}^{2.4} n \cdot 1.2\, dn + \int_{2.4}^{3.2} n \cdot (-2.7 + 1.625n)\, dn + \int_{3.2}^{3.8} n \cdot (5.7 - 0.5n)\, dn + \int_{3.8}^{4} n \cdot (2.05 - 0.25n)\, dn$$

$$Z1X := \int_{3.8}^{4} \frac{Q1X(y)^2}{2.05 - 0.25y}\, dy$$

$$Z2X := \int_{3.2}^{3.8} \frac{Q2X(y)^2}{5.7 - 0.5y}\, dy$$

$$Z3X := \int_{2.4}^{3.2} \frac{Q3X(y)^2}{-2.7 + 1.625y}\, dy$$

$$Z4X := \int_{0}^{2.4} \frac{Q4X(y)^2}{1.2}\, dy$$

Y – DIRECTION
**************************************************************************************************************************************

$$Q1Y(y) := \int_{y}^{2.25} n \cdot (-10 + 8n)\, dn$$

$$Q2Y(y) := \int_{y}^{1.85} n \cdot 8\, dn + \int_{1.85}^{2.25} n \cdot (-10 + 8n)\, dn$$

$$Q3Y(y) := \int_{y}^{1.65} n \cdot (-0.682 + 2.353n)\, dn + \int_{1.65}^{1.85} n \cdot 8\, dn + \int_{1.85}^{2.25} n \cdot (-10 + 8n)\, dn$$

$$Q4Y(y) := \int_{y}^{0.8} n \cdot 1.2\, dn + \int_{0.8}^{1.65} n \cdot (-0.682 + 2.353n)\, dn + \int_{1.65}^{1.85} n \cdot 8\, dn + \int_{1.85}^{2.25} n \cdot (-10 + 8n)\, dn$$

$$Z1Y := \int_{1.85}^{2.25} \frac{Q1Y(y)^2}{-10 + 8y}\, dy$$

$$Z2Y := \int_{1.65}^{1.85} \frac{Q2Y(y)^2}{8}\, dy$$

$$Z3Y := \int_{0.8}^{1.65} \frac{Q3Y(y)^2}{-0.682 + 2.353y}\, dy$$

$$Z4Y := \int_{0}^{0.8} \frac{Q4Y(y)^2}{1.2}\, dy$$

RESULTS
**************************************************************************************************************************************

$IX := 106.2213$ $\quad AsX := \dfrac{IX^2}{2 \cdot (Z1X + Z2X + Z3X + Z4X)}$ $\quad AsX = 10.076$

$IY := 38.2761$ $\quad AsY := \dfrac{IY^2}{2 \cdot (Z1Y + Z2Y + Z3Y + Z4Y)}$ $\quad AsY = 6.147$

# APPENDIX C

## MODE SHAPES OF MODEL 1B

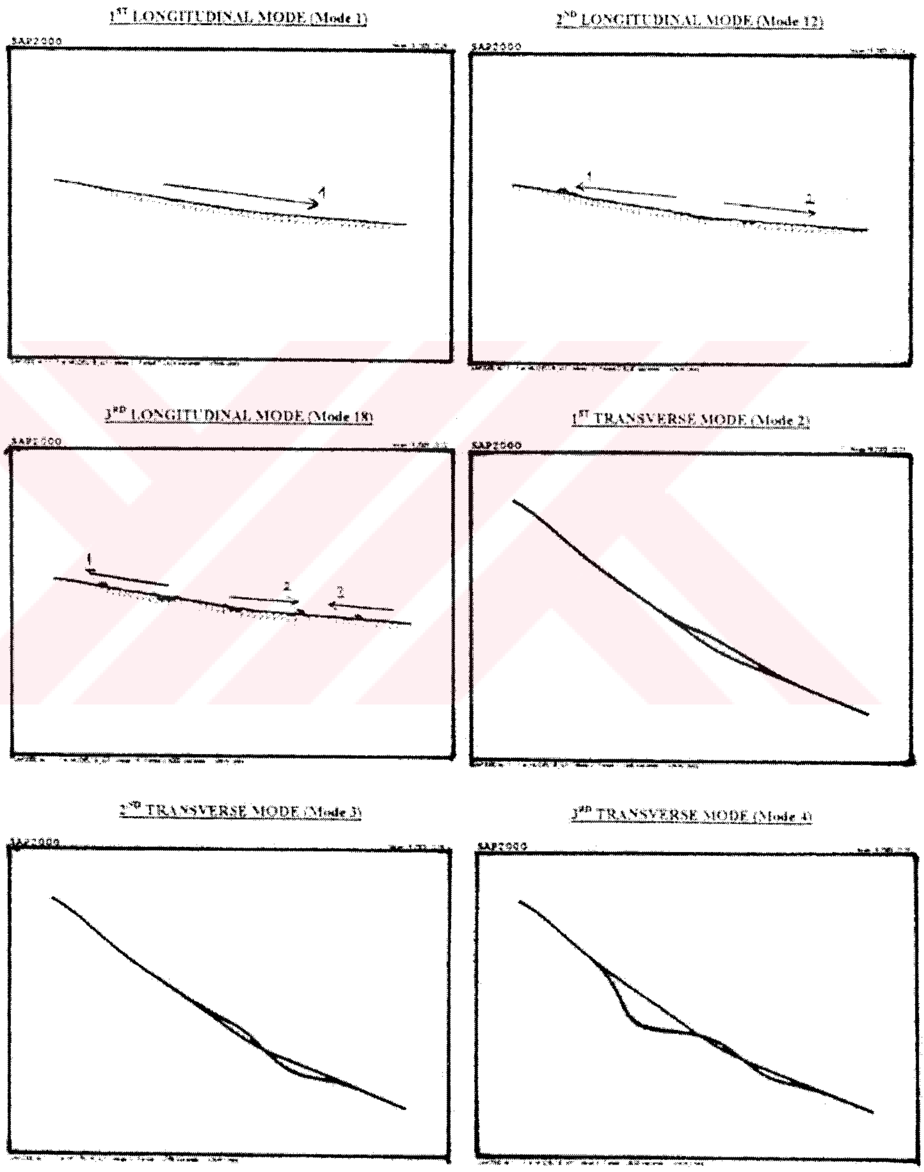


**Figure C.1 Mode Shapes of Model 1B**

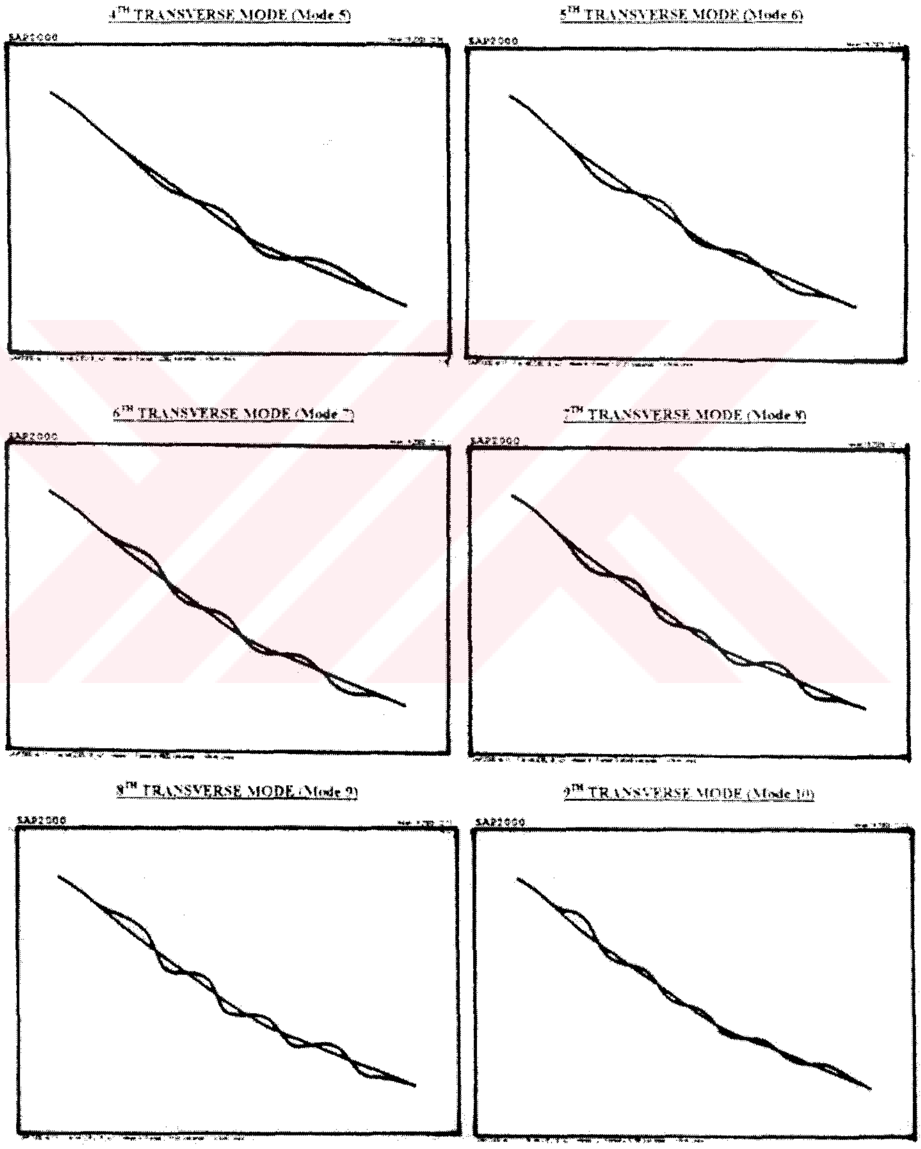


**Figure C.1 Mode Shapes of Model 1B (Continued)**

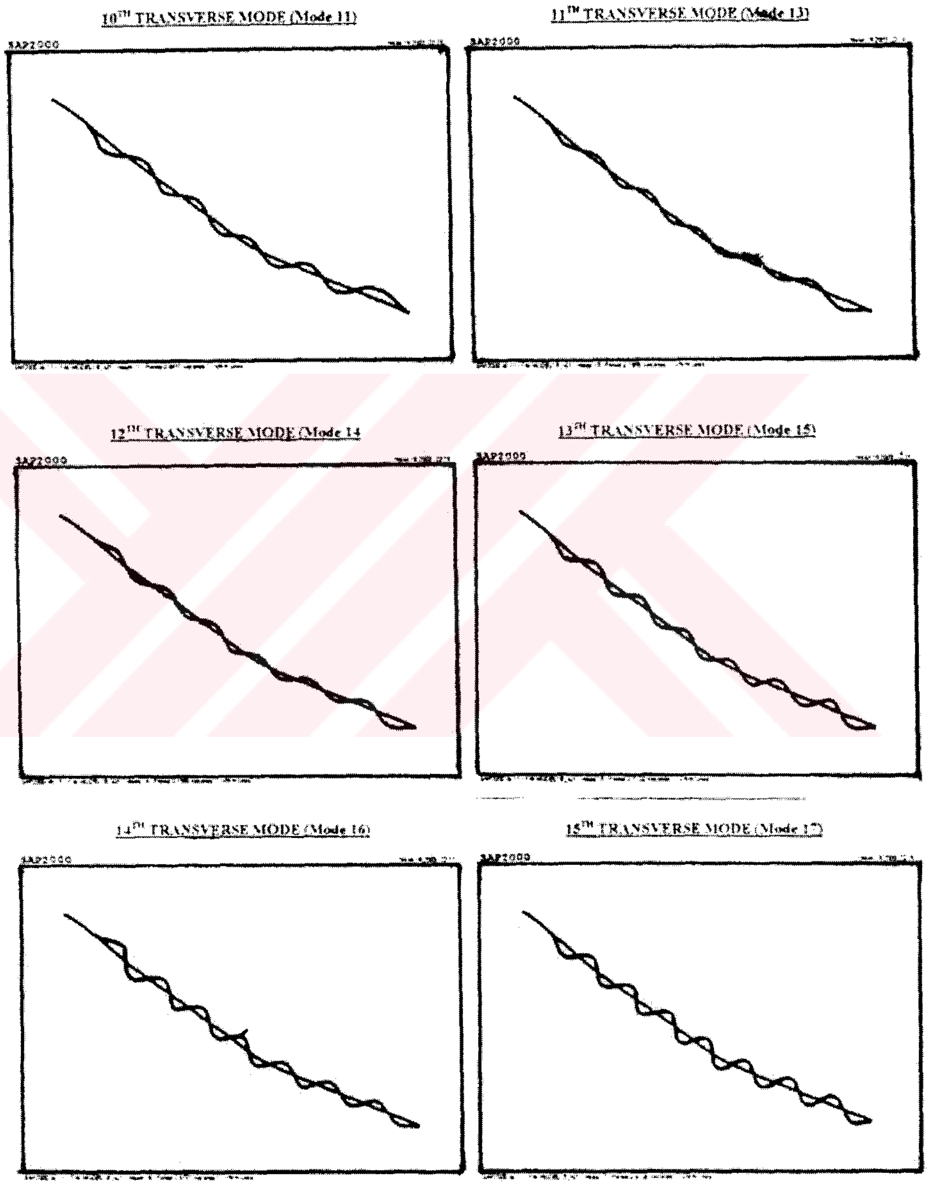


**Figure C.1 Mode Shapes of Model 1B (Continued)**

# APPENDIX D

## SHEAR FORCE, MOMENT AND DISPLACEMENT VALUES CALCULATED BY SAP 2000

In Appendix D, shear force, moment and displacement values calculated by SAP 2000 Structural Analysis Program are presented. Tables D.1, D.2 and D.3 show the values for case (a), and Tables D.4, D.5 and D.6 show the values for case (b). Table D.7 shows the shear force and moment values for "10-Span Segment Models", i.e. Astaldi's Model and Model 6B.

# Table D.1 Shear Force and Moment Values (CASE A)

| PIER NO | Frame # (Bottom) | $\lvert V22 \rvert_{MAX}$ (Transverse) (kN) | | | | | | $\lvert V33 \rvert_{MAX}$ (Longitudinal) (kN) | | | | | |
|---|---|---|---|---|---|---|---|---|---|---|---|---|---|
| | | MODEL1 | MODEL2 | MODEL3 | MODEL4 | MODEL5 | MODEL6 | MODEL1 | MODEL2 | MODEL3 | MODEL4 | MODEL5 | MODEL6 |
| 1 | 10 | 25445,110 | 28816,110 | 26989,790 | 30524,310 | 32707,720 | | 11653,010 | 11672,460 | 11700,540 | 11575,990 | 11660,170 | |
| 2 | 20 | 18227,790 | 21684,410 | 21672,430 | 23262,500 | 21244,540 | | 9265,258 | 9218,230 | 9215,875 | 9083,900 | 8871,544 | |
| 3 | 30 | 20788,020 | 24410,430 | 23644,030 | 25670,850 | 23209,700 | | 8005,875 | 8089,994 | 7803,237 | 8074,788 | 8219,940 | |
| 4 | 40 | 10638,970 | 10585,510 | 9539,909 | 13397,830 | 10610,170 | | 2559,215 | 3493,503 | 2376,755 | 2589,450 | 2668,493 | |
| 5 | 50 | 12859,960 | 10370,940 | 10851,360 | 9676,571 | 10315,910 | | 133823,600 | 125949,900 | 126560,400 | 98805,210 | 99918,720 | |
| 6 | 60 | 10384,690 | 10386,180 | 11474,350 | 9928,031 | 10773,160 | | 5311,768 | 5279,689 | 5204,308 | 5423,503 | 5555,478 | |
| 7 | 70 | 13109,420 | 12306,160 | 13105,290 | 12057,280 | 12151,590 | | 12054,480 | 12049,070 | 12049,810 | 11979,050 | 11670,990 | |
| 8 | 80 | 13928,070 | 13519,700 | 14846,010 | 13515,880 | 14232,940 | | 7328,621 | 7224,759 | 7334,161 | 7202,529 | 7037,409 | |
| 9 | 90 | 17277,710 | 16910,030 | 17766,170 | 17218,320 | 15752,300 | | 9929,807 | 10325,240 | 10504,670 | 10254,600 | 10426,680 | |
| 10 | 100 | 20294,580 | 18154,260 | 19592,430 | 18077,130 | 17784,570 | | 11252,660 | 11616,180 | 11654,050 | 11459,330 | 12066,850 | |
| 11 | 110 | 20534,910 | 20723,030 | 20662,290 | 22008,680 | 21454,850 | | 13088,370 | 12690,890 | 12994,280 | 13113,850 | 13434,820 | |
| 12 | 120 | 18631,320 | 20488,450 | 19375,300 | 22111,800 | 21712,030 | | 13614,690 | 13307,240 | 13497,680 | 13522,720 | 14255,080 | |
| 13 | 130 | 16568,810 | 18662,840 | 18162,540 | 21205,820 | 20675,560 | | 13636,140 | 13710,090 | 13809,880 | 13684,990 | 13995,580 | |
| 14 | 140 | 14979,400 | 16068,380 | 16857,900 | 19030,380 | 17719,380 | | 13750,420 | 13432,110 | 13638,940 | 13655,720 | 14259,000 | |
| 15 | 150 | 13438,320 | 14294,980 | 15446,600 | 15812,620 | 15055,540 | | 32462,730 | 31244,980 | 27240,920 | 24099,610 | 26327,050 | |
| 16 | 160 | 13393,520 | 14302,210 | 15659,510 | 15369,120 | 14425,910 | | 9556,682 | 9374,781 | 9457,617 | 9646,441 | 9707,101 | |
| 17 | 170 | 12438,880 | 13524,060 | 13987,650 | 15598,150 | 14723,230 | | 9544,479 | 9363,800 | 9450,722 | 9650,610 | 9707,101 | |
| 18 | 180 | 12385,830 | 12443,590 | 11550,110 | 14671,300 | 14250,750 | | 11054,320 | 10933,770 | 11016,220 | 11062,050 | 11224,170 | |
| 19 | 190 | 10336,690 | 10169,120 | 10202,710 | 11517,150 | 11716,170 | | 11047,870 | 10924,540 | 11008,950 | 11056,560 | 11217,810 | |
| 20 | 200 | 9408,530 | 9660,809 | 11636,170 | 11025,010 | 10103,130 | 11525,730 | 10339,840 | 10823,970 | 10905,320 | 10856,320 | 11089,960 | 11212,140 |
| 21 | 210 | 9555,774 | 10204,540 | 10563,380 | 10169,270 | 10021,170 | 10902,830 | 10023,060 | 10037,470 | 10039,810 | 10010,280 | 10235,940 | 10239,130 |
| 22 | 220 | 10166,910 | 10567,830 | 10085,450 | 12399,720 | 11959,260 | 11733,620 | 10024,530 | 10046,330 | 10040,870 | 10011,760 | 10237,790 | 10240,930 |
| 23 | 230 | 9931,792 | 11249,140 | 9744,128 | 12439,020 | 12343,740 | 11852,410 | 10024,010 | 10042,360 | 10040,480 | 10011,440 | 10237,790 | 10240,930 |
| 24 | 240 | 9317,158 | 10444,240 | 9341,922 | 12264,580 | 12044,280 | 12618,670 | 10024,200 | 10021,460 | 10040,780 | 10011,590 | 10237,790 | 10240,930 |
| 25 | 250 | 8433,945 | 9069,078 | 9855,652 | 10929,270 | 10575,980 | 12800,740 | 37890,680 | 35817,140 | 32890,410 | 25273,190 | 26765,280 | 26775,800 |
| 26 | 260 | 9026,035 | 10476,000 | 10345,970 | 10790,220 | 10743,340 | 12279,370 | 9553,114 | 9371,924 | 9458,809 | 9658,899 | 9697,788 | 9690,864 |
| 27 | 270 | 9582,521 | 10567,730 | 10320,310 | 12334,140 | 11969,040 | 11851,730 | 9552,980 | 9373,498 | 9458,748 | 9658,942 | 9697,788 | 9690,864 |
| 28 | 280 | 9582,405 | 10215,720 | 10520,260 | 12161,960 | 11483,250 | 12754,060 | 9544,406 | 9363,194 | 9450,646 | 9650,579 | 9707,101 | 9700,186 |
| 29 | 290 | 9200,248 | 9798,759 | 10262,370 | 10978,230 | 10337,720 | 13217,720 | 9545,233 | 9363,002 | 9452,977 | 9651,686 | 9707,101 | 9700,185 |
| 30 | 300 | 8825,469 | 9306,878 | 9520,119 | 10112,040 | 9687,740 | 13216,500 | 9809,512 | 9258,823 | 9461,604 | 9601,240 | 9698,170 | 9690,864 |

| PIER NO | Frame # (Bottom) | $\lvert M22 \rvert_{MAX}$ (Longitudinal) (kN.m) | | | | | | $\lvert M33 \rvert_{MAX}$ (Transverse) (kN.m) | | | | | |
|---|---|---|---|---|---|---|---|---|---|---|---|---|---|
| | | MODEL1 | MODEL2 | MODEL3 | MODEL4 | MODEL5 | MODEL6 | MODEL1 | MODEL2 | MODEL3 | MODEL4 | MODEL5 | MODEL6 |
| 1 | 10 | 232629,500 | 232296,300 | 233073,200 | 233033,800 | 233556,000 | | 661067,400 | 705569,600 | 689793,400 | 744532,400 | 791028,400 | |
| 2 | 20 | 201309,800 | 200639,400 | 201199,500 | 199897,500 | 193713,600 | | 532053,700 | 573509,500 | 617547,500 | 603030,000 | 551648,400 | |
| 3 | 30 | 112486,400 | 113681,500 | 111586,200 | 111957,600 | 114691,800 | | 431421,400 | 467528,400 | 471522,500 | 489176,800 | 438025,100 | |
| 4 | 40 | 17782,900 | 25969,870 | 16147,730 | 18081,950 | 17748,440 | | 137708,000 | 120622,700 | 110301,000 | 143703,900 | 110838,300 | |
| 5 | 50 | 1494631,000 | 1501888,000 | 1478002,000 | 1090641,000 | 1079061,000 | | 172174,400 | 120020,600 | 142100,100 | 109724,900 | 117384,000 | |
| 6 | 60 | 68381,980 | 67710,090 | 68879,050 | 67920,130 | 69697,920 | | 202088,300 | 176804,600 | 208868,500 | 175121,600 | 197229,200 | |
| 7 | 70 | 238514,700 | 239017,300 | 238631,900 | 239237,200 | 233722,500 | | 332124,500 | 299136,800 | 321292,100 | 290623,500 | 306399,500 | |
| 8 | 80 | 168528,700 | 168292,800 | 168491,900 | 168380,600 | 163448,600 | | 437907,500 | 399110,200 | 444443,600 | 396706,800 | 444454,300 | |
| 9 | 90 | 263784,300 | 272864,100 | 274930,800 | 271848,000 | 273510,500 | | 627099,600 | 592487,900 | 615063,200 | 593430,800 | 561467,900 | |
| 10 | 100 | 398421,900 | 408850,200 | 407654,800 | 400807,700 | 420869,100 | | 851374,800 | 739931,600 | 806180,300 | 728237,100 | 716885,000 | |
| 11 | 110 | 436569,900 | 432836,700 | 435727,300 | 437136,300 | 444868,900 | | 855131,800 | 852063,900 | 855158,100 | 878331,300 | 851550,800 | |
| 12 | 120 | 447411,800 | 444574,100 | 446346,800 | 446667,900 | 464190,800 | | 768849,000 | 838133,300 | 803131,100 | 881806,600 | 865841,200 | |
| 13 | 130 | 454629,000 | 454663,600 | 456253,400 | 455180,600 | 462591,600 | | 681781,800 | 755343,000 | 727167,100 | 837847,200 | 815670,600 | |
| 14 | 140 | 450862,000 | 447919,100 | 449862,300 | 450106,700 | 464225,400 | | 624952,600 | 680107,500 | 685114,700 | 770190,800 | 725135,000 | |
| 15 | 150 | 1449492,000 | 1323146,000 | 1089242,000 | 823452,900 | 899193,900 | | 586507,400 | 625592,500 | 650759,900 | 677418,000 | 640770,400 | |
| 16 | 160 | 346795,400 | 345850,800 | 347240,500 | 346928,000 | 353945,100 | | 582805,600 | 625302,700 | 666646,900 | 657047,000 | 629884,000 | |
| 17 | 170 | 347038,900 | 346052,900 | 347445,900 | 347598,800 | 353945,100 | | 551990,400 | 590955,900 | 602948,400 | 663891,300 | 632513,900 | |
| 18 | 180 | 383453,700 | 382944,700 | 382924,300 | 384032,300 | 386712,400 | | 544996,100 | 554015,700 | 517867,100 | 621879,700 | 612723,500 | |
| 19 | 190 | 383232,800 | 382704,500 | 382696,500 | 383829,600 | 386592,800 | | 461465,600 | 463260,900 | 450627,200 | 508581,600 | 516544,500 | |
| 20 | 200 | 369579,500 | 384879,100 | 381709,400 | 378491,500 | 385756,300 | 386596,200 | 401464,100 | 420370,800 | 490024,200 | 448044,900 | 455164,700 | 489253,300 |
| 21 | 210 | 327806,000 | 325995,300 | 328085,800 | 327720,200 | 338584,300 | 338602,700 | 423608,400 | 450128,800 | 471268,300 | 452295,400 | 446768,900 | 473028,800 |
| 22 | 220 | 327825,200 | 325794,700 | 328103,400 | 327738,500 | 338610,700 | 338628,900 | 456949,100 | 482902,000 | 463795,200 | 528909,100 | 514610,900 | 513646,400 |
| 23 | 230 | 327810,700 | 325814,600 | 328087,800 | 327722,700 | 338610,700 | 338628,900 | 456833,400 | 492373,700 | 444021,700 | 553114,300 | 547605,700 | 539290,300 |
| 24 | 240 | 327815,200 | 326087,900 | 328095,000 | 327730,100 | 338610,700 | 338628,900 | 438681,000 | 447741,900 | 436556,600 | 535578,700 | 524295,600 | 559893,400 |
| 25 | 250 | 1747111,000 | 1583994,000 | 1388359,000 | 900537,800 | 955738,100 | 956112,600 | 422311,800 | 426923,200 | 447561,800 | 476116,000 | 454699,900 | 553172,000 |
| 26 | 260 | 347229,000 | 346281,600 | 347639,500 | 347772,800 | 354144,900 | 354165,600 | 434627,700 | 457122,400 | 466496,100 | 470551,200 | 465563,900 | 540742,900 |
| 27 | 270 | 347223,600 | 346249,700 | 347634,800 | 347780,100 | 354144,900 | 354165,600 | 442453,600 | 468819,200 | 454606,300 | 520963,200 | 507154,700 | 524505,500 |
| 28 | 280 | 347036,800 | 346049,900 | 347454,500 | 347593,500 | 353945,100 | 353965,800 | 444857,300 | 453714,300 | 457480,000 | 522593,200 | 496805,800 | 550569,000 |
| 29 | 290 | 347215,400 | 346212,600 | 347619,600 | 347783,600 | 353945,100 | 353965,800 | 430166,000 | 435272,900 | 447374,500 | 486455,300 | 467681,300 | 566972,800 |
| 30 | 300 | 334874,800 | 345821,200 | 346841,800 | 345866,900 | 352268,400 | 354165,600 | 411117,400 | 429073,700 | 428151,700 | 445417,000 | 443083,300 | 568790,200 |

## Table D.1 Shear Force and Moment Values (CASE A) (Continued)

| PIER NO | Frame # (Bottom) | $\|V22\|_{MAX}$ (Transverse) (kN) | | | | | | $\|V33\|_{MAX}$ (Longitudinal) (kN) | | | | | | $\|M22\|_{MAX}$ (Longitudinal) (kN.m) | | | | | | $\|M33\|_{MAX}$ (Transverse) (kN.m) | | | | | |
|---|---|---|---|---|---|---|---|---|---|---|---|---|---|---|---|---|---|---|---|---|---|---|---|---|---|
| | | MODEL1 | MODEL2 | MODEL3 | MODEL4 | MODEL5 | MODEL6 | MODEL1 | MODEL2 | MODEL3 | MODEL4 | MODEL5 | MODEL6 | MODEL1 | MODEL2 | MODEL3 | MODEL4 | MODEL5 | MODEL6 | MODEL1 | MODEL2 | MODEL3 | MODEL4 | MODEL5 | MODEL6 |
| 31 | 310 | 8980,759 | 8839,502 | 8977,422 | 9622,653 | 9386,263 | | 10091,040 | 10129,580 | 10108,170 | 10081,900 | 10237,790 | | 331267,800 | 329477,600 | 331557,900 | 331259,600 | 338610,700 | | 424493,900 | 424173,900 | 424281,600 | 443306,300 | 436196,000 | |
| 32 | 320 | 8933,619 | 8918,417 | 9256,267 | 9103,683 | 9143,920 | | 10138,330 | 10364,450 | 10129,340 | 10292,190 | 10225,300 | | 335092,900 | 335978,000 | 335498,800 | 335378,300 | 339272,600 | | 421313,200 | 421129,000 | 420805,000 | 434378,700 | 432791,100 | |
| 33 | 330 | 9041,189 | 8591,405 | 9160,251 | 9581,445 | 9482,324 | | 9558,783 | 9470,026 | 9511,188 | 9466,766 | 9376,259 | | 332854,800 | 328394,600 | 332575,600 | 332238,800 | 331202,700 | | 404397,800 | 404476,100 | 407393,000 | 417734,900 | 421979,500 | |
| 34 | 340 | 9625,458 | 9087,654 | 9522,866 | 10357,570 | 10171,480 | | 10202,660 | 10408,760 | 10189,760 | 10344,990 | 10225,290 | | 341236,600 | 339674,500 | 341609,900 | 341164,900 | 339272,700 | | 441947,300 | 411095,800 | 411600,300 | 434986,700 | 435036,200 | |
| 35 | 350 | 9748,531 | 8981,586 | 9010,494 | 9906,284 | 9664,149 | | 38573,000 | 38750,310 | 36034,230 | 27241,850 | 27362,550 | | 1827589,000 | 1743477,000 | 1549791,000 | 994579,100 | 982363,600 | | 445505,500 | 408064,400 | 389675,800 | 423231,300 | 429744,900 | |
| 36 | 360 | 9711,118 | 9311,684 | 9387,474 | 11324,640 | 10777,340 | | 10482,150 | 10579,310 | 10449,030 | 10492,170 | 10237,790 | | 347233,500 | 345867,300 | 347551,000 | 347514,600 | 338610,700 | | 439262,600 | 414808,700 | 405730,800 | 481703,600 | 460941,900 | |
| 37 | 370 | 11428,730 | 10523,840 | 10501,630 | 12244,740 | 10912,170 | | 10986,240 | 11173,600 | 11042,530 | 11183,100 | 10237,790 | | 365351,500 | 369006,600 | 368515,000 | 372368,600 | 338610,700 | | 482577,800 | 487147,000 | 472779,800 | 522386,100 | 463661,300 | |
| 38 | 380 | 9044,396 | 10319,210 | 9869,670 | 10610,750 | 9800,219 | | 10206,770 | 10381,330 | 10189,840 | 10339,880 | 10225,290 | | 348840,200 | 346105,900 | 349144,500 | 348994,200 | 339272,600 | | 381324,800 | 447921,000 | 428136,800 | 454698,100 | 422076,500 | |
| 39 | 390 | 9281,679 | 10465,000 | 10142,030 | 9666,008 | 9607,146 | | 10201,570 | 10370,670 | 10183,580 | 10331,840 | 10225,290 | | 349399,100 | 346683,600 | 349694,200 | 349587,900 | 339272,700 | | 416191,000 | 453459,300 | 445426,800 | 435621,400 | 433751,600 | |
| 40 | 400 | 10551,560 | 11107,710 | 10867,150 | 10468,850 | 10954,970 | | 10876,830 | 10750,880 | 10872,270 | 10942,800 | 10371,950 | | 359816,700 | 352208,100 | 361954,500 | 364074,600 | 338438,500 | | 465127,100 | 494030,200 | 480164,600 | 432212,500 | 466923,800 | |
| 41 | 410 | 8715,077 | 9912,465 | 10340,780 | 9915,985 | 10568,640 | | 10617,830 | 10706,650 | 10584,390 | 10626,160 | 10237,790 | | 352178,100 | 352647,400 | 351832,800 | 351997,700 | 338610,700 | | 384933,000 | 421678,600 | 432512,300 | 446416,800 | 480266,300 | |
| 42 | 420 | 8021,853 | 8648,829 | 9888,322 | 9292,677 | 9621,951 | | 10197,540 | 10365,220 | 10180,340 | 10327,880 | 10225,290 | | 349623,200 | 346945,800 | 349916,400 | 349831,300 | 339272,700 | | 367315,500 | 391117,600 | 431555,200 | 417568,800 | 438590,500 | |
| 43 | 430 | 8397,223 | 9276,131 | 8454,125 | 9350,503 | 9299,073 | | 10197,260 | 10365,640 | 10180,320 | 10327,870 | 10225,290 | | 349625,800 | 346935,400 | 349916,300 | 349831,600 | 339272,700 | | 369330,800 | 378882,000 | 386412,200 | 407214,300 | 416206,300 | |
| 44 | 440 | 8702,396 | 8948,022 | 8637,615 | 9017,967 | 10006,540 | | 10618,090 | 10705,070 | 10584,330 | 10626,110 | 10237,790 | | 352180,000 | 352545,000 | 351830,800 | 351996,300 | 338610,700 | | 389235,100 | 398187,600 | 369920,500 | 428134,000 | 452389,000 | |
| 45 | 450 | 8632,612 | 9266,826 | 9433,896 | 9694,476 | 10604,720 | | 33323,110 | 33019,790 | 28319,760 | 28335,150 | 26322,550 | | 1476630,000 | 1432551,000 | 1153657,000 | 988544,400 | 899398,100 | | 411388,400 | 430301,800 | 406055,000 | 447514,500 | 487031,300 | |
| 46 | 460 | 8468,456 | 9599,506 | 9579,612 | 11124,290 | 11749,090 | | 11431,310 | 11336,300 | 11524,070 | 11360,090 | 11217,810 | | 400763,400 | 399240,200 | 399890,700 | 401893,500 | 386592,800 | | 401476,200 | 415525,900 | 428941,100 | 469749,400 | 497111,400 | |
| 47 | 470 | 9131,805 | 10401,870 | 10426,060 | 11840,210 | 12321,830 | | 10255,000 | 10243,660 | 10280,550 | 10270,090 | 9707,101 | | 366744,300 | 369367,800 | 366667,100 | 367184,400 | 353945,100 | | 417329,600 | 459560,300 | 471320,300 | 523752,600 | 558830,700 | |
| 48 | 480 | 11029,170 | 12804,620 | 11731,810 | 14083,680 | 14316,670 | | 10254,370 | 10239,810 | 10280,130 | 10269,740 | 9707,101 | | 366737,300 | 369528,300 | 366648,800 | 367172,700 | 353945,100 | | 494189,200 | 560423,900 | 537286,300 | 614903,200 | 649110,900 | |
| 49 | 490 | 13171,060 | 14434,620 | 13660,170 | 15695,770 | 16586,840 | | 10254,580 | 10240,630 | 10280,470 | 10269,990 | 9707,101 | | 366727,600 | 369487,100 | 366652,400 | 367180,900 | 353945,100 | | 585914,100 | 633416,100 | 616972,800 | 691430,100 | 719591,300 | |
| 50 | 500 | 14021,250 | 14150,260 | 14464,980 | 15790,630 | 16542,870 | | 10778,520 | 10654,430 | 10669,470 | 10706,620 | 10374,860 | | 356220,800 | 349766,200 | 354501,300 | 355029,000 | 338568,500 | | 625998,200 | 639390,300 | 646279,800 | 683378,800 | 710031,400 | |
| 51 | 510 | 15360,280 | 16992,360 | 17301,880 | 18809,870 | 19258,020 | | 14656,230 | 14473,950 | 14597,480 | 14553,440 | 14004,990 | | 465193,100 | 463437,400 | 464596,300 | 463853,500 | 462669,600 | | 625513,800 | 688712,700 | 691846,600 | 744951,200 | 759574,100 | |
| 52 | 520 | 16213,930 | 16727,390 | 17071,040 | 17592,180 | 18104,290 | | 14656,370 | 14476,020 | 14597,440 | 14553,650 | 14004,990 | | 465199,200 | 463503,700 | 464604,800 | 463858,300 | 462669,600 | | 644702,800 | 662736,300 | 672270,400 | 684482,200 | 701914,600 | |
| 53 | 530 | 19099,070 | 19329,690 | 19741,130 | 19858,290 | 20512,130 | | 14072,140 | 14077,470 | 14166,430 | 14157,750 | 14440,510 | | 435961,200 | 432706,300 | 436858,500 | 435189,400 | 432984,100 | | 745103,300 | 751045,800 | 764560,000 | 752933,100 | 771693,300 | |
| 54 | 540 | 16313,770 | 15446,750 | 16654,130 | 15797,460 | 16520,730 | | 20419,420 | 20700,270 | 20894,110 | 23813,740 | 22314,230 | | 831886,800 | 802293,200 | 778765,600 | 755274,800 | 698075,400 | | 653035,300 | 614936,700 | 660322,600 | 614622,900 | 635472,400 | |
| 55 | 550 | 12929,210 | 11850,900 | 12286,040 | 12062,090 | 12825,580 | | 14419,120 | 14705,950 | 14449,800 | 14499,630 | 14088,610 | | 460436,400 | 462252,100 | 460705,100 | 460683,700 | 451192,600 | | 502724,600 | 458776,000 | 477039,500 | 451495,500 | 466023,800 | |
| 56 | 560 | 17119,800 | 15663,090 | 14427,020 | 16573,780 | 17523,980 | | 11023,760 | 11117,260 | 11067,010 | 10977,850 | 11664,300 | | 221800,300 | 221984,100 | 221905,300 | 222481,200 | 233620,000 | | 467002,000 | 414078,000 | 369759,100 | 424245,400 | 448205,900 | |
| 57 | 570 | 9898,699 | 8904,055 | 8378,610 | 8775,777 | 9949,563 | | 8601,354 | 8738,319 | 8578,311 | 8633,446 | 8537,537 | | 130982,900 | 130878,300 | 130481,200 | 127860,200 | 128774,500 | | 195889,600 | 165076,200 | 155700,400 | 159030,600 | 180372,900 | |

## Table D.2 Absolutely Maximum Displacement Values at Pier Caps in Global X-Direction (East) and Global Y-Direction (North) (CASE A)

| PIER NO | Frame # (Bottom) | $\|Ux\|_{MAX}$ (m) | | | | | | $\|Uy\|_{MAX}$ (m) | | | | | |
|---|---|---|---|---|---|---|---|---|---|---|---|---|---|
| | | MODEL1 | MODEL2 | MODEL3 | MODEL4 | MODEL5 | MODEL6 | MODEL1 | MODEL2 | MODEL3 | MODEL4 | MODEL5 | MODEL6 |
| 1 | 10 | 0,0424 | 0,0578 | 0,0500 | 0,0598 | 0,0434 | | 0,0672 | 0,0782 | 0,0793 | 0,0697 | 0,0597 | |
| 2 | 20 | 0,0378 | 0,0651 | 0,0530 | 0,0673 | 0,0466 | | 0,0762 | 0,0696 | 0,0812 | 0,0650 | 0,0530 | |
| 3 | 30 | 0,0177 | 0,0184 | 0,0175 | 0,0192 | 0,0118 | | 0,0185 | 0,0206 | 0,0204 | 0,0221 | 0,0192 | |
| 4 | 40 | 0,0017 | 0,0016 | 0,0015 | 0,0018 | 0,0006 | | 0,0019 | 0,0019 | 0,0016 | 0,0022 | 0,0018 | |
| 5 | 50 | 0,0608 | 0,0609 | 0,0600 | 0,0443 | 0,0475 | | 0,0477 | 0,0485 | 0,0476 | 0,0349 | 0,0022 | |
| 6 | 60 | 0,0093 | 0,0089 | 0,0095 | 0,0095 | 0,0064 | | 0,0074 | 0,0068 | 0,0070 | 0,0071 | 0,0079 | |
| 7 | 70 | 0,0383 | 0,0353 | 0,0376 | 0,0366 | 0,0434 | | 0,0455 | 0,0499 | 0,0462 | 0,0513 | 0,0236 | |
| 8 | 80 | 0,0440 | 0,0450 | 0,0437 | 0,0489 | 0,0465 | | 0,0744 | 0,0674 | 0,0709 | 0,0662 | 0,0526 | |
| 9 | 90 | 0,1112 | 0,0961 | 0,1038 | 0,0934 | 0,0978 | | 0,1467 | 0,1405 | 0,1430 | 0,1370 | 0,0837 | |
| 10 | 100 | 0,2765 | 0,2760 | 0,2741 | 0,2797 | 0,2272 | | 0,1730 | 0,1619 | 0,1663 | 0,1449 | 0,1512 | |
| 11 | 110 | 0,2278 | 0,2418 | 0,2382 | 0,2527 | 0,2265 | | 0,2259 | 0,2042 | 0,2141 | 0,1907 | 0,1723 | |
| 12 | 120 | 0,1901 | 0,1993 | 0,2019 | 0,2096 | 0,2264 | | 0,2460 | 0,2466 | 0,2453 | 0,2450 | 0,1694 | |
| 13 | 130 | 0,1568 | 0,1615 | 0,1615 | 0,1677 | 0,2189 | | 0,2431 | 0,2550 | 0,2497 | 0,2664 | 0,1534 | |
| 14 | 140 | 0,1667 | 0,1734 | 0,1691 | 0,1800 | 0,2264 | | 0,2421 | 0,2511 | 0,2471 | 0,2604 | 0,1436 | |
| 15 | 150 | 0,8244 | 0,7427 | 0,6113 | 0,4371 | 0,4799 | | 0,6675 | 0,5901 | 0,4803 | 0,3474 | 0,1440 | |
| 16 | 160 | 0,2077 | 0,2151 | 0,2105 | 0,2322 | 0,2097 | | 0,1988 | 0,2013 | 0,1944 | 0,2063 | 0,1469 | |
| 17 | 170 | 0,1968 | 0,2024 | 0,2009 | 0,2156 | 0,2097 | | 0,1887 | 0,1878 | 0,1914 | 0,1975 | 0,1464 | |
| 18 | 180 | 0,1930 | 0,1972 | 0,2031 | 0,1937 | 0,2208 | | 0,2118 | 0,2122 | 0,2090 | 0,2150 | 0,1368 | |
| 19 | 190 | 0,1989 | 0,2031 | 0,2044 | 0,2019 | 0,2208 | | 0,1979 | 0,1977 | 0,1999 | 0,2018 | 0,1165 | |
| 20 | 200 | 0,2068 | 0,2048 | 0,1981 | 0,2116 | 0,2204 | 0,2208 | 0,1849 | 0,2039 | 0,1982 | 0,1960 | 0,1025 | 0,1090 |
| 21 | 210 | 0,1943 | 0,1981 | 0,1934 | 0,2094 | 0,1991 | 0,1991 | 0,1657 | 0,1701 | 0,1654 | 0,1723 | 0,1085 | 0,1138 |
| 22 | 220 | 0,1831 | 0,1859 | 0,1871 | 0,1974 | 0,1991 | 0,1991 | 0,1691 | 0,1709 | 0,1715 | 0,1824 | 0,1252 | 0,1238 |
| 23 | 230 | 0,1822 | 0,1858 | 0,1866 | 0,1915 | 0,1991 | 0,1991 | 0,1744 | 0,1768 | 0,1786 | 0,1795 | 0,1322 | 0,1319 |
| 24 | 240 | 0,1833 | 0,1885 | 0,1881 | 0,2009 | 0,1991 | 0,1991 | 0,1753 | 0,1797 | 0,1738 | 0,1822 | 0,1262 | 0,1361 |
| 25 | 250 | 1,0817 | 0,9706 | 0,8591 | 0,4806 | 0,5497 | 0,5499 | 0,8675 | 0,7699 | 0,6416 | 0,3773 | 0,1115 | 0,1347 |
| 26 | 260 | 0,1910 | 0,1945 | 0,1942 | 0,2015 | 0,2098 | 0,2098 | 0,1806 | 0,1838 | 0,1835 | 0,1849 | 0,1082 | 0,1264 |
| 27 | 270 | 0,1935 | 0,1979 | 0,1984 | 0,2026 | 0,2098 | 0,2098 | 0,1763 | 0,1772 | 0,1798 | 0,1816 | 0,1167 | 0,1234 |
| 28 | 280 | 0,1972 | 0,2015 | 0,2010 | 0,2051 | 0,2097 | 0,2097 | 0,1740 | 0,1754 | 0,1740 | 0,1792 | 0,1164 | 0,1277 |
| 29 | 290 | 0,2006 | 0,2029 | 0,2037 | 0,2067 | 0,2097 | 0,2097 | 0,1733 | 0,1733 | 0,1699 | 0,1777 | 0,1107 | 0,1313 |
| 30 | 300 | 0,1991 | 0,2009 | 0,2038 | 0,2037 | 0,2093 | 0,2098 | 0,1638 | 0,1723 | 0,1699 | 0,1737 | 0,1074 | 0,1317 |
| 31 | 310 | 0,1922 | 0,1932 | 0,1955 | 0,1982 | 0,1991 | | 0,1568 | 0,1582 | 0,1632 | 0,1622 | 0,1108 | |
| 32 | 320 | 0,2112 | 0,2122 | 0,2144 | 0,2149 | 0,2101 | | 0,1535 | 0,1582 | 0,1519 | 0,1499 | 0,1146 | |
| 33 | 330 | 0,2175 | 0,2214 | 0,2212 | 0,2240 | 0,2189 | | 0,1548 | 0,1423 | 0,1511 | 0,1396 | 0,1162 | |
| 34 | 340 | 0,2167 | 0,2167 | 0,2117 | 0,2118 | 0,2101 | | 0,1507 | 0,1518 | 0,1532 | 0,1585 | 0,1153 | |
| 35 | 350 | 1,3422 | 1,2355 | 1,0727 | 0,6070 | 0,5848 | | 0,7822 | 0,7243 | 0,6152 | 0,3824 | 0,1138 | |
| 36 | 360 | 0,2021 | 0,2040 | 0,2061 | 0,2057 | 0,1991 | | 0,1470 | 0,1526 | 0,1528 | 0,1582 | 0,1106 | |
| 37 | 370 | 0,2222 | 0,2224 | 0,2209 | 0,2257 | 0,1991 | | 0,1451 | 0,1515 | 0,1471 | 0,1533 | 0,1110 | |
| 38 | 380 | 0,2177 | 0,2177 | 0,2151 | 0,2195 | 0,2101 | | 0,1387 | 0,1452 | 0,1403 | 0,1535 | 0,1103 | |
| 39 | 390 | 0,2226 | 0,2269 | 0,2211 | 0,2303 | 0,2101 | | 0,1373 | 0,1527 | 0,1489 | 0,1497 | 0,1144 | |
| 40 | 400 | 0,2198 | 0,2183 | 0,2246 | 0,2364 | 0,1996 | | 0,1363 | 0,1506 | 0,1489 | 0,1475 | 0,1161 | |
| 41 | 410 | 0,2165 | 0,2177 | 0,2182 | 0,2196 | 0,1991 | | 0,1481 | 0,1545 | 0,1582 | 0,1607 | 0,1170 | |
| 42 | 420 | 0,2225 | 0,2202 | 0,2246 | 0,2168 | 0,2101 | | 0,1466 | 0,1541 | 0,1549 | 0,1531 | 0,1122 | |
| 43 | 430 | 0,2196 | 0,2157 | 0,2181 | 0,2111 | 0,2101 | | 0,1504 | 0,1595 | 0,1564 | 0,1534 | 0,1110 | |
| 44 | 440 | 0,2177 | 0,2215 | 0,2234 | 0,2227 | 0,1991 | | 0,1401 | 0,1539 | 0,1528 | 0,1553 | 0,1138 | |
| 45 | 450 | 1,0038 | 0,9586 | 0,7142 | 0,5499 | 0,4800 | | 0,4463 | 0,4384 | 0,3620 | 0,2973 | 0,1114 | |
| 46 | 460 | 0,2295 | 0,2289 | 0,2322 | 0,2284 | 0,2208 | | 0,1625 | 0,1742 | 0,1694 | 0,1905 | 0,1124 | |
| 47 | 470 | 0,2262 | 0,2251 | 0,2246 | 0,2278 | 0,2097 | | 0,1696 | 0,1848 | 0,1767 | 0,1876 | 0,1323 | |
| 48 | 480 | 0,2262 | 0,2270 | 0,2266 | 0,2324 | 0,2097 | | 0,1785 | 0,1885 | 0,1856 | 0,1956 | 0,1531 | |
| 49 | 490 | 0,2267 | 0,2330 | 0,2324 | 0,2439 | 0,2097 | | 0,1936 | 0,1960 | 0,1953 | 0,1970 | 0,1672 | |
| 50 | 500 | 0,2550 | 0,2498 | 0,2566 | 0,2535 | 0,1996 | | 0,1736 | 0,1629 | 0,1692 | 0,1586 | 0,1697 | |

**Table D.2 Absolutely Maximum Displacement Values at Pier Caps in Global X-Direction (East) and Global Y-Direction (North) (CASE A) (Continued)**

| PIER NO | Frame # (Bottom) | $\|Ux\|_{MAX}$ (m) | | | | | | $\|Uy\|_{MAX}$ (m) | | | | | |
|---|---|---|---|---|---|---|---|---|---|---|---|---|---|
| | | MODEL1 | MODEL2 | MODEL3 | MODEL4 | MODEL5 | MODEL6 | MODEL1 | MODEL2 | MODEL3 | MODEL4 | MODEL5 | MODEL6 |
| 51 | 510 | 0,2000 | 0,2010 | 0,2022 | 0,2018 | 0,2189 | | 0,2084 | 0,2167 | 0,2180 | 0,2215 | 0,1428 | |
| 52 | 520 | 0,2158 | 0,2172 | 0,2183 | 0,2193 | 0,2189 | | 0,1945 | 0,1931 | 0,1967 | 0,1919 | 0,1309 | |
| 53 | 530 | 0,1666 | 0,1690 | 0,1672 | 0,1718 | 0,1868 | | 0,2004 | 0,1951 | 0,1964 | 0,1905 | 0,1320 | |
| 54 | 540 | 0,4703 | 0,4381 | 0,4177 | 0,3683 | 0,3120 | | 0,2378 | 0,2145 | 0,2063 | 0,1630 | 0,1187 | |
| 55 | 550 | 0,2172 | 0,2232 | 0,2222 | 0,2267 | 0,2029 | | 0,1425 | 0,1301 | 0,1328 | 0,1245 | 0,0821 | |
| 56 | 560 | 0,0412 | 0,0424 | 0,0409 | 0,0422 | 0,0434 | | 0,0459 | 0,0460 | 0,0490 | 0,0482 | 0,0344 | |
| 57 | 570 | 0,0172 | 0,0168 | 0,0170 | 0,0170 | 0,0146 | | 0,0119 | 0,0114 | 0,0108 | 0,0115 | 0,0085 | |

**Table D.3 Modified Displacement Values at Pier Caps of Central Fixed Piers $[U=(UX^2+UY^2)^{1/2}]$ (CASE A)**

| PIER NO | Frame # (Bottom | $\|U\|_{MAX}$ $[=(dx^2+dy^2)^{1/2}]$ (m) | | | | | |
|---|---|---|---|---|---|---|---|
| | | MODEL1 | MODEL2 | MODEL3 | MODEL4 | MODEL5 | MODEL6 |
| 5 | 50 | 0,0773 | 0,0779 | 0,0766 | 0,0564 | 0,0476 | 0,0000 |
| 15 | 150 | 1,0542 | 0,9399 | 0,7509 | 0,5142 | 0,4809 | 0,0000 |
| 25 | 250 | 1,3772 | 1,2226 | 1,0437 | 0,6093 | 0,5498 | 0,5535 |
| 35 | 350 | 1,5068 | 1,4000 | 1,2096 | 0,7013 | 0,5862 | 0,0000 |
| 45 | 450 | 1,0716 | 1,0285 | 0,8007 | 0,6236 | 0,4838 | 0,0000 |
| 54 | 540 | 0,5062 | 0,4776 | 0,4533 | 0,3981 | 0,3121 | 0,0000 |

# Table D.4 Shear Force and Moment Values (CASE B)

| PIER NO | Frame # (Bottom) | $\|V22\|_{MAX}$ (Transverse) (kN) | | | | | | $\|V33\|_{MAX}$ (Longitudinal) (kN) | | | | | |
|---|---|---|---|---|---|---|---|---|---|---|---|---|---|
| | | MODEL1 | MODEL2 | MODEL3 | MODEL4 | MODEL5 | MODEL6 | MODEL1 | MODEL2 | MODEL3 | MODEL4 | MODEL5 | MODEL6 |
| 1 | 10 | 26360,610 | 30163,580 | 28577,030 | 30918,900 | 32705,430 | | 5910,532 | 5893,803 | 6490,321 | 7077,418 | 6450,434 | |
| 2 | 20 | 18874,860 | 21984,320 | 22659,620 | 23355,520 | 21209,780 | | 5654,218 | 5200,947 | 5827,361 | 6013,329 | 6412,955 | |
| 3 | 30 | 20846,890 | 23935,440 | 23696,180 | 25414,400 | 23199,190 | | 10905,010 | 11554,950 | 13069,200 | 13359,940 | 13428,000 | |
| 4 | 40 | 9646,736 | 9618,252 | 8526,060 | 11955,170 | 10539,430 | | 44593,270 | 50530,130 | 51047,990 | 51022,900 | 52138,530 | |
| 5 | 50 | 11290,870 | 9198,292 | 9473,130 | 10353,560 | 10317,790 | | 43253,400 | 48914,320 | 49915,660 | 50427,950 | 51229,230 | |
| 6 | 60 | 10284,550 | 11436,450 | 11801,660 | 9778,094 | 10782,900 | | 18977,130 | 20443,490 | 22454,200 | 23060,910 | 23322,100 | |
| 7 | 70 | 10632,740 | 11942,460 | 12318,320 | 11587,530 | 12145,180 | | 9163,724 | 10649,670 | 12469,590 | 13229,300 | 13227,520 | |
| 8 | 80 | 12012,780 | 12041,910 | 12405,650 | 13286,780 | 14222,160 | | 6650,243 | 7616,072 | 9070,547 | 9688,938 | 9926,976 | |
| 9 | 90 | 16091,880 | 16360,240 | 16983,970 | 17456,890 | 15757,700 | | 5543,876 | 7131,459 | 8255,728 | 9009,516 | 9040,344 | |
| 10 | 100 | 17289,870 | 15921,260 | 16681,100 | 18606,380 | 17659,380 | | 5157,537 | 5385,011 | 7005,838 | 7544,416 | 7753,870 | |
| 11 | 110 | 20282,700 | 21076,490 | 21412,380 | 23318,770 | 21399,040 | | 7219,645 | 6641,514 | 7882,459 | 8546,870 | 8665,050 | |
| 12 | 120 | 21362,860 | 22464,600 | 22209,190 | 24083,180 | 21655,780 | | 7249,799 | 7422,680 | 8786,603 | 9604,674 | 9730,018 | |
| 13 | 130 | 20925,470 | 22370,290 | 21754,540 | 23897,930 | 20709,350 | | 8673,405 | 8438,820 | 9955,662 | 10877,610 | 11163,220 | |
| 14 | 140 | 18692,320 | 19220,210 | 18989,970 | 21276,580 | 17756,360 | | 8916,099 | 8944,479 | 10157,040 | 11243,560 | 11333,850 | |
| 15 | 150 | 15068,460 | 15576,610 | 16554,770 | 17197,340 | 15035,860 | | 8446,350 | 8578,166 | 9903,860 | 11076,260 | 10876,700 | |
| 16 | 160 | 14050,170 | 14630,150 | 16531,220 | 16381,360 | 14431,240 | | 8934,521 | 8671,348 | 10040,910 | 11237,420 | 11050,480 | |
| 17 | 170 | 13401,490 | 13915,130 | 14793,520 | 16350,010 | 14723,560 | | 9105,047 | 9257,749 | 10579,470 | 11892,730 | 11653,920 | |
| 18 | 180 | 12625,370 | 12819,390 | 12795,590 | 14720,580 | 14238,930 | | 9555,009 | 9915,558 | 11390,920 | 12873,730 | 12696,080 | |
| 19 | 190 | 10894,020 | 11456,500 | 11420,750 | 12339,060 | 11692,240 | | 9708,266 | 10201,520 | 11783,060 | 13491,010 | 13255,660 | |
| 20 | 200 | 10438,960 | 10405,800 | 10381,570 | 11709,450 | 10089,580 | 11525,730 | 10377,610 | 10560,020 | 12146,310 | 13781,720 | 13769,640 | 12528,870 |
| 21 | 210 | 8686,437 | 8688,580 | 10933,550 | 9810,189 | 10022,380 | 10902,830 | 10018,820 | 10102,130 | 11640,350 | 13238,190 | 13127,110 | 14343,980 |
| 22 | 220 | 10173,170 | 10797,510 | 10847,700 | 12209,720 | 11967,940 | 11733,620 | 9897,737 | 10339,050 | 11784,200 | 13341,760 | 13410,330 | 14114,500 |
| 23 | 230 | 10892,610 | 11459,310 | 10825,760 | 12663,620 | 12320,300 | 11852,410 | 10130,520 | 10558,200 | 11964,520 | 13542,040 | 13677,470 | 14116,350 |
| 24 | 240 | 10831,310 | 11567,560 | 9866,996 | 12668,460 | 12041,120 | 12618,670 | 10283,390 | 10805,920 | 12099,580 | 13604,810 | 13814,830 | 14116,270 |
| 25 | 250 | 9652,284 | 10428,980 | 10493,550 | 10954,240 | 10579,070 | 12800,740 | 10506,890 | 11048,910 | 12324,890 | 13560,900 | 13899,020 | 14141,150 |
| 26 | 260 | 8980,880 | 10086,100 | 11369,540 | 10823,420 | 10742,290 | 12279,370 | 11250,340 | 11588,920 | 12831,570 | 14069,610 | 14492,880 | 14663,440 |
| 27 | 270 | 10126,410 | 11158,820 | 10398,400 | 11908,020 | 11961,300 | 11851,730 | 11565,800 | 11748,430 | 12937,670 | 14004,600 | 14517,220 | 14654,780 |
| 28 | 280 | 9713,385 | 10295,280 | 9967,513 | 11587,770 | 11471,760 | 12754,060 | 11684,390 | 11849,390 | 12993,260 | 13904,530 | 14521,730 | 14626,820 |
| 29 | 290 | 9158,990 | 9452,146 | 9877,419 | 10829,010 | 10329,460 | 13217,720 | 11467,060 | 11856,640 | 12997,390 | 13869,600 | 14584,760 | 14799,620 |
| 30 | 300 | 8996,650 | 8889,626 | 9536,988 | 10136,990 | 9679,936 | 13216,500 | 11751,630 | 11858,750 | 12969,190 | 13988,750 | 14741,110 | 12034,170 |

| PIER NO | Frame # (Bottom) | $\|M22\|_{MAX}$ (Longitudinal) (kN.m) | | | | | | $\|M33\|_{MAX}$ (Transverse) (kN.m) | | | | | |
|---|---|---|---|---|---|---|---|---|---|---|---|---|---|
| | | MODEL1 | MODEL2 | MODEL3 | MODEL4 | MODEL5 | MODEL6 | MODEL1 | MODEL2 | MODEL3 | MODEL4 | MODEL5 | MODEL6 |
| 1 | 10 | 123560,900 | 119971,200 | 121201,000 | 115649,900 | 116742,800 | | 679240,200 | 735181,500 | 726217,700 | 752956,400 | 791117,100 | |
| 2 | 20 | 105495,900 | 99737,050 | 101938,300 | 104051,500 | 105657,900 | | 546768,500 | 575350,200 | 643116,900 | 604628,900 | 551496,600 | |
| 3 | 30 | 185676,800 | 202695,300 | 200222,400 | 194940,600 | 196955,900 | | 435642,300 | 455712,000 | 473798,800 | 484010,000 | 438111,200 | |
| 4 | 40 | 439257,200 | 531262,100 | 485848,000 | 485344,800 | 491710,800 | | 117110,100 | 105822,400 | 88313,270 | 127166,900 | 110787,900 | |
| 5 | 50 | 468000,000 | 556491,600 | 520323,500 | 513032,900 | 519295,500 | | 144092,300 | 107323,300 | 120599,600 | 119525,700 | 117452,500 | |
| 6 | 60 | 316528,000 | 346961,100 | 345350,600 | 334992,300 | 338497,300 | | 194327,500 | 193445,700 | 210109,400 | 178862,300 | 197185,500 | |
| 7 | 70 | 212568,800 | 241536,700 | 250731,500 | 246301,500 | 250409,500 | | 272252,700 | 296113,400 | 304370,200 | 278200,800 | 306308,100 | |
| 8 | 80 | 178377,100 | 201733,800 | 212041,800 | 209609,800 | 214928,200 | | 376577,100 | 375633,000 | 380179,200 | 390227,300 | 444385,000 | |
| 9 | 90 | 161097,600 | 200405,100 | 208455,600 | 206313,200 | 214520,900 | | 591225,500 | 579004,600 | 599121,600 | 612210,500 | 561468,700 | |
| 10 | 100 | 165004,200 | 168453,700 | 179247,600 | 184599,800 | 189122,000 | | 728382,600 | 667053,100 | 704127,500 | 753826,700 | 715565,200 | |
| 11 | 110 | 222295,500 | 200515,200 | 205246,600 | 211995,700 | 215128,300 | | 845482,200 | 867041,900 | 878766,400 | 933887,400 | 850980,900 | |
| 12 | 120 | 234963,500 | 226600,400 | 233709,200 | 241231,000 | 243868,600 | | 877717,100 | 918591,300 | 915021,400 | 965572,800 | 865234,100 | |
| 13 | 130 | 271615,800 | 255756,800 | 264490,600 | 272972,800 | 276542,700 | | 849671,100 | 890884,900 | 868408,400 | 938142,500 | 815995,800 | |
| 14 | 140 | 282713,100 | 267606,800 | 279077,500 | 287048,400 | 287982,600 | | 773730,900 | 797263,600 | 781394,400 | 861572,500 | 725471,000 | |
| 15 | 150 | 273408,300 | 263598,600 | 272107,100 | 284315,500 | 282860,200 | | 669302,400 | 694852,900 | 717502,600 | 749548,900 | 640595,000 | |
| 16 | 160 | 286374,600 | 272822,600 | 283364,900 | 297493,300 | 291906,400 | | 626913,400 | 654516,100 | 710358,300 | 720398,600 | 629817,900 | |
| 17 | 170 | 298165,900 | 292348,000 | 302036,100 | 315806,500 | 308858,200 | | 590791,200 | 612450,500 | 649178,300 | 697248,300 | 632507,300 | |
| 18 | 180 | 320666,000 | 315460,300 | 327792,500 | 339855,600 | 334263,300 | | 548896,700 | 552691,900 | 539339,700 | 629594,400 | 612570,700 | |
| 19 | 190 | 329106,200 | 328193,200 | 342431,000 | 354787,900 | 349508,100 | | 477257,500 | 471961,500 | 469962,700 | 506339,300 | 516258,700 | |
| 20 | 200 | 352503,900 | 341179,800 | 354572,800 | 365190,300 | 363256,600 | 397503,400 | 456327,900 | 449818,900 | 438796,600 | 475895,400 | 455599,100 | 489253,300 |
| 21 | 210 | 349528,700 | 331842,900 | 345393,600 | 356067,600 | 355555,000 | 416902,600 | 394281,200 | 400006,300 | 466315,800 | 436395,400 | 446789,800 | 473028,800 |
| 22 | 220 | 351707,800 | 341553,900 | 352129,300 | 361955,500 | 365158,900 | 413767,100 | 448664,500 | 472396,200 | 488509,800 | 523835,600 | 514516,800 | 513646,400 |
| 23 | 230 | 360261,800 | 350175,400 | 358851,800 | 369344,400 | 373423,100 | 413897,100 | 485642,800 | 516486,700 | 468113,100 | 559353,300 | 547332,900 | 539290,300 |
| 24 | 240 | 366877,100 | 358327,200 | 366326,600 | 375495,600 | 380022,100 | 413750,100 | 472395,700 | 503335,300 | 440986,000 | 548258,800 | 524389,700 | 559893,400 |
| 25 | 250 | 374005,900 | 365690,200 | 372853,700 | 380368,200 | 385498,300 | 413993,000 | 437688,400 | 441062,900 | 461934,400 | 484623,800 | 454662,300 | 553172,000 |
| 26 | 260 | 393709,600 | 382436,300 | 387477,100 | 393030,800 | 400076,200 | 425982,800 | 431593,900 | 444702,800 | 486105,100 | 471704,300 | 465542,100 | 540742,900 |
| 27 | 270 | 403336,500 | 387415,100 | 391084,000 | 395483,400 | 403482,600 | 425823,300 | 435856,100 | 479461,100 | 453560,800 | 504322,600 | 507057,300 | 524505,500 |
| 28 | 280 | 409744,400 | 391102,300 | 393268,000 | 396486,300 | 405615,800 | 425435,700 | 434467,200 | 455302,800 | 435271,800 | 498848,200 | 496796,300 | 550569,000 |
| 29 | 290 | 410278,900 | 393316,300 | 394267,200 | 396729,300 | 406897,800 | 427687,300 | 425590,900 | 428056,800 | 427489,900 | 482438,900 | 467808,800 | 566972,800 |
| 30 | 300 | 423766,300 | 395075,900 | 394581,700 | 396886,800 | 411031,900 | 384852,000 | 413217,600 | 427987,200 | 431502,400 | 458724,800 | 443000,700 | 568790,200 |

# Table D.4 Shear Force and Moment Values (CASE B) (Continued)

| PIER NO | Frame # (Bottom) | $\lvert V22 \rvert_{MAX}$ (Transverse) (kN) | | | | | | $\lvert V33 \rvert_{MAX}$ (Longitudinal) (kN) | | | | | | $\lvert M22 \rvert_{MAX}$ (Longitudinal) (kN.m) | | | | | | $\lvert M33 \rvert_{MAX}$ (Transverse) (kN.m) | | | | | |
|---|---|---|---|---|---|---|---|---|---|---|---|---|---|---|---|---|---|---|---|---|---|---|---|---|---|
| | | MODEL1 | MODEL2 | MODEL3 | MODEL4 | MODEL5 | MODEL6 | MODEL1 | MODEL2 | MODEL3 | MODEL4 | MODEL5 | MODEL6 | MODEL1 | MODEL2 | MODEL3 | MODEL4 | MODEL5 | MODEL6 | MODEL1 | MODEL2 | MODEL3 | MODEL4 | MODEL5 | MODEL6 |
| 31 | 310 | 9602,013 | 10492,490 | 9843,722 | 10632,430 | 9379,349 | | 11920,950 | 11473,650 | 12288,410 | 13935,950 | 14269,730 | | 427393,300 | 385172,300 | 379330,500 | 385306,800 | 400674,200 | | 427004,700 | 461903,600 | 441274,500 | 450612,800 | 436220,800 | |
| 32 | 320 | 10456,650 | 11618,280 | 10958,910 | 11687,280 | 9144,799 | | 11345,280 | 11342,640 | 11887,330 | 13888,190 | 14195,210 | | 416173,200 | 380179,500 | 366380,100 | 377392,400 | 392104,000 | | 469560,400 | 515913,700 | 498176,200 | 490821,300 | 432897,800 | |
| 33 | 330 | 9115,720 | 10363,860 | 11243,810 | 11039,930 | 9470,270 | | 10921,900 | 11198,990 | 11649,010 | 13840,150 | 14168,050 | | 407321,300 | 374449,300 | 353468,700 | 371453,800 | 386633,700 | | 436248,600 | 487444,600 | 511623,400 | 469086,400 | 422041,400 | |
| 34 | 340 | 9882,723 | 10896,720 | 10837,040 | 12150,400 | 10169,500 | | 11919,080 | 11406,570 | 11701,760 | 14061,910 | 14488,230 | | 432822,700 | 383821,600 | 362766,600 | 382397,000 | 398330,100 | | 436262,600 | 474362,100 | 482236,800 | 501421,300 | 435035,900 | |
| 35 | 350 | 10701,160 | 11428,780 | 10080,340 | 10553,000 | 9672,520 | | 12375,020 | 11371,390 | 11619,490 | 13979,230 | 14578,930 | | 442660,700 | 383575,000 | 363461,900 | 383324,000 | 402011,700 | | 476603,100 | 504015,200 | 441748,900 | 458475,400 | 429824,100 | |
| 36 | 360 | 11295,950 | 12106,170 | 11238,420 | 12049,150 | 10784,890 | | 13282,160 | 11570,180 | 12424,620 | 14098,290 | 14925,440 | | 465255,400 | 392124,800 | 370325,800 | 393678,700 | 414919,600 | | 516875,000 | 528258,300 | 481250,300 | 515498,200 | 460989,800 | |
| 37 | 370 | 11155,340 | 11976,030 | 11503,410 | 12480,090 | 10916,510 | | 13506,170 | 11633,630 | 12130,350 | 13972,620 | 14996,100 | | 469811,000 | 391293,600 | 371011,300 | 390158,300 | 415324,800 | | 510453,900 | 520280,700 | 496367,200 | 531638,600 | 463674,800 | |
| 38 | 380 | 10001,770 | 10792,470 | 10900,280 | 11284,780 | 9799,175 | | 12839,120 | 11439,540 | 12204,330 | 13490,770 | 14482,330 | | 453769,800 | 376357,800 | 355051,300 | 377879,500 | 403362,000 | | 449016,300 | 470411,100 | 474544,500 | 484319,400 | 422060,400 | |
| 39 | 390 | 9003,805 | 9282,421 | 10100,400 | 9805,527 | 9602,120 | | 12782,890 | 11384,210 | 11989,230 | 13329,060 | 14430,570 | | 452777,300 | 372388,100 | 354587,800 | 374209,400 | 401356,500 | | 398486,900 | 413591,700 | 439036,600 | 442547,400 | 433786,800 | |
| 40 | 400 | 8710,712 | 9592,092 | 10264,960 | 10366,750 | 10958,010 | | 13356,080 | 11578,050 | 12215,350 | 13753,660 | 14868,720 | | 463982,400 | 380506,100 | 369734,000 | 390319,100 | 409492,300 | | 396283,800 | 424513,500 | 466019,300 | 428625,000 | 466920,000 | |
| 41 | 410 | 8682,642 | 9541,121 | 10305,360 | 9858,840 | 10580,040 | | 12922,510 | 11535,180 | 12013,930 | 13688,910 | 14636,140 | | 452803,400 | 375408,900 | 364727,800 | 385545,900 | 404204,400 | | 384662,200 | 414897,500 | 427380,900 | 443139,700 | 480388,100 | |
| 42 | 420 | 8117,047 | 9082,448 | 9108,093 | 9436,380 | 9617,427 | | 12190,760 | 11310,750 | 11455,910 | 12831,190 | 13865,870 | | 433374,700 | 359830,800 | 353215,800 | 370510,900 | 387106,400 | | 359358,400 | 388252,500 | 416462,800 | 420052,100 | 438613,500 | |
| 43 | 430 | 8599,960 | 8879,021 | 9581,519 | 9706,290 | 9302,356 | | 12023,970 | 11306,840 | 11511,130 | 12799,310 | 13534,590 | | 427182,900 | 355743,000 | 351994,700 | 367502,900 | 380220,300 | | 364532,300 | 378480,000 | 388297,100 | 414072,700 | 416220,900 | |
| 44 | 440 | 8810,082 | 8877,195 | 9273,873 | 9546,379 | 10004,950 | | 12491,280 | 11488,710 | 11893,940 | 13294,210 | 13689,050 | | 435873,600 | 360283,500 | 359382,200 | 375227,300 | 386282,400 | | 398985,000 | 415394,800 | 408379,700 | 430954,300 | 452384,100 | |
| 45 | 450 | 9121,730 | 9462,084 | 10111,730 | 10196,550 | 10608,000 | | 13289,420 | 11789,830 | 12599,920 | 13938,950 | 14611,720 | | 457463,500 | 379801,400 | 375938,100 | 389510,200 | 401380,800 | | 431905,700 | 435515,800 | 450958,600 | 452371,300 | 486859,000 | |
| 46 | 460 | 10410,090 | 10303,250 | 10085,500 | 11645,560 | 11762,050 | | 13021,050 | 11648,520 | 12680,750 | 13872,280 | 14288,780 | | 447508,700 | 373355,300 | 372291,700 | 384009,200 | 392782,900 | | 422003,000 | 433313,300 | 448504,300 | 490696,200 | 496925,500 | |
| 47 | 470 | 10328,110 | 11515,340 | 11000,070 | 11794,810 | 12320,670 | | 12389,600 | 11226,100 | 11997,080 | 13088,060 | 13378,290 | | 425402,900 | 357974,800 | 354722,700 | 365191,300 | 371840,500 | | 443247,300 | 485489,900 | 481376,000 | 522767,000 | 558876,800 | |
| 48 | 480 | 12875,580 | 13653,380 | 12937,400 | 14162,780 | 14333,420 | | 11733,700 | 10982,180 | 11753,810 | 12429,610 | 13081,440 | | 409780,100 | 351031,900 | 343787,800 | 351513,700 | 360506,300 | | 546563,600 | 591262,000 | 560016,400 | 615880,100 | 649280,900 | |
| 49 | 490 | 13838,280 | 14416,900 | 13860,040 | 15586,020 | 16578,620 | | 11562,890 | 10695,310 | 11565,150 | 12082,250 | 12722,790 | | 402959,300 | 343345,500 | 334961,900 | 341482,600 | 348762,400 | | 617767,400 | 648225,800 | 627846,800 | 686740,700 | 719487,900 | |
| 50 | 500 | 14452,900 | 14193,890 | 14220,290 | 15713,860 | 16525,670 | | 10151,770 | 10185,770 | 11008,920 | 11483,670 | 12018,750 | | 362779,700 | 324296,800 | 318603,300 | 324913,000 | 328795,000 | | 634535,600 | 627545,100 | 623714,400 | 679576,800 | 709841,600 | |
| 51 | 510 | 16745,420 | 17838,450 | 17893,850 | 18733,960 | 19260,290 | | 12449,530 | 12651,760 | 13495,010 | 14303,640 | 14528,460 | | 420596,700 | 386411,200 | 375556,400 | 374541,600 | 380476,100 | | 679645,500 | 716685,400 | 712430,600 | 741086,300 | 759539,600 | |
| 52 | 520 | 15928,600 | 16235,170 | 16787,990 | 17082,850 | 18084,520 | | 12531,410 | 12209,740 | 13010,470 | 13697,540 | 14101,570 | | 413646,700 | 372507,800 | 361485,700 | 359868,900 | 368138,900 | | 633747,900 | 653517,900 | 667080,600 | 669668,000 | 701717,600 | |
| 53 | 530 | 18333,350 | 19096,060 | 20080,630 | 19862,510 | 20502,900 | | 13366,820 | 12944,520 | 13951,390 | 14495,610 | 14718,790 | | 430405,800 | 387839,900 | 376011,700 | 372710,100 | 378109,600 | | 709814,900 | 740219,500 | 773756,600 | 754315,600 | 771604,300 | |
| 54 | 540 | 14722,700 | 14986,630 | 15675,070 | 15926,280 | 16469,140 | | 11709,990 | 11590,720 | 12089,470 | 12638,410 | 13065,410 | | 380515,700 | 348833,800 | 331420,300 | 333024,100 | 338814,400 | | 588857,300 | 595339,600 | 623222,800 | 621941,100 | 835845,000 | |
| 55 | 550 | 11222,180 | 11041,840 | 11523,420 | 12287,290 | 12797,890 | | 11791,970 | 11574,610 | 12464,750 | 13191,860 | 13700,940 | | 378550,400 | 348139,900 | 335639,600 | 335542,500 | 338358,300 | | 439628,700 | 427094,300 | 446669,000 | 461216,200 | 465820,200 | |
| 56 | 560 | 15129,860 | 14979,790 | 15220,610 | 16929,010 | 17514,720 | | 34425,820 | 30952,960 | 31860,480 | 33294,140 | 33949,120 | | 809923,100 | 714891,900 | 655907,300 | 646317,300 | 658733,000 | | 390188,900 | 377970,800 | 375976,700 | 434542,600 | 448158,900 | |
| 57 | 570 | 8478,245 | 8552,412 | 8458,604 | 8793,426 | 9950,434 | | 60980,200 | 53098,700 | 50043,990 | 49359,420 | 50566,110 | | 1182955,000 | 1047821,000 | 920087,900 | 891024,900 | 908803,100 | | 160787,900 | 157447,200 | 158915,200 | 157656,400 | 180290,500 | |

## Table D.5 Absolutely Maximum Displacement Values at Pier Caps in Global X-Direction (East) and Global Y-Direction (North) (CASE B)

| PIER NO | Frame # (Bottom) | $\lvert Ux \rvert_{MAX}$ (m) | | | | | | $\lvert Uy \rvert_{MAX}$ (m) | | | | | |
|---|---|---|---|---|---|---|---|---|---|---|---|---|---|
| | | MODEL1 | MODEL2 | MODEL3 | MODEL4 | MODEL5 | MODEL6 | MODEL1 | MODEL2 | MODEL3 | MODEL4 | MODEL5 | MODEL6 |
| 1 | 10 | 0,0457 | 0,0439 | 0,0446 | 0,0389 | 0,0213 | | 0,0544 | 0,0562 | 0,0597 | 0,0585 | 0,0597 | |
| 2 | 20 | 0,0482 | 0,0471 | 0,0521 | 0,0403 | 0,0219 | | 0,0564 | 0,0565 | 0,0680 | 0,0595 | 0,0530 | |
| 3 | 30 | 0,0237 | 0,0257 | 0,0255 | 0,0210 | 0,0204 | | 0,0249 | 0,0233 | 0,0242 | 0,0228 | 0,0192 | |
| 4 | 40 | 0,0165 | 0,0192 | 0,0176 | 0,0174 | 0,0187 | | 0,0117 | 0,0139 | 0,0130 | 0,0130 | 0,0018 | |
| 5 | 50 | 0,0195 | 0,0225 | 0,0208 | 0,0204 | 0,0228 | | 0,0150 | 0,0180 | 0,0169 | 0,0168 | 0,0022 | |
| 6 | 60 | 0,0291 | 0,0318 | 0,0300 | 0,0281 | 0,0324 | | 0,0255 | 0,0264 | 0,0273 | 0,0267 | 0,0079 | |
| 7 | 70 | 0,0423 | 0,0414 | 0,0375 | 0,0346 | 0,0442 | | 0,0382 | 0,0403 | 0,0421 | 0,0420 | 0,0236 | |
| 8 | 80 | 0,0595 | 0,0577 | 0,0539 | 0,0546 | 0,0564 | | 0,0551 | 0,0586 | 0,0580 | 0,0586 | 0,0526 | |
| 9 | 90 | 0,0969 | 0,0980 | 0,0945 | 0,0960 | 0,0681 | | 0,0834 | 0,0810 | 0,0756 | 0,0757 | 0,0837 | |
| 10 | 100 | 0,1564 | 0,1453 | 0,1434 | 0,1532 | 0,0804 | | 0,1117 | 0,1074 | 0,1112 | 0,1169 | 0,1512 | |
| 11 | 110 | 0,1789 | 0,1724 | 0,1695 | 0,1768 | 0,0908 | | 0,1250 | 0,1293 | 0,1404 | 0,1419 | 0,1723 | |
| 12 | 120 | 0,1784 | 0,1720 | 0,1659 | 0,1739 | 0,1007 | | 0,1343 | 0,1366 | 0,1392 | 0,1449 | 0,1694 | |
| 13 | 130 | 0,1678 | 0,1605 | 0,1527 | 0,1659 | 0,1100 | | 0,1416 | 0,1380 | 0,1389 | 0,1376 | 0,1534 | |
| 14 | 140 | 0,1616 | 0,1502 | 0,1688 | 0,1703 | 0,1195 | | 0,1523 | 0,1482 | 0,1466 | 0,1406 | 0,1436 | |
| 15 | 150 | 0,1838 | 0,1803 | 0,1997 | 0,2015 | 0,1292 | | 0,1607 | 0,1576 | 0,1519 | 0,1540 | 0,1440 | |
| 16 | 160 | 0,2127 | 0,2109 | 0,2239 | 0,2269 | 0,1379 | | 0,1591 | 0,1586 | 0,1395 | 0,1575 | 0,1469 | |
| 17 | 170 | 0,2291 | 0,2291 | 0,2263 | 0,2357 | 0,1459 | | 0,1450 | 0,1421 | 0,1267 | 0,1382 | 0,1464 | |
| 18 | 180 | 0,2319 | 0,2288 | 0,2177 | 0,2239 | 0,1531 | | 0,1540 | 0,1254 | 0,1209 | 0,1154 | 0,1368 | |
| 19 | 190 | 0,2313 | 0,2205 | 0,2002 | 0,1989 | 0,1600 | | 0,1548 | 0,1304 | 0,1257 | 0,1144 | 0,1165 | |
| 20 | 200 | 0,2341 | 0,2120 | 0,1843 | 0,1787 | 0,1665 | 0,2206 | 0,1590 | 0,1431 | 0,1244 | 0,1270 | 0,1025 | 0,1277 |
| 21 | 210 | 0,2344 | 0,2056 | 0,1782 | 0,1750 | 0,1730 | 0,2069 | 0,1673 | 0,1492 | 0,1255 | 0,1335 | 0,1085 | 0,1138 |
| 22 | 220 | 0,2277 | 0,2042 | 0,1841 | 0,1832 | 0,1783 | 0,2069 | 0,1725 | 0,1516 | 0,1279 | 0,1397 | 0,1252 | 0,1238 |
| 23 | 230 | 0,2348 | 0,2147 | 0,2008 | 0,1977 | 0,1829 | 0,2070 | 0,1787 | 0,1503 | 0,1350 | 0,1391 | 0,1322 | 0,1319 |
| 24 | 240 | 0,2391 | 0,2287 | 0,2190 | 0,2126 | 0,1868 | 0,2070 | 0,1830 | 0,1537 | 0,1391 | 0,1395 | 0,1262 | 0,1361 |
| 25 | 250 | 0,2492 | 0,2393 | 0,2275 | 0,2216 | 0,1899 | 0,2069 | 0,1852 | 0,1578 | 0,1375 | 0,1401 | 0,1115 | 0,1347 |
| 26 | 260 | 0,2543 | 0,2411 | 0,2225 | 0,2202 | 0,1921 | 0,2065 | 0,1856 | 0,1545 | 0,1357 | 0,1374 | 0,1082 | 0,1264 |
| 27 | 270 | 0,2551 | 0,2361 | 0,2134 | 0,2119 | 0,1941 | 0,2064 | 0,1876 | 0,1470 | 0,1349 | 0,1335 | 0,1167 | 0,1234 |
| 28 | 280 | 0,2568 | 0,2328 | 0,2090 | 0,2034 | 0,1956 | 0,2063 | 0,1898 | 0,1427 | 0,1278 | 0,1323 | 0,1164 | 0,1277 |
| 29 | 290 | 0,2571 | 0,2331 | 0,2092 | 0,2003 | 0,1968 | 0,2062 | 0,1883 | 0,1417 | 0,1193 | 0,1326 | 0,1107 | 0,1313 |
| 30 | 300 | 0,2666 | 0,2378 | 0,2101 | 0,2036 | 0,1977 | 0,2042 | 0,1843 | 0,1391 | 0,1233 | 0,1325 | 0,1074 | 0,1317 |
| 31 | 310 | 0,2821 | 0,2441 | 0,2136 | 0,2108 | 0,1987 | | 0,1801 | 0,1388 | 0,1367 | 0,1451 | 0,1108 | |
| 32 | 320 | 0,2944 | 0,2495 | 0,2186 | 0,2130 | 0,1996 | | 0,1760 | 0,1404 | 0,1439 | 0,1522 | 0,1146 | |
| 33 | 330 | 0,3051 | 0,2528 | 0,2190 | 0,2083 | 0,2003 | | 0,1770 | 0,1380 | 0,1402 | 0,1522 | 0,1162 | |
| 34 | 340 | 0,3070 | 0,2476 | 0,2119 | 0,1981 | 0,2006 | | 0,1808 | 0,1349 | 0,1528 | 0,1533 | 0,1153 | |
| 35 | 350 | 0,3118 | 0,2489 | 0,2021 | 0,1906 | 0,2011 | | 0,1837 | 0,1358 | 0,1568 | 0,1616 | 0,1138 | |
| 36 | 360 | 0,3136 | 0,2501 | 0,1938 | 0,1869 | 0,2009 | | 0,1798 | 0,1379 | 0,1472 | 0,1670 | 0,1106 | |
| 37 | 370 | 0,3130 | 0,2493 | 0,1946 | 0,1893 | 0,2006 | | 0,1728 | 0,1291 | 0,1437 | 0,1665 | 0,1110 | |
| 38 | 380 | 0,3105 | 0,2454 | 0,2029 | 0,1961 | 0,2004 | | 0,1693 | 0,1231 | 0,1417 | 0,1603 | 0,1103 | |
| 39 | 390 | 0,3060 | 0,2400 | 0,2098 | 0,2034 | 0,1998 | | 0,1676 | 0,1397 | 0,1357 | 0,1461 | 0,1144 | |
| 40 | 400 | 0,3039 | 0,2378 | 0,2081 | 0,2067 | 0,1985 | | 0,1613 | 0,1407 | 0,1386 | 0,1462 | 0,1161 | |
| 41 | 410 | 0,2978 | 0,2386 | 0,2014 | 0,1998 | 0,1970 | | 0,1509 | 0,1291 | 0,1386 | 0,1374 | 0,1170 | |
| 42 | 420 | 0,2953 | 0,2362 | 0,1934 | 0,1909 | 0,1954 | | 0,1488 | 0,1374 | 0,1407 | 0,1424 | 0,1122 | |
| 43 | 430 | 0,2945 | 0,2391 | 0,1911 | 0,1894 | 0,1928 | | 0,1517 | 0,1357 | 0,1338 | 0,1352 | 0,1110 | |
| 44 | 440 | 0,2913 | 0,2466 | 0,1993 | 0,1950 | 0,1895 | | 0,1571 | 0,1195 | 0,1289 | 0,1236 | 0,1138 | |
| 45 | 450 | 0,2859 | 0,2491 | 0,2101 | 0,2083 | 0,1853 | | 0,1584 | 0,1160 | 0,1140 | 0,1307 | 0,1114 | |
| 46 | 460 | 0,2809 | 0,2491 | 0,2192 | 0,2184 | 0,1814 | | 0,1567 | 0,1194 | 0,1256 | 0,1349 | 0,1124 | |
| 47 | 470 | 0,2763 | 0,2434 | 0,2246 | 0,2213 | 0,1773 | | 0,1570 | 0,1353 | 0,1310 | 0,1378 | 0,1323 | |
| 48 | 480 | 0,2693 | 0,2308 | 0,2171 | 0,2125 | 0,1725 | | 0,1537 | 0,1519 | 0,1499 | 0,1519 | 0,1531 | |
| 49 | 490 | 0,2637 | 0,2157 | 0,2021 | 0,1991 | 0,1672 | | 0,1575 | 0,1536 | 0,1527 | 0,1539 | 0,1672 | |
| 50 | 500 | 0,2492 | 0,2022 | 0,1857 | 0,1916 | 0,1618 | | 0,1514 | 0,1412 | 0,1370 | 0,1429 | 0,1697 | |

**Table D.5 Absolutely Maximum Displacement Values at Pier Caps in Global X-Direction (East) and Global Y-Direction (North) (CASE B) (Continued)**

| PIER NO | Frame # (Bottom) | $\lvert Ux \rvert_{MAX}$ (m) | | | | | | $\lvert Uy \rvert_{MAX}$ (m) | | | | | |
|---|---|---|---|---|---|---|---|---|---|---|---|---|---|
| | | MODEL1 | MODEL2 | MODEL3 | MODEL4 | MODEL5 | MODEL6 | MODEL1 | MODEL2 | MODEL3 | MODEL4 | MODEL5 | MODEL6 |
| 51 | 510 | 0,2276 | 0,1956 | 0,1781 | 0,1879 | 0,1539 | | 0,1235 | 0,1194 | 0,1062 | 0,1115 | 0,1428 | |
| 52 | 520 | 0,2159 | 0,1940 | 0,1745 | 0,1807 | 0,1478 | | 0,1104 | 0,1108 | 0,1049 | 0,0953 | 0,1309 | |
| 53 | 530 | 0,1995 | 0,1902 | 0,1720 | 0,1768 | 0,1409 | | 0,1143 | 0,1197 | 0,1205 | 0,1066 | 0,1320 | |
| 54 | 540 | 0,1864 | 0,1836 | 0,1592 | 0,1627 | 0,1353 | | 0,1114 | 0,1147 | 0,1164 | 0,1078 | 0,1187 | |
| 55 | 550 | 0,1807 | 0,1715 | 0,1344 | 0,1400 | 0,1290 | | 0,0955 | 0,0922 | 0,0970 | 0,0905 | 0,0821 | |
| 56 | 560 | 0,1719 | 0,1521 | 0,1287 | 0,1218 | 0,1178 | | 0,0757 | 0,0643 | 0,0640 | 0,0632 | 0,0344 | |
| 57 | 570 | 0,1598 | 0,1393 | 0,1219 | 0,1170 | 0,1091 | | 0,0631 | 0,0612 | 0,0469 | 0,0459 | 0,0085 | |

**Table D.6 Modified Displacement Values at Pier Caps of Central Fixed Piers $[U=(UX^2+UY^2)^{1/2}]$ (CASE B)**

| PIER NO | Frame # (Bottom | $\lvert U \rvert_{MAX}$ $[=(dx^2+dy^2)^{1/2}]$ (m) | | | | | |
|---|---|---|---|---|---|---|---|
| | | MODEL1 | MODEL2 | MODEL3 | MODEL4 | MODEL5 | MODEL6 |
| 5 | 50 | 0,0242 | 0,0288 | 0,0268 | 0,0264 | 0,0228 | 0,0000 |
| 15 | 150 | 0,1880 | 0,1877 | 0,2004 | 0,2026 | 0,1532 | 0,0000 |
| 25 | 250 | 0,2682 | 0,2526 | 0,2385 | 0,2316 | 0,1959 | 0,2336 |
| 35 | 350 | 0,3247 | 0,2643 | 0,2358 | 0,2304 | 0,2022 | 0,0000 |
| 45 | 450 | 0,2966 | 0,2495 | 0,2157 | 0,2116 | 0,1916 | 0,0000 |
| 54 | 540 | 0,2127 | 0,1879 | 0,1797 | 0,1800 | 0,1571 | 0,0000 |

## Table D.7 Shear Force and Moment Values For "10-Span Segment Models"

| PIER NO | Frame # (Bottom) | $\lvert V22\rvert_{MAX}$ (kN) (Transverse) | | $\lvert V33\rvert_{MAX}$ (kN) (Longitudinal) | | $\lvert M22\rvert_{MAX}$ (kN.m) (Longitudinal) | | $\lvert M33\rvert_{MAX}$ (kN.m) (Transvese) | |
|---|---|---|---|---|---|---|---|---|---|
| | | ASTALDI | MODEL6B | ASTALDI | MODEL6B | ASTALDI | MODEL6B | ASTALDI | MODEL6B |
| 10 | 100 | 11872,000 | | 11520,000 | | 205900,000 | | 271000,000 | |
| 11 | 110 | 11910,000 | | 10730,000 | | 216300,000 | | 253500,000 | |
| 12 | 120 | 11750,000 | | 10770,000 | | 218600,000 | | 250500,000 | |
| 13 | 130 | 13150,000 | | 11610,000 | | 233000,000 | | 276200,000 | |
| 14 | 140 | 12800,000 | | 11120,000 | | 228600,000 | | 266500,000 | |
| 15 | 150 | 12020,000 | | 12780,000 | | 241300,000 | | 263100,000 | |
| 16 | 160 | 13190,000 | | 14370,000 | | 262900,000 | | 273700,000 | |
| 17 | 170 | 11920,000 | | 14520,000 | | 253700,000 | | 273100,000 | |
| 18 | 180 | 12000,000 | | 14420,000 | | 257200,000 | | 266200,000 | |
| 19 | 190 | 14120,000 | | 13920,000 | | 245100,000 | | 280200,000 | |
| 20 | 200 | 15112,000 | 11525,730 | | 12528,870 | | 397503,400 | 285600,000 | 489253,300 |
| 21 | 210 | | 10902,830 | | 14343,980 | | 416902,600 | | 473028,800 |
| 22 | 220 | | 11733,620 | | 14114,500 | | 413767,100 | | 513646,400 |
| 23 | 230 | | 11852,410 | | 14116,350 | | 413897,100 | | 539290,300 |
| 24 | 240 | | 12618,670 | | 14116,270 | | 413750,100 | | 559893,400 |
| 25 | 250 | | 12800,740 | | 14141,150 | | 413993,000 | | 553172,000 |
| 26 | 260 | | 12279,370 | | 14663,440 | | 425982,800 | | 540742,900 |
| 27 | 270 | | 11851,730 | | 14654,780 | | 425823,300 | | 524505,500 |
| 28 | 280 | | 12754,060 | | 14626,820 | | 425435,700 | | 550569,000 |
| 29 | 290 | | 13217,720 | | 14799,620 | | 427687,300 | | 566972,800 |
| 30 | 300 | | 13216,500 | | 12034,170 | | 384852,000 | | 568790,200 |